Dear Climate of the Past Editorial Board, dear Referees,

We would like to express our gratitude to both anonymous Referees for their thoughtful review of our manuscript titled "An assessment of latest Cretaceous *Pycnodonte vesicularis* (Lamarck, 1806) shells as records for palaeoseasonality: A multi-proxy investigation" submitted to the journal Climate of the Past. After careful consideration of all the criticisms and suggestions raised by the Referees, we herewith provide a point-by-point reply to the report of both Referees. In this rebuttal, we will first summarize the major points of criticism raised by the Referees and then proceed to cite parts of the review reports and provide our reactions directly below the citations.

Major points of criticism

1. **Offset between independent temperature reconstructions**

One of the major concerns raised by Referee #1 is the way in which our manuscript describes the offset between the various independent temperature reconstructions we attempted. The point we were trying to make in our discussion of this offset is that TEX86 temperatures seem to overestimate the water temperatures, or at least those in the part of the water column where the *Pycnodonte* shells grew. We make the case that clumped isotope thermometry should be the most sensitive and well-constrained of the methods we applied. Given that it yields lower temperatures, we conclude that it is likely that the TEX86 reconstructions are overestimating the local water temperatures. Referee #1 suggests that our clumped isotope measurements might be subject to diagenetic alteration or solid state reordering after burial, but this effect would increase the reconstructed temperature, not lower it. We include diagenetically altered clumped-isotopic values in our manuscript that illustrate this effect and indeed yield higher temperatures (26-35 degrees). In a revised version of the manuscript, we will include these altered clumped isotope measurements into our discussion as an illustration of the burial temperatures (as suggested by Referee #1). Following the Referee's suggestion, we will also clarify that we do not think that the temperature gradient with (50-75m) depth can fully explain the offset between TEX86 and clumped isotope reconstructions. Similarly, we agree that extreme summer temperatures might not fully explain this offset while still maintaining relatively cool mean temperatures and moderate seasonality. However, we do not wish to fully abandon the hypothesis that shell growth happened preferentially in the cooler months. If summer maxima in temperature or minima in salinity were extreme enough to produce conditions that limited shell growth, we reckon that this may still be a valid explanation. Indeed, our records suggest that lowest salinities are reached in winter to spring. In the Cretaceous lower mid-latitudes of the South Atlantic the growth of ostreid bivalves may not be limited by low winter temperatures, as they are in the cool temperate seas of the present North Sea Basin (NW Europe) (as in Ullmann et al., 2010,2013). It may, in our opinion, therefore not be ruled out that preferential growth in cool seasons biased reconstructions of mean annual temperatures from these bivalves towards lower temperatures. The part of the discussion that deals with this offset between temperature reconstructions will be revisited in the revised version and we will attempt to restructure the arguments to make the discussion of the points mentioned above more convincing.

2. **Stratigraphic constraint**

A point is raised over the lack of stratigraphic constraints of the samples used in our manuscript. We admit that Figure 1 could be clearer and also realize that it may be interesting to constrain the stratigraphy of the specimens more rigorously. Besides, we agree with the Referees that it may be interesting for future research to briefly state how abundant *Pycnodonte* shells are in the

stratigraphy. We therefore propose to restructure paragraph 4.1 and reconsider Figure 1 to clarify these points. In the meantime, we will include more detailed information about the taphonomic condition of the specimens. We agree that any variation or uncertainty in the stratigraphic location of the specimens may have bearing on the discussion of differences in seasonality recorded in the multi-proxy records through the shells, and will take this into account in the discussion while revising our manuscript.

3. Vital effects and comparison with other species

Some comments were raised with regard to the species with which we compare our *Pycnodonte* records in the manuscript. For these comparisons, we have tried to stick to the closest modern relatives of *Pycnodonte vesicularis*. We do however, concede that these modern analogues may not be a perfect fit in terms of their environment. Most notably the species *Neopycnodonte zibrowii* may not be a good modern analogue. We will reduce the discussion of the comparison with this species and focus on the discussion with *Hyotissa*, which has a more similar environment.

Length of the manuscript text

Both Referees rightly comment on the fact that our manuscript is quite long. We realize that the text has become quite convoluted in some places (most notably in the discussion) as a result of the various methods applied in this multi-proxy study. We thank both Referees for their advice on how to amend this and will try to use their suggestions to improve the readability of the manuscript text. We will try to shorten methodological descriptions and move parts of the methodology to supplementary files. We will shorten the Abstract and Conclusion chapters and will attempt to remove any recurring parts from the discussion to make the argumentation easier to follow.

Point-by-point replies to comments of referees

Anonymous Referee #1

In the manuscript "An assessment of latest Cretaceous Pycnodonte vesicularis (Lamarck, 1806) shells as records for palaeoseasonality: A multi-proxy investigation", de Winter and co-authors report observations of shell preservation and geochemistry of Pycnodonte vesicularis and potential implications for palaeoclimate and palaeoenvironmental research that can be drawn from these results.

The authors advocate that, based on conventional oxygen isotope data, Mg/Ca ratios and clumped oxygen isotopes, P. vesicularis of the late Maastrichtian of the Neuquén Basin experienced limited annual seasonality with temperatures fluctuating around 11_C or slightly more. These temperature estimates are markedly lower than existing TEX86 estimates. Additionally, general suitability of P. vesicularis for palaeoclimate research, water mass stratification and fresh water input into the Neuquén Basin are discussed.

The authors present a rigorously constrained, extensive dataset of high quality and remain generally cautious about interpretation of the data. The text, figures and tables are clear and easy to follow, even though the text is relatively long. The questions addressed are in the scope of CP and this study contains a wealth of novel data using partly very recently developed analytical techniques. Scientific methods are clearly outlined and valid, even though I partly disagree with interpretations in detail (see below). Description of the methodology is mostly sufficient to understand the workflows (see specific comments below). It is great to see that most raw data

generated to write this manuscript is included in the supplements, but giving the reader some guidance to the significance of the data and more intuitive headers in the excel file would be useful. Could stable isotope ratio and clumped isotope data also be included in the supplements? In my opinion, after moderate revision, this contribution would be very suitable for Climate of the Past:

The one point I am struggling with is the inference that the oyster-based temperature estimate of 11_C can be reconciled with the 27_C TEX86 SST estimate. The authors acknowledge that the discrepancy is surprisingly large, putting forward that 1) TEX86 may be biased towards summer SST, 2) oysters are benthic creatures and bottom water temperatures at 50-75m depth would have been somewhat lower, 3) oyster growth may have been biased towards preferential shell formation in the cold season, 4) there may be an unconstrained bias on the oxygen isotope temperature estimate and Mg-based temperature estimates might be more accurate. I do fully agree with 1) and 2) even though the inferred SST-bottom water temperature gradient would be very large. In particular – if TEX86 may be biased towards high summer temperatures and oyster calcite towards winter lows, why is the seasonality recorded in the oysters so limited? After all the authors put forward an interpretation of continuous oyster growth over the entire year with somewhat reduced _18O values only in the austral spring (October- December; Fig. 9) 3) It appears odd to me that oysters should have preferentially grown in the cold season. Modern oysters shut down growth in the cold season and show increased growth and fitness in warm temperatures (e.g., Pauley, 1988 for a review of the older literature). Average oxygen isotope values for oyster transects of modern specimens therefore show a bias towards warm temperatures (more than 5_C in a specimen from N Germany, Ullmann et al., 2010) and characteristic saw-tooth patterns with flat summer minima and sharp winter maxima of _18O (Ullmann et al., 2010, 2013). 4) It is my understanding that clumped isotope measurements are thought to represent palaeotemperatures and ambient water isotopic composition unaffected by vital effects or any other potential bias. It is not clear to me how these temperatures (if the clumped signal is indeed preserved perfectly) could be underestimated. It is unfortunate that no clumped isotope measurements for the M0 specimen are available as the authors argue this fossil shell is overall best preserved and should yield the most trustworthy data. Connected to the clumped isotopes, is there an estimate of maximum burial depth of the late Maastrichtian strata (maximum burial temperatures) in the Neuquén Basin? Can re-equilibration at the atomic scale be excluded with confidence? As the authors rightly point out there are problems with identifying a suitable transfer function for Mg/Ca temperature reconstruction for Cretaceous oysters because of secular change of seawater Mg/Ca and a multitude of available oyster (and related species) calibrations. Any argument relating to such a tentative reconstruction based on the calibration that "appears to fit best" must therefore carry some element of circularity. Could the authors revisit their chain of arguments and address these points?

As mentioned above, this is one of the major points in the discussion that we will try to clarify in a revised version of the manuscript. We will put in effort to more clearly reconcile the outcomes of various techniques of temperature reconstruction described in the manuscript.

Abstract and Conclusion seem quite long-winded and could be shortened with nonessential information being transferred into other sections or deleted. The referencing and reference list require a thorough check for consistency and missing information.

Both Referees have noted that our reference list is not up to date. In a revised version of the manuscript, we will take care to update the reference list according to the guidelines of Climate of

the Past. As mentioned above, we will restructure Abstract and Conclusions to make them more concise.

Specific points:

Line 20: "the late Maastrichtian of the Neuquén Basin". At the moment it reads as if only Maastrichtian sediments are present in Neuquén Basin.

We will rephrase this to "the late Maastrichtian strata exposed within the Neuquén Basin succession"

Line 43: "allowed for a tentative"

This will be rephrased

Line 57: References in wrong sequence.

We will update the reference list and citations through the text.

Line 68: Another point here is the rapid secretion of such shells allowing for the high time-resolution required.

We thank Referee #1 for this suggestion and incorporate this into our manuscript text.

Line 78: What is meant here by "long timescale reconstruction"?

We mean to refer to the superposition of seasonality records from bivalves into the framework of longer timescale palaeoclimate records. This will be rephrased to: "seasonally-resolved bivalve records are rarely combined with longer timescale palaeoclimate records"

Line 79: Could this sentence be rephrased? I am not sure "caveat" can be used in the way it is put here.

We will rephrase this to "disadvantage"

Line 86: References in wrong sequence

References and citations will be updated

Line 106: "Fischer von Waldheim, 1835"

This will be corrected

Line 106: "shell" instead of "shelf"?

The term "commissural shelf" refers to the shelflike part of the bivalve shell that faces the place where both valves meet (the commissure).

Line 113: Oysters in general grow very rapidly as compared to other calcite secreting marine animals and the Maastrichtian Pycnodonte does not seem to be an exception.

We will take this into account while rephrasing this sentence. In this context we mean to say that bivalves (as far as we know) seem to precipitate their shell calcite in isotopic equilibrium with the extrapallial fluid (certainly with respect to oxygen isotopes).

Line 116: "tridacnid bivalves"?

This will be corrected

Line 119: "Al-Aasm"

This will be corrected

Line 131: Here and in the following, please be consistent in the use of "paleo" or "palaeo"

In the revised version of the manuscript, we will go through the text and consistently use the British spelling ("palaeo") wherever applicable.

*Line 164: Missing space after 2_*

This will be corrected

Line 196: "5m below the Cretaceous-Paleogene". Regardless of style, the spelling of "Paleogene" is fixed by the International Commission on Stratigraphy (e.g., Cohen et al., 2013).

Agreed, this will be corrected

Line 226: "half shell"?

This will be corrected

Line 255: "Elderfield and Ganssen, 2000". This reference is missing in the reference list

We will add it to the reference list

Line 263: This statement is somewhat vague. Is this meant to be with reference to the composition of the ambient seawater or the mantle fluid?

We agree that this sentence could require clarification and will adapt it in the next version. What is meant is that trace element concentrations (in this case those of Mg) are not necessarily taken into the shell in equilibrium with the ambient seawater.

Line 271: It should be kept in mind that the Sr distribution coefficient is negatively correlated with temperature (Rimstidt et al., 1998). Studies inferring a temperature control on Sr in bivalve calcite are rare and conversely point towards higher Sr/Ca in shell secreted at higher temperature (Wanamaker et al., 2008). The article cited in line 271 does not promote a Sr calibration but one for Mg.

We apologize for the mixing up of references in this sentence and will revisit this paragraph to provide the right background of Sr/Ca ratios in bivalve shells and how they should be interpreted.

Line 307: What is the 1sd uncertainty of the Marbella marble related to? Does this mean that its composition is only known within 0.2 permil for carbon and 0.4 permil for oxygen or that this is its heterogeneity? In the former case this would impose quite a large potential bias on analyses corrected against this standard. In the latter case I wonder how the analytical reproducibility can be so much better (Line 308) than the above stated uncertainty ranges.

This is a valid comment, as the description of the MAR2 standard contains errors. The uncertainty on the values of the Marbella marble is relative to the values of NBS-19 and the reported values should be of 2 standard deviations rather than one. A combination of machine error and reproducibility error on the MAR2 standard yields total uncertainties on the measurement of 0.1 and 0.2 permille for carbon and oxygen delta values respectively. We will clarify this in the revised text to avoid confusion.

Line 331: What is the meaning of "error" for the _47 measurements? Is that to be read as potential bias against other labs or is this purely a measurement uncertainty?

This error is a long-term measurement reproducibility error. We will mention this to avoid confusion.

Line 333: Is there a reference to these Santrock/Gonfiantini or Brand (Line 336) parameters that could be cited here?

Two references for these parameters are:

Daëron, M. et al., 2016. Absolute isotopic abundance ratios and the accuracy of Δ47 measurements. Chemical Geology, 442, pp.83–96.
Schauer, A.J. et al., 2016. Choice of 17O correction affects clumped isotope (Δ 47) values of CO 2measured with mass spectrometry. Rapid Communications in Mass Spectrometry, 30(24), pp.2607–2616.

We will include the reference to these studies in the revised version. In order to clarify and shorten the method description in this paragraph we will move some of the text to supplementary material.

Line 371: What is the evidence for diagenesis of the calcite comprising the vesicular material at this stage?

This is a valid point, in the revised version of the manuscript we will refrain from interpreting results in the results section and save interpretations for the discussion section.

Line 380: "consists"

This will be corrected

Line 391: "correspond to"

This will be corrected

Line 401: I am not entirely sure how interferences could cause noise in the XRF spectrum. An interference should cause a bias in the measurement which cannot be corrected for by applying a running mean smoothing routine. Noise should be bias-free and related only to the problems in quantifying low-amplitude signals precisely.

This is a valid point and we realize that the explanation of smoothing of the XRF records is somewhat vague as it is. In the revised version of the manuscript we will rephrase this sentence to explain that small-scale variations in the matrix of the sample (in this case the bivalve shell) causes variations in the spectral resolution of XRF spectra, which affect lighter elements with smaller peaks (e.g. Mg) more than elements with larger peaks in the XRF spectrum.

Line 403: Please check for grammar.

This sentence will be corrected

Line 454: The finding of seawater _18O values around -2 ‰be quite important. Previously some late Maastrichtian freshening of the Basin has been mentioned. Is a rough estimate of salinity possible from the reconstructed bottom water oxygen isotope ratio?

We will try to include an estimate of salinity changes in the Basin based on our data, but this will be discussed in the Discussion section.

Line 462: Recrystallization is a different process than cementation. This statement seems to be in contrast to what has been said in Line 371.

We agree and will rephrase by stating which process may affect the porosity of the shell on the microscale.

Line 477: "laminae"

This will be corrected

Line 505: Consider adding that this is a threshold for both Mn and Fe for clarity.

We will follow the suggestion and add a statement here.

Line 522: "LMC" is never used again in the text so I do not think there is a need to introduce this abbreviation.

Agreed, we will remove the reference to the abbreviation.

Line 536: "exceedingly" seems a slightly extreme term to use. Compared to heavily altered calcite samples the ones reported here are moderately depleted in 18O.

Agreed, we will use "relatively" instead.

Line 540: This concept of "remote biomineralisation" has been commented on by a few studies but I am not sure how much acceptance it currently has.

Neither are we, but we would like to include the reference to this hypothesis for sake of completeness.

Line 558: The partially to fully (?) altered samples subjected to clumped isotope measurements may yield some interesting information about the type of diagenesis the samples underwent. Is there any meaningful information about burial conditions during recrystallization that can be extracted from these data?

We thank Referee #1 for this suggestion, which, as mentioned above, will be included in a revision of the discussion. Indeed, diagenetically altered clumped isotope results may feature more prominently in this part of the discussion to show that the samples considered reliable are not affected by the same degree of diagenesis.

Line 595: Here and Line 596 – "Quaternary"

This will be corrected

Line 611: "altered vesicular calcite in the shell"

This will be corrected

Line 651: References in wrong sequence.

This will be corrected

Line 664: "alternating"

This will be corrected

Line 667: "correlate with"

This will be corrected

Line 677: "extrapallial fluid"

This will be corrected

Line 693: Is this meant to be a reference to Wisshak et al. (2009)? See also lines 704, 705.

This will be corrected

Line 704: Wisshak et al. (2009) report a minor (0.5 ‰ enrichment of 18O in N. zibrowii on the basis of the Anderson and Arthur (1983) oxygen isotope thermometer. I would not count this as a strong vital effect because their assessment would have been the opposite (enrichment of 16O of similar magnitude) if they had employed the Coplen (2007) oxygen isotope thermometer. At the sub-permil level it is very hard to make strong inferences about kinetic isotope effects.

We will take this into account while discussing differences between our results and those of Wisshak et al. 2009. As mentioned above, we will limit the discussion of *N. zibrowii* as a modern analogue because its environment is not likely to be representative for that of *P. vesicularis*.

Line 705: References in wrong sequence.

This will be corrected

Line 731: "evaporitic setting"? Or "setting characterized by common evaporites"?

This will be corrected

Line 780: If Sr/Ca was indeed controlled by growth rate and P. vesicularis would have grown more slowly in spring (why would this be the case?), this effect should be seen as an ontogenetic drift of Sr/Ca towards lower ratios as the shell extends more slowly as the animal ages. The only shell that may show this effect is potentially M11, however (Fig. 5).

We thank Referee #1 for the input on this part of the discussion and will take these considerations into account in the revision of our discussion. We acknowledge that the relationship of Sr/Ca with growth rate does not show up as an ontogenetic trend. Sr/Ca ratios in bivalve calcite are controversial and our current interpretation of these records is based on a small amount of earlier studies. As it stands, the interpretation of Sr/Ca ratios was mostly driven by their anti-phase relationship with carbon isotopes, which were tentatively interpreted as proxy for light conditions based on the comparison with *Hyotissa*. As mentioned above, we may have to partly revise and restructure our interpretation of the phase relationship between the proxies. Therefore, we will revise the discussion of Sr/Ca ratios in the new version of the manuscript and be more careful in interpreting Sr/Ca ratios. We will put forward other interpretations for this record and its apparent seasonality to show that the relationship with growth rate is not certain.

Line 823: The way it is expressed here is potentially misleading. The Mouchi et al. (2013) calibration is not only a calibration based on juvenile specimens, it is also reported as a calibration that can only be employed for juvenile specimens.

We will rephrase this expression to avoid confusion. The attempted temperature reconstructions using Mg/Ca ratios are subject to considerable uncertainty. We will shorten the discussion of these Mg/Ca temperatures and further emphasize that these reconstructions are based on assumptions that are uncertain. The reason these attempted temperature reconstructions are added is to illustrate how different independent reconstructions lead to different temperatures and to allow discussion between temperature proxies.

Line 847: I am not entirely sure how the estimate of 20 psu was derived. Could this be elaborated on? If this model is based on water _18O it must depend on the isotopic composition of the fresh water source which I suppose is poorly constrained?

Both referees mention this issue. We acknowledge that the estimate of salinity is not very certain. We will rephrase this sentence in the revised version and refrain from giving absolute estimates of salinity since we cannot constrain all the variables needed to do so with any certainty. Instead, we will discuss relative salinity changes.

Line 901: Secondary carbonates may be enriched in Mn and Fe and depleted in 13C and 18O, but this is not necessarily always the case.

We will rephrase this to "recrystallization and precipitation of secondary carbonates in equilibrium with these reducing pore fluids may raise the concentration of Mn and Fe and lower stable isotope ratios"

Line 916: This seems to be a repetition of lines 886 and following.

Agreed, we will shorten this paragraph and remove repetitive elements to improve readability of the text.

Line 937: "Maastrichtian of the Neuquén Basin"

This will be corrected

Line 956: I agree that the clumped isotope numbers appear to make some sense, but is there any independent evidence that they truly reflect environmental conditions at the time of shell formation? I have the feeling that clumped isotope values are accepted once they give values reasonably close to where one would expect them and reconstructed ambient water composition is not too far off the expected marine value.

In the revised manuscript we will revisit the discussion of clumped isotope results and discuss any potential for diagenetic alteration in more detail using the altered clumped isotope measurements that yield higher temperatures.

All comments and suggestions regarding the reference list were incorporated in the revised manuscript.

Figure 3: Why are the sum of Mn and Fe shown in panel be? Fe is a quenching element and Mn an activator of cathodoluminescence, so I would expect that an image of Mn only would more closely resemble the CL pattern. As it stands there seems very little communality between the CL and the XRF trace which is a bit surprising. Could the small panels (C-I) be enlarged? I find it very hard to see the blocky calcite crystals in C and the thin layer of vesicular calcite in G in print. Also I do not find panel I) very convincing as evidence for a Fe and Mn corona around a boring. This boring rather seems to be Mn and Fe depleted.

This figure and its caption will be restructured to better highlight the observations they are meant to illustrate. The corona of higher Mn and Fe concentrations is maybe better visible in the larger image Figure 3B.

Figure 4E): How was the porograph constructed? Does it present porosity strictly on the pixels covered by the red arrow or does it integrate pixels in the depth domain or even pixels in depth and with?

Details on the processing of CT-scan data will be added to the part of the methods section that will be placed in supplementary data to allow for easier reading. The porographs are constructed by first segmenting the scanned object into two phases, i.e., shell material and porosity. Porographs are made by integrating density data parallel to the shell layers:

The segmentation is straightforward, given the large density difference between the shell material and the pore filling substance (air, Araldite resin did not penetrate into the internal pores). Secondly, the porosity is calculated (in Matlab, repetitive 2D approach) by taking the slice per slice ratio of pore pixels to pore + shell pixels (pore/pore+shell). The porograph shows the evolution of porosity from the bottom to the top slice in a given image stack. The slice per slice calculation allows to evaluate the evolution of porosity through the shell. The total shell porosity is then obtained by taking the average porosity of all values that were obtained in the slice per slice procedure. The calculated total shell porosity was confirmed by a voxel based volume approach (in Avizo fire, in 3D) that takes into account the total volume of pore and shell voxels.

Figure 6): Please rephrase "Cross plots showing cross plots". A): What this plot shows is a weak covariation of Mn with Fe, not that there is a link to diagenesis. This is an – admittedly well-founded – inference independent of this graph. C): This graph shows that there is no significant correlation of oxygen isotope ratios with Mn concentrations (p > 0.05). This contradicts the caption for this panel. In particular, most _18O values < -3 ‰ actually seem to be related to relatively low Mn (and Fe) concentrations.

We will rephrase the figure captions and better describe the trends shown in this figure. In addition, we will base our discussion of diagenesis in the records more on Figure 5, which shows the effect of local diagenesis on the records more clearly.

Figure 7: Axis title for y-axis of panel A should be "_47". Consider cutting the repetition of the symbol explanation in the caption for B) and state "Symbols as in A)".

We thank the referee for this suggestion and will implement it in the revised version.

Figure 8):

Line 1389: "Stack of proxy records for shell M0".

This will be corrected

Line 1402: A lot of the samples for which the Kim and O'Neil thermometer is employed yield results outside the calibration range (10-40_C). Consider opting for a different thermometer.

We will attempt a different thermometer to accommodate the samples with higher oxygen isotope values (lower temperatures).

Table 1: I do not understand how the average _47 value of 0.643 was calculated. The values given above should equate to _0.701.

Indeed it seems that this is an error in the table which will be corrected in the revised version of the manuscript.

References:

Anderson, T. F., and Arthur, M. A., 1983, Stable isotopes of oxygen and carbon and their application to sedimentologic and paleoenvironmental problems, in Arthur, M. A., Anderson, T. F., Kaplan, I.R., Veizer, J., and Land, L. S., eds., Stable isotopes in sedimentary geology: Society of Economic Paleontologists and Mineralogists Short Course 10, p. 1.1–1.151.

Cohen, K.M., Finney, S.C., Gibbard, P.L., Fan, J.-X., 2013, The ICS International Chronostratigraphic Chart. Episodes 36 (3), 199-204.

Coplen, T.B., 2007, Calibration of the calcite-water oxygen-isotope geothermometer at Devils Hole, Nevada, a natural laboratory. Geochimica et Cosmochimica Acta 71, 3948-3957.

Mouchi, V., de Rafélis, M., Lartaud, F., Fialin, M., Verrecchia, E., 2013, Chemical labelling of oyster shells used for time-calibrated high-resolution Mg/Ca ratios: A tool for estimation of past seasonal temperature variations. Palaeogeography, Palaeoclimatology, Palaeoecology 373, 66-74.

Pauley, G. B., Van Der Raay, B., Troutt, D., 1988, Species profiles: Life histories and environmental requirements of coastal fishes and invertebrates (Pacific Northwest)âˇAˇTPacific oyster, U.S. FishWildl. Serv. Biol. Rep. 82(11.85), U.S. Army Corps of Engineers, TR EL-82.4., Research and Development, National Wetlands Research Center, Washington, DC, 20240, 28 pp.

Ullmann, C.V., Wiechert, U., Korte, C., 2010, Oxygen isotope fluctuations in a modern North Sea oyster (Crassostrea gigas) compared with annual variations in seawater temperature: Implications for palaeoclimate studies. Chemical Geology 277, 160-166.

Ullmann, C.V., Böhm, F., Rickaby, R.E.M., Wiechert, U., Korte, C., 2013, The Giant Pacific Oyster (Crassostrea gigas) as a modern analog for fossil ostreoids: Isotopic (Ca, O, C) and elemental (Mg/Ca ,Sr/Ca, Mn/Ca) proxies. Geochemistry, Geophysics, Geosystems 14 (10), doi: 10.1002/ggge.20257.

Rimstidt, J.D., Balog, A., Webb, J., 1998. Distribution of trace elements between carbonate minerals and aqueous solutions. Geochimica et Cosmochimica Acta 62 (11), 1851-1863.
Wanamaker Jr, A.D., Kreutz, K.J., Wilson, T., Borns Jr, H.W., Introne, D.S., Feindel, S., 2008. Experimentally determined Mg/Ca and Sr/Ca ratios in juvenile bivalve calcite for Mytilus edulis: implications of paleotemperature reconstructions. Geo-Mar Lett 28, 359-368.

Wisshak, M., López Correa, M., Gofas, S., Salas, C., Taviani, M., Jakobsen, J., Freiwald, A., 2009, Shell architecture, element composition, and stable isotope signature of the giant deep-sea oyster Neopycnodonte zibrowii sp. N. from the NE Atlantic. Deep-Sea Research I 56, 374-407.

Anonymous Referee #2

The manuscript "An assessment of latest Cretaceous Pycnodonte vesicularis (Lamarck, 1806) shells as records for palaeoseasonality: A multi-proxy investigation" of de Winter and coauthors wants to assess the potential of shells of the bivalve Pycnodonte vesicularis as recorder of palaeoseasonality. They analyzed several specimens coming from the late Maastrichtian Neuquén Basin in Argentina, using different techniques to check the preservation of the shells (CT scanning, light microscopy, Micro- XRF and cathodoluminescence) and to reconstruct the palaeoclimatic and palaeoenvironmental variations recorded by the bivalve (stable isotope, trace

elements and clumped isotope analyses). They described in great details the methodology used and deeply discussed the advantages and disadvantages of the different methods. The authors discussed in a proper way their results making comparison with recent closely related genera and with data coming from the literature, providing a huge amount of new information.

Results are reported in great detail, which causes the manuscript to be very long and often not fluid, due to the wealth of information provided. I understand the need to document and discuss in details the trend observed; however, I think that shorten the manuscript would definitely improve the reading. Part of the method descriptions can be moved to the supplementary material, as well as parts of the comparison with other species should be reduced. Also, the discussion (6.4 temperature proxies) and the conclusions should be shortened, as many times they results in a repetition of the same concepts.

As mentioned above, we will take this major comment into account in our revision of the manuscript. We aim to shorten the manuscript text by moving parts of the methodology to the supplementary material and to shorten the discussion in the places suggested by Referee #2. The section about temperature proxies (6.4) will be rephrased following comments by Referee #1 and we will aim for a more concise discussion in this paragraph.

The manuscript address interesting scientific questions that are within the scope of Climate of the Past, so I recommend its publication after moderate revision.

Specific comments

A) Paragraph 4.1. According to Figure 1, it seems that only one level with Pycnodonte vesicularis is found in the section. The caption specifies that only the main Pycnodonte level is shown. From this, I understand that there are more levels with Pycnodonte but this is not adequately described and clarified in the text. The authors only said that Pycnodonte specimens were collected from the upper 5 m below the Cretaceous- Paleogene boundary. Were the seven specimens analyzed coming from different levels? Some of the differences the authors observed among the specimens may be due to the fact they did not live during the same time interval, thus not experiencing the same environmental oscillations. Also, it is worth to add something about the taphonomic condition of the specimens (e.g., articulated, disarticulated) and the associated fauna, if present.

As mentioned above, we will adapt paragraph 4.1 and Figure 1 according to the comments by Referee #2 and add information about the stratigraphic constraint on the shells and their state during collection. Furthermore, we will add some information about the abundance of *Pycnodonte* in these strata to Figure 1 to provide context to the discussion of the palaeoenvironment in which these animals lived.

B) Lines 436-437 and 449. A salinity decrease by fresh water input can also cause the low _18O and _13C values observed, lowering both the _18O and _13C values (fresh water is enriched in 16O and 12C) (Gillikin, 2005; Gillikin et al., 2006). The authors should add a sentence on this and better explain why they excluded the salinity effect. Lines 436-437, add a reference to: "Such a relationship between _18O and _13C has often been interpreted as a sign of diagenetic alteration."

Both Referees mention the role of salinity in their comments and we will discuss salinity changes in more detail in the revised discussion. We thank Referee #2 for the suggestions on how salinity changes may (partly) explain variations in stable isotope ratios in our records.

C) Paragraphs 6.3.1-6.3.3 (mainly lines 703-704). When comparing the isotope values of P. vesicularis with related species, the authors have to take in mind the different environmental settings in which the 3 species live (P. vesicularis, N. zibrowii and H. hyotis). As observed by the authors N. zibrowii lives in deep water, so its isotope signatures (especially the _18O values) are also controlled by this parameter. The higher _18O values recorded in N. zibrowii compared to P. vesicularis may be also explained with the deep sea habitat of the former species. So if they want to compare the isotope values, they have to consider species coming from similar environments.

See above, this is a valid comment and we will mostly restrict our discussion here to the comparison with *Hyotissa* while shortening the discussion of the comparison with *N. zibrowii*, see comment A) from Referee #2.

D) Lines 709-712. This sentence is strange; are you sure is the juvenile and not the adult part of the shells showing an ontogenetic trend in _13C? Usually bivalves incorporates isotopically light CO2 in the adult stages, showing an ontogenetic decrease in _13C (e.g., Gillikin, 2005; Gillikin et al., 2006, 2007). The model of Lorrain et al. (2004) suggests that the decrease in _13C through ontogeny is actually caused by increasing utilization of metabolic C (respiratory CO2 which is 13C-depleted) to satisfy carbon requirements for calcification. As bivalves grow and become older, the amount of available metabolic CO2 increases, while the amount needed for shell growth is reduced, resulting in more metabolic carbon (12C-enriched) being incorporated into the shell. A similar ontogenetic trend is observed in specimens M6 and M11. The authors should rewrite this part.

We thank Referee #2 for this comment which will allow us to better discuss carbon isotope ratios measured in our bivalve shells. We will apply the suggestions of the Referee to revise the concerning paragraph of the discussion and provide a better explanation of the stable carbon isotope records plotted in Figure 5 in terms of physiological changes. In addition, as mentioned above, we will limit the comparison with *N. zibrowii* because it is most likely not a very good modern analogue for *N. vesicularis*.

E) The authors provide a lot of data in the manuscript, analyzing in details the different methods used. I understand that the primary aim of the manuscript is to assess the potential of P. vesicularis shells as recorders of palaeoseasonality. However, the authors obtained some useful data for palaeoclimatic reconstructions which are not adequately discussed in the manuscript. How the data in terms of palaeotemperatures and palaeoseasonality fit into the larger context of the Cretaceous climate of the area? Which new information can they add to the knowledge of the late Cretaceous of the Neuquén basin?

In the current version of our manuscript, we deliberately kept the palaeoclimate interpretation of our shell records to a minimum, because of the many uncertainties discussed in the manuscript. Some of these uncertainties were picked up in a comment by Referee #1 about our interpretation of the various temperature proxies. We do not want to over-interpret our data sets, but we do agree that some palaeoclimatic context may be a good addition to the manuscript. In the revised version, we will therefore include a short paragraph at the end of the discussion in which tentative palaeoclimate reconstructions from *P. vesicularis* shells are placed in a broader context of palaeoclimate reconstructions in the late Cretaceous.

Minor comments

A) Be consistent through the manuscript on the use of English or American spelling (paleo -> palaeo, recrystallization, recrystallised, : : :)

We will scrutinize the text and correct inconsistencies in style.

B) When citing a paper within the manuscript use the same format. Some citations have comma before the year other not, e.g., Kiessling et al. 2005 (line 177) or Woelders et al., 2017 (line 182). Check carefully through the text.

This will be corrected

LINE 68-70 Bivalve shells are also important as they have a broad biogeographic distribution, occurring in different environmental settings, from shallow water to deep-sea environments, in freshwater, marine and brackish settings, from near the poles to the equator (e.g., Schöne et al., 2005a)

We thank Referee #2 for this addition and will implement it in the revised manuscript.

LINE 78 Add other references as Schöne et al., 2005b; Butler et al., 2013

These will be added

LINES 92-96 Add reference to Crippa et al., 2016

We will add this reference

LINE 111 ReconstructionS

This will be corrected

LINE 130 "The aim of this multi-approach is to characterize the MICROstructure". Refer also in other part of the text to microstructure and not structure, as you are observing shells at micrometrical scale

This will be corrected

LINE 196 "from the upper 5 m OF below the Cretaceous". Delete OF

This will be corrected

LINE 200 What do you mean by biodegradation? Please explain

We mean the extent to which the shells suffered from borings of predatory or parasitic organisms (e.g. sponges and polychaete worms). The sentence will be rephrased to clarify this.

LINE 242 It is not Figure 1, please correct

This should be Figure 2, we will change the reference

LINE 244 "See section 4.1.1 and 4.1.3". May it be section 5?

Indeed, this should refer to sections 5.1.1 and 5.1.3. We will change the references.

LINES 252 and 274 Gillikin et al., before Lorrain et al.

This will be corrected

LINE 257 Surge and Lohmann 2008 before Wanamaker et al. 2008

This will be corrected

LINE 294 Add space between 100 and _m

This will be corrected

LINE 345 Add reference to MacDonald et al., 2009

This reference will be added.

LINE 371 Diagenetic alteration instead of diagenesis

This will be corrected

LINES 384-385 and 476- 477 What about the CL of the vesicular layer? Add an image of this; if not in the main paper, add more images in the supplementary. It is important to document what you saw and described.

We will add more CL images in the supplementary data and add an appropriate image to Figure 3 to refer to in the text.

LINE 401 Delete space after record

This will be corrected

LINES 401-403 Rephrase this sentence

This sentence will be rephrased with reference to comments from both Referees.

LINE 405 "In three out of four specimens", delete OUT

This will be corrected

LINE 445 What does it mean from the same locality? Same stratigraphic level?

As mentioned above, we will add more detailed information on the stratigraphic context of the shells in a revised version of the manuscript.

LINE 446 Defliese et al., 2015; the year should be in parentheses

This will be corrected

LINES 471-474 Also, oystreids, due to their layered shell structure, may be more prone to infiltration of fluids inside the shells, which of course affected more the porous chalky fabric than the foliated ones.

Agreed, we will mention this in the text.

LINE 477 Laminae instead of lamina

This will be corrected

LINE 521 Measuring instead of measured

This will be corrected

LINE 566 "in vesicular calcite this close". Delete THIS

This will be corrected

LINE 596 ReconstructionS

This will be corrected

LINE 611 "vesicular calcite into the in the shell". Delete INTO THE

This will be corrected

LINE 651 Klein et al. before Ullmann et al.

This will be corrected

LINE 654 Delete "in the Late Cretaceous" at the end of the sentence; it is clear you are referring to the Late Cretaceous

This will be corrected

LINE 662 Hyotissa not Hytissa; add the name of the author who first describe the species

This will be corrected

LINE 683 "which complicates interpretation"; it should be "which complicates THE interpretation" or "which complicates interpretationS"

This will be corrected

LINE 693, 704 and other lines Wisshak et al., 2008, in the reference list is Wisshak et al., 2009

We will thoroughly check the citations and reference list in the revised version of the manuscript.

LINE 705 Titschack et al., 2010 before Ullmann et al., 2010

This will be corrected

LINE 731 Evaporitic setting

This will be corrected

LINE 732 Specify in which country Safaga Bay is

This will be corrected

LINE 732 Add + before 2.17 ‰

This will be corrected

LINE 734 "records OF H. hyotis". Add OF

This will be corrected

LINE 745 "a decrease in salinity in the spring". Delete THE

This will be corrected

LINE 781-782 It seems strange that during high productivity spring they growth slower, they should do the opposite. Is there any evidence in previous literature on this?

A similar point was made by Referee #2 and we will revise this part of the discussion, taking into account the comments from both referees, to better discuss the observed proxy relationships. We acknowledge that the discussion of the phase relationships between proxies may not be clear at this point. We hope that a revision and shortening of this part of the discussion will make the rationale easier to follow.

LINE 783 Gillikin et al., 2005 before Lorrain et al., 2005

This will be corrected

LINE 796 Such a decrease of nearly 10_C between surface and relatively deep sea water is comparable to present day situation?

We do not wish to argue that this depth temperature profile can explain the full temperature offset (see next line)..

LINE 801 "d18O", change with _18O

This will be corrected

LINE 806-808 During the spring-summer seasons the authors reported a salinity decrease; slow growth may be caused by this?

We thank Referee #2 for this suggestion and will implement it in a revision of the discussion. This decrease in salinity may indeed cause stress to the bivalve and diminish the growth rate, explaining the observed phase relationships between proxies.

LINE 815 "than parts of the year". Add OTHER parts of the year

This will be corrected

LINE 847 How was 20 PSU determined? It is a very big variations. For example in the Mediterranean Sea a salinity change of 2 PSU would correspond to a shift of _1‰ in _18Osw (Rohling and Bigg, 1998), which is equivalent to nearly 4-5_C in the temperatures calculated from the _18O of the shell. The authors observed a 10_C variation, which correspond to _2-3‰ in _18O. The salinity 20 PSU value seems overestimated. The authors should better explain this assertion

As mentioned above, we will discuss salinity changes in a more relative sense in the revised version of our manuscript. We realize that this conversion of d18O to psu values is unconventional and not well founded. We will refrain from any quantitative attempt to reconstruct salinity in the revised version, because we cannot constrain all the variables needed for this reconstruction.

LINE 869 10-15 _C at which water depth?

These are surface water temperatures. This will be clearly indicated in the text.

LINE 909 reconstructionS

This will be corrected

LINE 911 vesicular instead of vesulicar

This will be corrected

Reference list Please check very carefully the reference list. Some data are missing (pages), many specific names are not in italic, some references are in wrong chronological order, some present in the list are missing in the main text and viceversa. Some of the changes to make are listed hereafter:

The reference list will be thoroughly checked in a revised version and the helpful comments on the formatting and completeness of the references posed by both reviewers will be taken into account.

Figures

FIGURE 1 Is it possible to add a legend with the lithologies? Also, in the y-axis of the log correct BOUNDARY

This will be corrected, we will add a legend for the lithologies

FIGURE 2 To be more clear the direction of growth of the shell should be added.

The red arrow in this figure indicates the direction of growth. This will be explicitly mentioned in the caption.

FIGURE 3 Images C-G and H, I should be a bit larger. Images C and E are not very clear.

The figure will be edited according to these suggestions by making the microscope images larger and improving the figure caption.

FIGURES 5 and 9 Vertical bars have too similar colors (orange and red), change one to be more clear.

The figure will be edited according to these suggestions

FIGURE 6 Cross plots showing cross plots, please rephrase.

The figure caption will be edited according to these suggestions

FIGURE 8 "interpretation of annual cyclicity based on Sr/Ca ratios" and on _18O seasonality?

We will add this to the caption of the figure.

References

Butler, P.G., Wanamaker Jr., A.D., Scourse, J.D., Richardson, C.A. & Reynolds, D.J. (2011), Longterm stability of 13C with respect to biological age in the aragonite shell of mature specimens of the bivalve mollusk Arctica islandica, Palaeogeography, Palaeoclimatology, Palaeoecology, 302(1), 21-30.

Crippa G., Angiolini L., Bottini C., Erba E., Felletti F., Frigerio C., Hennissen J.A.I., Leng M.J., Petrizzo M.R., Raffi I., Raineri G., Stephenson M.H. (2016). Seasonality fluctuations recorded in fossil bivalves during the early Pleistocene: Implications for climate change. Palaeogeogr. Palaeoclimatol. Palaeoecol., 446, 234–251.

Gillikin, D.P. (2005), Geochemistry of Marine Bivalve Shells: the potential for paleoenvironmental reconstruction. Unpublished PhD thesis, Bruxelles University.

Gillikin, D.P., Lorrain, A., Bouillon, S., Willenz, P. & Dehairs, F. (2006), Stable carbon isotope composition of Mytilus edulis shells: Relation to metabolism, salinity, _13CDIC, and phytoplankton, J. Organic Geochemistry, 37, 1371–1382.

Gillikin, D.P., Lorrain, A., Meng, L. & Dehairs, F. (2007), A large metabolic carbon contribution to the _13C record in marine aragonitic bivalve shells, Geochimica et Cosmochimica Acta, 71, 2936–2946.

Lorrain, A., Paulet, Y.M., Chauvaud, L., Dunbar, R., Mucciarone, D. & Fontugne, M. (2004), _13C variation in scallop shells: increasing metabolic carbon contribution with body size?, Geochimica et Cosmochimica Acta, 68, 3509–3519.

MacDonald, J., Freer, A., & Cusack, M. (2009). Alignment of crystallographic c-axis throughout the four distinct microstructural layers of the oyster Crassostrea gigas. Crystal Growth & Design, 10(3), 1243-1246.

Rohling, E.J., Bigg, G.R. (1998). Paleosalinity and _18O: a critical assessment. J. Geophys. Res. Oceans 103 (C1), 1307–1318.

Schöne, B.R., Fiebig, J., Pfeiffer, M., Gle_, R., Hickson, J., Johnson, A.L.A., Dreyer, W. & Oschmann, W. (2005a), Climate records from a bivalved Methuselah (Arctica islandica, Mollusca; Iceland), Palaeogeography, Palaeoclimatology, Palaeoecology, 228(1), 130-148.

Schöne, B.R., Pfeiffer, M., Pohlmann, T. & Siegismund, F. (2005b), A seasonally resolved bottom water temperature record for the period of AD 1866–2002 based on shells of Arctica islandica (Mollusca, North Sea), Int. J. Climatol., 25, 947–962

1 **An assessment of latest Cretaceous *Pycnodonte vesicularis* (Lamarck, 1806) shells as records for**
2 **palaeoseasonality: A multi-proxy investigation**

3 de Winter, Niels J.*[1], Vellekoop, Johan*[1,2], Vorsselmans, Robin[2], Golreihan, Asefeh[2], Soete, Jeroen[2],
4 Petersen, Sierra V.[3], Meyer, Kyle W.[3], Casadio, Silvio[4], Speijer, Robert P.[2], Claeys, Philippe[1]

5 [1]*Analytical, Environmental and Geo-Chemistry (AMGC), Vrije Universiteit Brussel (VUB), Brussels,*
6 *Belgium.*
7 [2]*Department of Earth and Environmental Science, KU Leuven, Heverlee, Belgium*
8 [3]*Earth and Environmental Sciences Department, University of Michigan, Ann Arbor, Michigan, USA.*
9 [4] *Escuela de Geología, Paleontología y Enseñanza de las Ciencias, Universidad Nacional de Río Negro,*
10 *CONICET, General Roca, Argentina.*

12 *Niels J. de Winter and Johan Vellekoop contributed equally to this work

14 Corresponding author: niels.de.winter@vub.be

16 Target journal: Climate of the Past

18 **Abstract**

19 In order to assess the potential of the honeycomb oyster *Pycnodonte vesicularis* for the
20 reconstruction of palaeoseasonality, several specimens recovered from ~~the~~ late Maastrichtian strata
21 in the Neuquén Basin (Argentina) were subject to a multi-proxy investigation, involving scanning
22 techniques, trace element and isotopic analysis. Combined CT scanning and light microscopy reveals
23 two ~~major~~ calcite ~~micromorphologies~~microstructures in *P. vesicularis* shells (vesicular and foliated
24 calcite). Micro-XRF analysis and cathodoluminescence microscopy show that reducing pore fluids
25 were able to migrate through the vesicular portions of the shells (aided by bore holes) and cause
26 recrystallization ~~and precipitation of secondary carbonate in the porous micromorphology, thus~~
27 ~~rendering~~of the vesicular calcite. This renders the vesicular portions not suitable for
28 palaeoenvironmental reconstruction. In contrast, stable isotope and trace element compositions
29 show that the original chemical composition of the ~~shell~~foliated calcite is well-preserved ~~in the~~
30 ~~denser, foliated portions, which~~and can ~~therefore~~ be ~~reliably~~ used for the reconstruction of
31 palaeoenvironmental conditions. Stable oxygen and clumped isotope thermometry on carbonate
32 from the dense hinge ~~region~~of the shell yield sea water temperatures of 11°C, while previous TEX_{86}^H
33 palaeothermometry yielded much higher temperatures. The difference is ascribed to seasonal bias
34 in the growth of *P. vesicularis*, causing warm seasons to be underrepresented from the record, ~~and~~
35 ~~TEX₈₆ᴴ palaeothermometry being potentially biased towards warmer surface water temperatures.~~
36 ~~Superimposed on this annual mean is a seasonality in δ¹⁸O of about 1‰, which is ascribed to a~~
37 ~~combination of varying salinity due to fresh-water input in the winter and spring season and a~~
38 ~~moderate temperature seasonality.~~ while TEX_{86}^H palaeothermometry seems to be biased towards
39 warmer surface water temperatures. ~~Attempts to independently verify the seasonality in sea water~~
40 ~~temperature by Mg/Ca ratios of shell calcite are hampered by significant uncertainty due to the lack~~
41 ~~of proper transfer functions for pycnodontein oysters.~~ The multi-proxy approach employed here
42 enables us to differentiate between well-preserved and diagenetically altered portions of the shells

43 and provides an improved methodology for reconstructing palaeoenvironmental conditions in deep
44 time. While establishing a chronology for these shells was ~~severely~~ complicated by growth cessations
45 and diagenesis, cyclicity in trace elements and stable isotopes allowed for a tentative interpretation
46 of the ~~potential annual~~ seasonal cycle in ~~the~~ late Maastrichtian palaeoenvironment of the Neuquén
47 basin. Attempts to independently verify the seasonality in sea water temperature by Mg/Ca ratios of
48 shell calcite are hampered by significant uncertainty due to the lack of proper transfer functions for
49 pycnodontein oysters. Future studies of fossil ostreid bivalves should target dense foliated calcite
50 rather than sampling bulk or vesicular calcite. Successful application of clumped isotope
51 thermometry on fossil bivalve calcite in this study indicates that temperature seasonality in fossil
52 ostreid bivalves may be constrained by the sequential analysis of well-preserved foliated calcite
53 samples using this method.

54

55 **1. Introduction**

56 The Late Cretaceous is generally considered a greenhouse world (e.g. Hay, 2008). Indeed,
57 reconstructed global mean temperatures and atmospheric pCO_2 concentrations for this period
58 generally exceed those of the present-day climate (e.g., Berner, 1990; Andrews et al., 1995; Ekart et
59 al., 1999; Hunter et al., 2008; Quan et al., 2009; Wang et al., 2013). As such, the Late Cretaceous
60 may be considered an analogue for climate ~~in~~of the near future if anthropogenic greenhouse gas
61 emissions continue unabated (Hay, 2013; IPCC, 2014; ~~Hay, 2013;~~ Dlugokencky, 2017). Many studies
62 have yielded reconstructions of Late Cretaceous climates using either climate models or a variety of
63 proxies in temporally long archives, such as deep-sea cores and continental sections (Pearson et al.,
64 2001; Huber et al., 2002; Otto-Bliesner et al., 2002; Miller et al., 2003; Friedrich et al., 2012; de
65 Winter et al., 2014; Vellekoop et al., 2016). Yet, although most deep-time climate reconstructions so
66 far have focused on reconstructing mean annual temperatures (MAT), climate change also involves
67 changes in other climate parameters, such as precipitation, seasonality and the frequency of
68 extreme weather events, which all take place on timescales shorter than those that can be resolved
69 in the above mentioned long archives. Therefore, it is important that these climate variations are
70 understood on a shorter timescale.

71 One way to achieve such high-resolution palaeoclimate and palaeoenvironmental reconstructions is
72 by using marine organisms that ~~form~~grow their shells ~~that grow~~ incrementally. Marine ~~bivalve shells~~
73 bivalves are excellent palaeoclimate recorders, ~~and the~~ since they have a broad geographic
74 distribution and because the rapid secretion of their shells allows for the high time resolution
75 needed to resolve climate parameters on a sub-annual scale (e.g. Jones, 1983; Dettman and
76 Lohmann, 1993; Steuber, 1996; Schöne et al., 2005a;b). The relationship between ~~their~~ shell
77 chemistry and the environmental conditions in which ~~they~~bivalves grow has been studied intensively
78 (~~Jones, 1983; Dettman and Lohmann, 1993; Steuber, 1996;~~Gillikin et al., 2005a; Elliot et al., 2009~~.~~
79 ~~Many~~; Marali and Schöne, 2015). As a result, many geochemical proxies have been described based
80 on bivalve calcite. Examples include temperature calibrations for Mg/Ca and stable oxygen isotope
81 ratios ($\delta^{18}O$; e.g. Klein et al., 1996a; Richardson et al., 2004; Freitas et al., 2008; Wanamaker et al.,
82 2008), tentative salinity calibrations using Sr/Ca and the combination of Mg/Ca and $\delta^{18}O$ (Dodd and
83 Crisp, 1982; Klein et al., 1996a; Watanabe et al., 2001) and proxies for palaeoproductivity, such as
84 Ba/Ca and Mn/Ca (Lazareth et al., 2003; Gillikin et al., 2008).

85 Despite their potential for high-resolution palaeoenvironmental reconstruction, seasonally resolved
86 bivalve records ~~feature~~ rarely ~~in long~~combined with longer timescale reconstructions (e.g. Steuber~~,~~
87 et al., 2005; Schöne et al., 2005c; Harzhauser et al., 2011; Butler et al., 2013; Hallmann et al., 2013).

88 A ~~caveat in the use~~disadvantage of using bivalve records for long-term palaeoclimate

89 reconstructions is the potential problems that arise when using multiple bivalve species for

90 palaeoclimate reconstruction (Gillikin et al., 2005a; b; de Winter et al., 2017a). Culture experiments

91 in extant bivalve species have shown that palaeoenvironmental proxies in bivalve calcite may be

92 affected by ~~internal~~ mechanisms that are independent of the environment of the animal and are

93 controlled by parameters such as growth, reproductive cycle and metabolism (the so-called "vital

94 effects"; Dunbar and Wefer, 1984; Weiner and Dove, 2003; Gillikin et al., 2005b; Lorrain et al., 2005;

95 Carré et al., 2005). ~~Such internal factors~~These vital effects are often species-specific and limit the

96 applicability of proxy transfer functions from modern culture studies to multiple species in the same

97 study or ~~on~~to species for which no culture study data is available. The integration of different species

98 of bivalves in palaeoclimate studies is further complicated by the various ecological niches these

99 species of bivalves occupy, ~~which results~~resulting in great variability ~~between~~in their direct

100 environments (Chauvaud et al., 2005; Dreier et al., 2014). In addition, bivalves are ~~mostly restricted~~

101 ~~to~~often, though not exclusively, found in shallow marine and estuarine environments. This further

102 complicates the interpretation of bivalve records in terms of global climate (e.g. Surge et al~~.~~., 2001,

103 Richardson et al., 2004; Gillikin et al., 2008; Wisshak et al., 2009; Ullmann et al., 2010; Crippa et al.,

104 2016), as these environments are often characterized by large variations in temperature, salinity and

105 water chemistry, ~~which makes~~making it hard to disentangle the effect~~s~~ of different environmental

106 parameters on geochemical proxies (e.g. Duinker et al., 1982; Morrison et al., 1998; Pennington et

107 al., 2000).

108 The above-mentioned problem of combining different high-resolution climate records to study

109 climatic variations on a geological timescale can be overcome by combining results from multiple

110 well-preserved bivalve specimens of the same species and in the same geological setting. Several

111 studies have tried such a multi-specimen approach to trace changes in high-resolution climate

112 parameters, such as seasonal variations, over geological timescales (Dettman and Lohmann, 2000;

113 Dettman et al., 2001; Steuber~~,~~ et al., 2005; Gutiérrez-Zugasti et al., 2016). However, such

114 reconstructions require bivalve species that preserve well, are geographically widespread, have a

115 high occurrence frequency over longer timescales and record seasonal-scale variations within their

116 shell.

117 Potential candidate species for such studies are bivalves of the genus *Pycnodonte*. This genus of

118 oysters (Bivalvia: Ostreoida; Fis~~c~~her von Waldheim, 1835) is characterized by a well-developed

119 commissural shelf and ~~a~~ vesicular shell microstructure (hence the name "honeycomb oyster" or

120 "foam oyster"; Stenzel, 1971; Hayami and Kase, 1992). Members of the genus *Pycnodonte* are found

121 in geological deposits from the Lower Cretaceous to the Pleistocene. The appearance of *Pycnodonte*

122 shells in a wide range of palaeolatitudes and geological settings, especially in the Cretaceous, makes

123 them a promising archive for high-resolution climate reconstruction~~s~~ (Ayyasami, 2006; Fossilworks,

124 2017). As mentioned in Titschak et al. (2010), records from large and long-living bivalves, such as

125 *Pycnodonte*, provide several advantages in comparison with other seasonality archives. They are

126 slow-growing~~, reducing~~ in comparison to other ostreid taxa, have rather limited kinetic effects and

127 disequilibrium fractionation of stable isotopes (McConnaughey 1989; Abele et al., 2009). In addition,

128 *Pycnodonte* bivalves likely did not have symbionts, in contrast to, for example, ~~T~~tridacnid bivalves

129 (Elliot et al., 2009). This means that *Pycnodonte* bivalves take up nutrients and other elements

130 directly from their environment, simplifying the interpretation of their shell composition. Their low-

131 Mg calcite shells are less prone to diagenetic alteration than shells made of aragonite or high-Mg

132 calcite (Al-~~A~~aa~~s~~m and Veizer, 1986; Pirrie and Marshall, 1990), and their sedentary life mode ensures

133 that they fossilize in life position. The latter enables the integration of environmental information

134 extracted from the sediments in which they are fossilized into the discussion of their shell chemistry.

135   The species *Pycnodonte vesicularis* (Lamarck, 1806) is one of the most common and long-ranging

136   species of *Pycnodonte.* Therefore, in this study the potential for *P. vesicularis* to be used as a record

137   for sub-annual environmental variability in the Late Cretaceous is explored. The present study

138   focuses on the characteristics of fossil specimens of *P. vesicularis* from the upper Maastrichtian

139   Jagüel Formation of the Bajada de Jagüel section, Argentina (**Figure 1A**). A range of qualitative, semi-

140   quantitative and quantitative methods ~~are~~is applied to investigate the nature of the *P. vesicularis*

141   shell material, shell morphology and its preservation state. The aim of this multi-proxy approach is to

142   characterize the microstructure and chemical composition of the *P. vesicularis* shell and its

143   ontogenetic development ~~through the lifetime of the animal~~ and to assess its potential as a recorder

144   of palaeoseasonality.

145

146   **2. The species *Pycnodonte vesicularis***

147   *Pycnodonte vesicularis* was reclining and inhabited muddy bottoms on the shallow marine shelf with

148   a low sedimentation rate (e.g. Brezina et al., 2014). ~~The individual variability is very extensive in~~

149   Individual valves of *P. vesicularis*~~, involving, among others, the~~ vary considerably in dimension,

150   outline~~ of valves, their~~, convexity, ~~the~~wall thickness~~ of the walls, the dimensions, the~~, muscle scar

151   position, deepness~~, shape~~ and ~~position of the adductor muscle scar~~shape, as well as the

152   characteristics of chomata (Pugaczewska, 1977; Brezina et al., 2014). This variability depends on the

153   age of the individual and ~~on~~local environmental conditions, especially ~~on the character and grain~~

154   ~~size of~~ the substrate. According to Berzina et al. (2014), about one third of *P. vesicularis* valves at

155   Bajada de Jagüel are mature (gerontic) specimens, characterized by relatively thick valves (>10mm)

156   with a well-developed vesicular layer. Given their longer life span, ~~such~~ mature specimens of *P.*

157   *vesicularis* were considered most suitable for the present investigation.

158   In the past, several studies have ~~made an attempt~~attempted to calculate the age of individuals of *P.*

159   *vesicularis* based on the number of laminae in the complex of lamellar and vesicular layers (Nestler,

160   1965), or the number of growth lines ~~of~~in the ligament (Müller, 1970). Yet, so far no studies have

161   investigated the potential of *P. vesicularis* shells as palaeoseasonality records based on their

162   geochemical signature. ~~Given the species-specific relationships between environmental parameters~~

163   ~~and bivalve shell geochemistry, in an ideal situation, a culture experiment would be used to~~

164   ~~determine these relationships for *Pycnodonte* bivalves. Unfortunately, no extant species of the~~

165   ~~genus~~Unfortunately, no extant species of *Pycnodonte* are known, rendering culture experiments for

166   these species impossible. However, two species of the closely related ~~pycnodontein genus~~

167   *Neopycnodonte* (Stenzel, 1971) are found in deep-sea habitats today (*Neopycnodonte conchlear*,

168   Poli, 1795, and *Neopycnodonte zibrowii*; Videt, 2004; Wisshak et al., 2009), whereas the extant

169   pycnodontein genus *Hyotissa* is characterized by a shallow-marine distribution (Titschack et al.,

170   2010). Detailed studies of the shell morphology and chemical composition of *N. zibrowii* and

171   *Hyotissa hyotis* ~~a~~were reported in Wisshak et al., (2009) and Titschak et al., (2010), respectively, and

172   ~~can be~~are used as a basis for comparison of the *Pycnodonte* oyster shells.

173

174   **3. Geological Background**

175   **3.1 Paleogeographical context**

176   The studied specimens were collected from the Bajada de Jagüel (BJ) section (38°06'10.5"S,

177   68°23'20.5"W). The site is situated in the Neuquén Basin in Argentina~~. The Neuquén Basin~~, which is

4

178   bordered to the south by the North Patagonian massif and to the northeast by the Sierra Pintada
179   massif (**Figure 1B and 1C**). The Bajada de Jagüel section has a palaeolatitude of ~43˚S ± 2˚ relative to
180   the palaeomagnetic reference frame of Torsvik et al. (2012) according to palaeolatitude.org (van
181   Hinsbergen et al., 2015). A large transgression from the South Atlantic into the basin (Bertels, 2013)
182   occurred from the late Maastrichtian to early Danian, during a time of relative tectonic quiescence
183   and low magmatic activity (Malumian et al., 2011).

3.2 Palaeoenvironment

185   The Maastrichtian mudstones of the Jagüel Fm. are homogeneous and intensely bioturbated,
186   indicating a well-oxygenated seafloor, with palaeodepths of approximately 50-75 m (Scasso et al.,
187   2005; Woelders et al., 2017; see also **Figure 1**). A coarse-grained, mottled, clayey sandstone bed, 15-
188   25 cm thick, separates the Maastrichtian and Danian mudstones. This sandstone bed represents the
189   K-Pg boundary and is ~~interpreted~~thought to have resulted from a tsunami wave, related to the
190   Chicxulub impact event (Scasso et al., 2005). During the late Maastrichtian and early Danian, North
191   and Central Patagonia experienced a warm, humid climate. Pollen records suggest rainforests,
192   coastal mangrove forests and swamp communities in the region (Baldoni, 1992; Kiessling et al.,
193   2005; Barreda and Palazzesi, 2007; Iglesias et al., 2007; Palazzesi and Barreda, 2007). This
194   vegetation type is classified as megathermal and indicates average air temperature of 24°C or higher
195   (Barreda and Palazzesi, 2007; Palazzesi and Barreda, 2007; Barreda et al., 2012). Average annual sea
196   surface temperatures are estimated to have been 26-29°C in the latest Maastrichtian at Bajada de
197   Jagüel, based on TEX_{86}^{H}-palaeothermometry (Woelders et al., 2017; **Figure 1D**). An average of these
198   TEX_{86}^{H}-temperatures weighted to the stratigraphic abundance of *P. vesicularis* (Aberhan and
199   Kiessling, 2014) yields a temperature of 27.3°C ± 2.5°C for the environment of *P. vesicularis* in the
200   Bajada de Jagüel formation (see **suppl_Weighted_TEX**). While hypersaline conditions have been
201   inferred for the northernmost part of the Neuquén Basin, the central part of the Neuquén Basin,
202   where the BJ site is located, is suggested to have experienced more normal marine conditions. The
203   latter is evidenced by the presence of planktic foraminifera, dinocysts and relatively few terrestrial
204   palynomorphs (Prámparo et al., 1996; Prámparo and Papú 2006; Woelders et al., 2017). Yet,
205   Woelders et al. (2017) inferred enhanced runoff and stratification of the water column at the Bajada
206   de Jagüel site during the late Maastrichtian warming (450-150 kyr before the K-Pg boundary). Hence,
207   salinity may have deviated from normal marine during the lifetime of the *Pycnodonte* specimens
208   studied here.

4. Materials and methods

4.1 Sample acquisition and preparation

212   Seven specimens of *Pycnodonte vesicularis* were collected from the upper Maastrichtian Jagüel
213   Formation in the Bajada de Jagüel section (**Figure 1**), labelled "M0", "M4", "M5", "M6", "M8",
214   "M10" and "M11". All shells were collected from the upper 5m of below the Cretaceous-Palaeogene
215   boundary (see **Figure 1**). The abundance of *Pycnodonte* in these strata, based on the data of
216   Aberhan and Kiessling (2014), is indicated in **Figure 1**. There is a *Pycnodonte*-bed approximately 50
217   cm below the K-Pg boundary, which is the likely source of most of the specimens. Yet, the specimens
218   studied here were collected as surface finds, so downhill transport cannot be excluded with
219   certainty. Therefore, a more precise stratigraphic position cannot be provided. For associated fauna,
220   see Aberhan et al. (2007), Aberhan and Kiessling (2014) and Woelders et al. (2017).

Commented [NdW1]: Add abundance-weighed average of TEX values

5

221 Four of these specimens ("M0", "M4", "M6" and "M11", see **Figure 2**) represent completely
222 preserved left valves of mature specimens of *P. vesicularis* (c.f. Pugaczewska, 1977), while the
223 remaining three ("M5", "M8" and "M10") were incomplete. Specimens were selected that differ
224 from each other in morphology, body size and extent of biodegradation~~,~~ (e.g. bore holes), to assess
225 both the potentials and possible pitfalls of this taxon as a palaeoseasonality recorder. The four
226 complete shells were cleaned and cast into Araldite® 2020 epoxy resin (Araldite, Basel, Switzerland)
227 before being cut along the major growth axis of the shell using a slow rotating rotary saw (Ø 1 mm).
228 A parallel slab was cut out of one half of the shell, while the other half was preserved (archive half).
229 The resulting thick section, with a typical thickness of 4 mm, was polished using a series of
230 progressively higher-grade silicon carbide polishing disks (up to P2400) to allow a smooth surface for
231 sampling and imaging. The ~~remaining~~ three incomplete shells were left untreated and were only
232 used for bulk analysis.

4.2 Colour scanning and microscopy

234 Polished surfaces of shell sections were colour-scanned at 6400 dpi ~~resolution~~ (~4 μm resolution)
235 using an Epson 1850 flatbed scanner. Shell microstructures were studied and imaged at 50x
236 magnification using an Olympus BX60 optical microscope (KU Leuven, Belgium). In order to study the
237 preservation of pristine calcite in ~~the~~ *P. vesicularis* ~~shells~~, shell slabs were studied using
238 cathodoluminescence microscopy using a Technosyn Cold Cathodoluminescence model 8200, mark
239 II microscope operated at 16-20 kV electron gun potential, 420 μA beam current, 0.05 Torr (6.6 * 10^{-5}
240 bar) vacuum and 5 mm beam width (KU Leuven, Belgium). Cathodoluminescence (CL) refers to the
241 emission of light from material during excitation by an electron beam. The wavelength (i.e. colour)
242 of the emitted light depends on the crystal lattice structure and on activators, i.e. light emitting
243 centres constituted by chemical elements or crystal defects. CL microscopic observations of the shell
244 sections thus enable the recognition of crystal defects and ~~to evaluate~~evaluation of the preservation
245 state of the ~~samples~~shells (e.g. overgrowth, recrystallisation, dissolution~~). They allow to assess to~~
246 ~~what extent the~~), and is used to evaluate whether obtained element concentrations and isotopic
247 ratios reflect the original shell signature (Barbin, 2000).

4.3 Porosity and trace element analysis

249 In order to visualize shell microstructure and the pore network, high-resolution 3D micro-
250 tomography analysis was carried out on the archive half of *Pycnodonte* specimens using a General
251 Electric Nanotom microCT X-Ray CT scanner (KU Leuven, Belgium). One ~~entire~~half shell ~~halve~~ was
252 scanned at a 30 μm spatial resolution while representative shell pieces of interest were scanned at
253 1.5 μm resolution. The CT images were segmented in Matlab by applying a dual thresholding
254 algorithm. The shell porosity was rendered in 3D and labelled in Avizo Fire 7.0. Pore parameters
255 were calculated in Avizo and Matlab~~.~~ (see **SI_CT_scanning** for details). Micro-XRF measurements
256 were carried out using a Bruker M4 Tornado micro-XRF scanner ~~at the XRF platform of the Analytical,~~
257 ~~Environmental and Geochemistry group at the Vrije Universiteit Brussel (~~(AMGC, VUB, Brussels,
258 Belgium). Details on the setup and methodology of the M4 Tornado μXRF scanner can be found in de
259 Winter and Claeys (2016~~). μXRF mapping was done using the M4 Tornado's Rh-anode X-Ray tube~~
260 ~~under maximum source energy settings (50kV, 600 μA) using two silicon drift detectors, a spatial~~
261 ~~pixel resolution of 50 μm and an integration time of 1 ms per pixel. μXRF line scans of the hinges of~~
262 ~~shells M0, M4, M6 and M11 were measured on the M4 Tornado in point-by-point mode (see~~), de
263 Winter et al~~., 2017a)~~ using maximum source energy settings (50kV, 600 μA), a spot size of 25 μm, a
264 ~~spatial sampling resolution of 50 μm and an integration time per point of 60 seconds (1085~~
265 ~~measurements in total). This measurement strategy allowed XRF spectra to accumulate enough~~
266 ~~counts to reach the Time of Stable Reproducibility and Accuracy (de Winter et al.,~~. (2017b~~). Line~~

267 ~~scans were carried out in growth direction on polished cross sections through the hinge of the four~~
268 ~~*P. vesicularis* shells (see **Figure 1**).~~) and in **suppl_XRF_IRMS**. Care was taken to limit sampling to the
269 dense calcite in the hinge of the shells, though observations of the microstructure of the shell hinge
270 show that incorporation of vesicular calcite into the profile could not ~~always~~ be fully avoided (see
271 section 4~~5~~.1.1 and 4~~5~~.1.3).

272 **4.4 Trace elements in bivalves**

273 The use of trace element concentrations in fossil bivalve shells as a means of reconstructing
274 palaeoenvironmental conditions is subject to ongoing debate. As ~~briefly~~ mentioned above, some
275 tentative calibrations have been made that link trace element ratios in shell carbonate to
276 environmental conditions in modern bivalves (e.g. Jones ~~et al.,~~ 1980; Klein et al., 1996a; Freitas et
277 al., 2005; Wanamaker et al., 2008). However, the degree by which the incorporation of these trace
278 element concentrations is controlled by the ~~shell's~~ environment of the bivalve, as opposed to
279 ~~internal mechanisms (~~vital effects~~)~~, is often uncertain (e.g. Weiner and Dove, 2003; ~~Lorrain et al.,~~
280 ~~2005;~~ Gillikin et al., 2005b~~)~~; Lorrain et al., 2005). An example ~~of this~~ is the Mg/Ca ratio, which is
281 ~~widely~~ thought to reflect the calcification temperature of the shell (e.g. Klein et al., 1996a). While
282 the Mg/Ca palaeothermometer is commonly applied in foraminifera studies (e.g. Ederfield and
283 Ganssen, 2000; Lear et al., 2000), calibrations of this proxy for different bivalve taxa vary widely
284 (Klein et al., 1996a; Vander Putten et al., 2000; Takesue and van Geen, 2004; Freitas et al., 2005;
285 ~~Wanamaker et al., 2008;~~ Surge and Lohmann, 2008; Wanamaker et al., 2008; Mouchi et al., 2013;
286 see also de Winter et al., 2017a). Even Mg/Ca calibration curves for oyster species within the same
287 genus (*Crassostrea virginica* ~~and *Crassostrea gigas*;~~in Surge and Lohmann~~,~~ (2008) and *Crassostrea*
288 *gigas* in Mouchi et al~~.,~~. (2013~~, respectively~~) yield very different results, illustrating that the
289 temperature dependence of Mg/Ca ratios in bivalve calcite is not straightforward. ~~Furthermore, it~~
290 ~~has been shown that the incorporation of Mg (and other trace elements, such as Sr and Mn) into~~
291 ~~bivalve shells does not happen in equilibrium with ambient concentrations (Weiner and Dove, 2003).~~
292 Relationships of bivalve Mg/Ca ratios with temperature are ~~also~~ known to break down during
293 periods of growth stress (Lorens and Bender, 1980; Weiner and Dove, 2003; Takesue and van Geen,
294 2004). ~~Some~~Part of the Mg in bivalve shells is associated with organic molecules in the matrix in the
295 shell rather than being substituted for Ca in the crystals of bivalve calcite (Lorens and Bender, 1980).
296 ~~Hence~~In addition, factors determining ~~elemental~~ incorporation of Mg in bivalve carbonate are partly
297 controlled by physiological processes and are therefore species or even specimen specific (e.g.
298 Freitas et al., 2006; 2008).
299
300 Another commonly reported ratio, that of Sr/Ca, has ~~yielded good correlations with water~~
301 ~~temperature for some bivalve taxa (e.g.~~ been demonstrated to co-vary~~Freitas et al., 2005), while~~
302 ~~others have shown that it strongly covaries~~ with changes in growth and metabolic rate in ~~a range~~
303 ~~of~~some taxa (Klein et al., 1996b; ~~Lorrain et al., 2005;~~ Gillikin et al., 2005b; Lorrain et al., 2005).
304 However, a few studies have shown a positive correlation with water temperature in other species
305 (e.g. Freitas et al., ~~)~~2005; Wanamaker et al., 2008). These results are somewhat counterintuitive
306 since the partition coefficient of Sr into calcite is negatively correlated with temperature (Rimstidt et
307 al., 1998). The above shows that the extent of vital effects is highly taxon-specific and that
308 palaeoclimate reconstructions based on trace element records in bivalve shells need to be
309 interpreted with great care.
310 Beside~~s~~ sea water temperature, attempts have been made to reconstruct other environmental
311 parameters, such as redox conditions and palaeoproductivity, based on trace element records in
312 bivalves. Examples of such proxies include elements that are enriched in skeletons of primary
313 producers such as Ba (Gillikin et al., 2008; Marali et al., 2017), redox-sensitive elements like Mn
314 (Freitas et al., 2006) and micronutrients such as Zn and Cd, which are known to be taken up into
315 bivalve shells and whose concentration profiles reflect changes in palaeoproductivity (Carriker et al.,
316 1980a; Calmano et al., 1993; Jackson et al., 1993; Wang and Fisher, 1996; Guo et al., 1997). ~~It has~~

Formatted: Font: Italic

317 ~~been demonstrated that seasonal~~Seasonal records of these proxies are reproducible between
318 different shells in the same environment (Gillikin et al., 2008). While these proxies have not been
319 explored in detail, their interpretation gives additional information about the ambient sea water
320 chemistry and illustrates the advantage of applying the multi-proxy approach to reconstruct
321 palaeoseasonality from bivalve shells (de Winter et al., 2017a).
322

4.5 Stable isotope analyses

324 Samples for stable isotope analysis were drilled using a microscope-guided Merchantek drill, coupled
325 to Leica GZ6 microscope, equipped with a 300 μm diameter tungsten carbide drill bit ~~(AMGC group,~~
326 ~~VUB, Belgium).~~. Spatial sample resolutions smaller than the diameter of the drill were obtained by
327 abrading consecutive samples off the side of the sampling front. This was achieved by moving in
328 steps of ~~100μm~~100 μm along a ±2 mm wide linear sampling path, oriented parallel to the growth
329 lines of the shell and in the growth direction of the shell (447 measurements in total; see also Van
330 Rampelbergh et al., 2014~~; Vansteenberge et al., in review CHEMGEO~~).~~)~~. Dense foliated calcite in the
331 hinge of the shells was targeted ~~in~~while sampling for stable isotope analysis, but as a result of the
332 shell structure (see discussion below) the incorporation of some vesicular calcite could not always be
333 excluded. Note that, as a consequence of the abrading sampling strategy, the width of the sampling
334 path for IRMS samples is much larger (2 mm) than the width of the sampling path of a μXRF line scan
335 (25 μm). This caused more vesicular calcite to be incorporated into stable isotope measurements
336 than in μXRF measurements, as it was easier to avoid the vesicular microstructure in ~~the~~ μXRF
337 ~~measurements.~~ line scans.

338 Aliquots of ±50 μg of sampled calcite were allowed to react with 104% phosphoric acid (H_3PO_4) at
339 70°C in a NuCarb carbonate preparation device and stable oxygen and carbon isotope ratios ($\delta^{13}C$
340 and $\delta^{18}O$) were measured using a NuPerspective Isotope Ratio Mass Spectrometer (~~AMGC group,~~
341 ~~VUB, Belgium). Analytical uncertainty was determined by repeated measurement (N = 110) of the in-~~
342 ~~house reference material MAR2 (Marbella marble, $\delta^{13}C$: 3.41 ± 0.10 ‰VPDB; $\delta^{18}O$: 0.13 ± 0.20~~
343 ~~‰VPDB; 1 standard deviation, SD) and found to be 0.02‰ and 0.08‰ for $\delta^{13}C$ and $\delta^{18}O$ values (1~~
344 ~~SD), respectively. This MAR2 reference material was previously calibrated using the international~~
345 ~~NBS-19 stable isotope standard (Friedman et al., 1982). All stable isotope values are reported in~~
346 ~~permil~~Nu Instruments Ltd, Wrexham, UK) at the AMGC lab of the VUB. For analytical uncertainties
347 and reproducibiltiy, see **suppl_XRF_IRMS**. All stable isotope values are reported in permille relative
348 to the Vienna Pee Dee Belemnite standard (‰VPDB). While μXRF and IRMS measurements were
349 carried out on the same transect, small differences in the length of the records did occur and these
350 were corrected by linearly rescaling the stable isotope records to match the length of trace element
351 records in the same shell.

4.6 Clumped isotope analysis

353 The stable and clumped isotopic composition of samples from five shells (M4, M5, M8, M10 and
354 M11) was measured at the University of Michigan Stable Isotope Laboratory. Bulk sampling for
355 clumped isotope analysis was carried out in two ways: 1) ~~Of three shells (M5, M8 and M10),~~
356 ~~slabs~~Slabs of dense calcite were broken off the ventral margin of three shells (M5, M8 and M10) and
357 powdered by hand. 2) ~~Of four shells (M4, M5, M8 and M11), samples~~Samples were drilled from the
358 dense hinge area~~.~~ of four shells (M4, M5, M8 and M11). Sample preparation was performed on a
359 manual extraction line following Defliese et al. (2015), with the temperature of the Porapak™ trap
360 increased to avoid fractionating stable isotope values (Petersen et al., 2016). Aliquots of 3.5-5 mg
361 carbonate powder were reacted with phosphoric acid (H_3PO_4) at 75°C and sample CO_2 was analysed

362 on a ThermoFinnegan MAT253 equipped with Faraday cups to measure m/z 44-49. ~~Each sample was~~
363 ~~analysed for 5 acquisitions of 12 cycles each and calibrated relative to heated (1000°C) and H$_2$O-~~
364 ~~equilibrated (25°C) gas standards and two in-house carbonate standards (Carrara Marble and~~
365 ~~Aragonitic Bahamanian Ooids). Gas standards were used to convert unknowns into the absolute~~
366 ~~reference frame (Dennis et al., 2011) and carbonate standards (Carrara Marble and Aragonitic~~
367 ~~Bahamanian Ooids) were used to quantify reproducibility of reacted samples. δ^{18}O$_{water}$ values were~~
368 ~~calculated using the calcite-H$_2$O equation of Kim and O'Neil (1997). External (long term) error on the~~
369 ~~Δ$_{47}$ value was found to be 0.011‰ (1σ), based on companion measurements of carbonate standards~~
370 ~~(see **supplementary data 1**). Data presented in the main manuscript were processed using the~~
371 ~~Santrock/Gonfiantini parameters~~. Data presented in the main manuscript were processed using the
372 Santrock/Gonfiantini parameters (Daëron et al., 2016; Schauer et al., 2016) and the high-
373 temperature composite calibration of Defliese et al. (2015). Further details on the measurement and
374 calibration procedure of clumped isotope thermometry are found in **supplementary data 1**, along
375 with raw data processed using both Santrock/Gonfiantini and Brand parameters.

376

377 **5. Results**

378 **5.1 *Pycnodonte vesicularis* shell structure**

379 **5.1.1 Shell microstructures**

380 An overview of the results of colour scanning, microscopic analyses and µXRF mapping on ~~one of the~~
381 ~~*P. vesicularis* specimens (~~specimen M11~~)~~ reveals the microstructure of the shells ~~of these~~
382 ~~honeycomb oysters~~ (**Figure 3; supplementary data 2**~~).~~, supplementary microscopy). A cross section
383 through the shell in direction of maximum growth (**Figure 3A**) ~~reveals~~shows a layered shell structure
384 with laterally continuous growth increments similar to those ~~found~~ in modern ~~ostreid shells~~ostreids
385 (e.g. Carriker et al., 1980b; Surge and Lohmann, 2008; MacDonald et al., 2009; Ullmann et al., 2013).
386 Growth increments are characterized by an alternation of dense, foliated calcite layers with lighter
387 coloured, more porous, vesicular ("chalky") calcite layers that are characteristic for the family
388 Gryphaeidae (Linnaeus, 1758; Carriker et al., 1980b; Bieler et al., 2004; Surge and Lohmann, 2008).
389 The porosity ~~in~~of these vesicular layers is visualized in microscopic images (**Figure ~~3C-E). Microscopic~~
390 ~~images also show that the~~3D-F). The hinge of the shell is mostly devoid of this vesicular ~~structure,~~
391 ~~and~~microstructure, but instead consists of a close packing of foliated calcite layers (**Figure 3A** and
392 **Figure ~~3G~~3H**). However, in parts of the hinge small layers of vesicular calcite are also visible between
393 the foliated layers ~~in~~ (**Figure 3~~G~~H**). In places where these vesicular layers are interlocked between
394 foliated layers, the transition between the two microstructures is gradual. ~~Microscopic images~~
395 ~~(Figure 3D-E) show that farther~~Further away from the shell hinge, the transitions between foliated
396 calcite and vesicular calcite are sharp~~,~~ and ~~that~~ individual layers of foliated and chalky calcite can be
397 very thin (<30 µm; **Figure ~~3D~~3E-G**). Pores in the vesicular calcite are heterogeneous in size and shape
398 and can be up to 200 µm wide. While the shell structure is in general very well preserved (**Figure ~~3C-~~
399 ~~G~~3D-H**), it is disturbed in some areas by patches of different texture, or holes that have been
400 previously ascribed to boring by polychaete worms (Brezina et al., 2014).

401 **5.1.2 Porosity**

402 Micro-CT images of ~~one of the *P. vesicularis* specimens (~~specimen M4~~)~~ further illustrate the
403 distribution of porosity in the shell (**Figure 4**). Porosity analysis based on micro-CT scanning confirms
404 the microscopic observations of porous vesicular calcite and denser foliated calcite layers in the
405 shells. Quantitative analyses of porosity through the shell (porosity logs) on the high-resolution CT

9

406 scan of a small part of the shell (**Figure 4B**) shows that the distribution of porosity strictly relates to
407 growth layering of the shell. The porosity log perpendicular to the ~~growth layering~~layers (**Figure 4E**)
408 shows that porosity is almost absent in the foliated calcite layers and reaches up to 65% of the shell
409 volume in the most porous vesicular layers. Total shell CT scan results reveal that the average
410 porosity in the shell is 21%. ~~Results of CT scanning and microscopy show that, while the calcite in the~~
411 ~~vesicular microstructure was affected by diagenesis, the original porosity in these *P. vesicularis* shells~~
412 ~~has been preserved almost completely, and the filling of pores by recrystallized calcite is relatively~~
413 ~~uncommon (see **Figure 3D-E**).~~

414 **5.1.3 Chemical heterogeneity and cathodoluminescence**

415 Heterogeneity in the *P. vesicularis* shell is also evidenced by the distribution of iron (Fe) and
416 manganese (Mn) in the shell, as illustrated by µXRF mapping (**Figure 3B-C**). The ~~map shows~~maps
417 show that the vesicular layers ~~in the shell~~ are characterized by higher concentrations of Fe and Mn
418 than the dense foliated calcite layers. Parts of the shell that were perforated by bore holes have
419 especially high concentrations of Fe and Mn, and these holes are surrounded by a corona of elevated
420 Fe and Mn concentrations (**Figure ~~3H and I~~3I-L**). A close-up of ~~the~~a shell hinge ~~in~~ (**Figure 3B and C**)
421 confirms that it consists almost entirely of dense foliated calcite with low Fe and Mn concentrations.
422 It also shows occasional thin layers of vesicular calcite with higher Mn concentrations between
423 foliated calcite layers in the shell hinge (**Figure 3B**). The same close-up also illustrates that, due to
424 the ~~limitations of µXRF mapping with a~~ spot size of 25 µm~~,~~. ~~Tt~~he method is not able to resolve
425 variations in the concentration of Fe and Mn on the scale of fine (<30 µm) laminations in the shell
426 hinge. A composite of cathodoluminescence microscopy images of the same area (insert in **Figure**
427 **3A**) complements µXRF mapping by showing in more detail that the foliated calcite of the shell hinge
428 is characterized by microscopic growth increments that show a dull luminescence. At the same time,
429 the vesicular calcite microstructure shows bright luminescence (**Figure 3A, supplementary data 3**).
430 Only the largest increments can be distinguished on the µXRF map, while thin alternations between
431 microstructures are generally too small for the 25 µm XRF spot size to detect. In calcite, Mn^{2+} is the
432 main luminescence activator causing emission of yellow to orange light (~620 nm; Machel and
433 Burton, 1991) of which the intensity is positively correlated with the Mn concentration (de Lartaud
434 et al., 20~~10~~0a; Habermann, 2002; Langlet et al., 2006; de Winter and Claeys, 2016). Indeed, brighter
435 layers in the CL image correspond ~~with~~to higher Mn values in the XRF map. An enlarged version of
436 the CL composite shown in **Figure 3** ~~is~~as well as CL-images of other parts of the shells are given in
437 **supplementary data 3** and XRF Mn and Fe maps of all shells are given in **supplementary data 2**.

438 **5.2 Trace element profiles**

439 ~~Results~~Raw results of XRF line scans through all *P. vesicularis* shells featuring in this study are given
440 in **supplementary data 4**. Quantitative XRF line scans through the ~~hinge of the *P. vesicularis*~~
441 ~~shells~~hings yield records of [Ca], [Si], S/Ca, Zn/Ca, Sr/Ca, Mg/Ca, [Mn] and [Fe] in growth direction
442 through the dense hinge area of the shells (**Figure 5**). All measured XRF data ~~is~~are directly
443 represented in **Figure 5**, only the Mg/Ca record is plotted with a three point running average. This
444 ~~running average smoothes out~~smoothing is necessary because ~~the~~ ~~variation between individual~~Kα-
445 energy in which Mg~~/Ca~~ fluoresces X-rays is low, causing measurements~~, because~~ and quantification
446 of Mg ~~is slightly~~to be more susceptible to ~~interferences on~~small-scale changes in the sample matrix
447 along the XRF ~~spectrum, causing noise on the Mg/Ca record~~. ~~This results from the fact that Mg is on~~
448 ~~the edge of the spectrum of elements measurable by the M4 Tornado µXRF scanner and is~~
449 ~~therefore~~scan, which can be smoothed out by a moving average (see de Winter and Claeys, 2016; de
450 Winter et al., 2017b). ~~A plot of these results shows that concentrations~~Concentrations of calcium
451 (Ca) and silicon (Si) in all ~~shells~~shell records generally remain above 38 mass% and below 0.5 mass%,

10

452 respectively. In three ~~out~~ of the four specimens (M0, M4 and M6), absolute concentrations of Fe and
453 Mn rarely exceed 800 μg/g (**Figure 5**). The ~~exception is the~~ iron record of specimen M11~~, which~~
454 shows maxima often exceeding 2000 μg/g. Fe concentrations in M6 are also elevated in comparison
455 with M0 and M4, leading to the suggestion that there might be a link between the presence of bore
456 holes (observed in M6 and M11) and elevated Fe-concentrations. A cross plot in **Figure 6A** shows
457 that the concentrations of Fe and Mn are weakly correlated in XRF line scan measurements.
458 Furthermore, samples with elevated concentrations of Mn generally have lower Sr concentrations ~~of~~
459 ~~Sr~~, especially when Mn concentrations ~~are higher than~~exceed 800 μg/g (**Figure 6B**). Both are a sign
460 of diagenetic alteration because Mn and Fe have been shown to be preferentially enriched in
461 recrystallized shell carbonates, while Sr is preferentially removed during the recrystalli~~s~~zation
462 process (Brand and Veizer, 1980; Al-Aasm and Veizer, 1986a). Trace element profiles through the
463 four *P. vesicularis* specimens show that there is ~~a~~ good ~~overall~~ agreement between shells both in
464 terms of absolute concentration of magnesium (Mg), strontium (Sr), zinc (Zn) and sulphur (S) and
465 their internal variation. Records of ratios of Mg/Ca, Sr/Ca, Zn/Ca and S/Ca show quasi-cyclic
466 oscillations. In records of Mg/Ca and Sr/Ca, these oscillations ~~are quasi~~appear sinusoidal, while
467 records of Zn/Ca and S/Ca are characterized by short-lived increases relative to a baseline value.
468 Trace element ratios generally oscillate around a stable baseline value, though in some cases (e.g.
469 Sr/Ca and Mg/Ca in M11) there is a slight evolution of this baseline value in the direction of growth.

470 **5.3 Stable isotope analysis**

471 **5.3.1 Stable isotope records**

472 Records of ~~stable oxygen isotope ratios (~~$\delta^{18}O$~~)~~ and ~~stable carbon isotope ratios (~~$\delta^{13}C$~~)~~ are plotted
473 together with trace element ratios in **Figure 5**. As in ~~the~~ trace element records, absolute values as
474 well as internal variation of stable isotope records show good agreement between shells. Values in
475 the $\delta^{18}O$ record oscillate around a baseline value of -1.5‰. The $\delta^{13}C$ baseline values are ~~a bit~~ more
476 variable, possibly showing a late ontogenetic trend in M6 and M11, but remaining stable at 2‰ in
477 the other specimens. Stable oxygen and carbon isotope records seem to show quasi-periodic
478 variations around these baseline values, with amplitudes of about 1‰ and 0.5‰ respectively (**Figure**
479 **5**). Stable oxygen isotope ratios remain between -2.5‰ and -0.5‰ for the majority of the records,
480 ~~exceptions being $\delta^{18}O$ values~~only dropping below -3‰ in a few measurements in M4, the central
481 part of the M6 record, and a few measurements in the youngest part of the M0 record. Similarly,
482 $\delta^{13}C$ ratios in all shells remain between 1.5‰ and 3.5‰, except for the latter cases. Cross plots
483 between isotope ratios show that samples with exceptionally low $\delta^{18}O$ values (<-3‰) often also
484 exhibit decreased $\delta^{13}C$ values (<1.5‰; **Figure 6D**). This relationship between $\delta^{18}O$ and $\delta^{13}C$~~values,~~
485 which is significant in shells M4, M6 and M11~~, and~~ but not in M0~~. Such a relationship between $\delta^{18}O$~~
486 ~~and $\delta^{13}C$ has,~~ is often ~~been~~ interpreted as a sign of diagenetic alteration~~.~~ (Al-Aasm and Veizer,
487 1986b; Banner and Hanson, 1990). Therefore, the absence of this relationship in M0 in contrast to
488 the other shells shows that the stable isotope profile from the hinge of shell M0 is least affected by
489 diagenetic alteration. The fact~~Stable oxygen and carbon isotope records seem to show quasi-~~
490 ~~periodic variations around these baseline values, with amplitudes of about 1‰ and 0.5‰~~
491 ~~respectively (Figure 5). Cross plots of proxy records show~~ that $\delta^{18}O$ and $\delta^{13}C$ values are generally
492 lower in samples with elevated concentrations of Mn and Fe (**Figure 6A and 6C**~~).~~) supports the
493 hypothesis that these parts of the shell are affected by diagenesis.

494 **5.3.2 Clumped isotope analysis**

495 Clumped isotope analyses of ventral margin calcite from three *P. vesicularis* shells from the same
496 ~~locality~~palaeoenvironment (M5, M8 and M10; see **Figure 1** and section 4.1) yielded Δ_{47} values of

11

497 0.699 to 0.707‰, equivalent to a temperature range of 21-25°C using the high temperature
498 composite calibration of Defliese et al~~.,~~. (2015 ~~(;~~ see **Table 1**). Both reconstructed temperatures and
499 $\delta^{18}O_{seawater}$ values varied significantly between these samples, with $\delta^{18}O_{seawater}$ ranging from -0.6‰ in
500 M10 to -2.2‰ and -5.9‰ in M5 and M8 respectively, likely indicating the influence of altered calcite
501 material. This is supported by shell $\delta^{18}O$ values, which ~~deviate to~~contain very low values (-4‰ to -
502 7‰VPDB in M5 and M8) well outside of the range of samples micromilled from the well-preserved
503 hinge carbonate (**Figure 5**). The same samples (M5 and M8) also show relatively decreased $\delta^{13}C$
504 values (<1‰), ~~further~~indicating that these decreased stable isotope ratios are likely indicative of
505 diagenetic alteration. In comparison, samples of the dense hinge calcite from M4, M5, M8 and M11,
506 yielded ~~$\delta^{18}O_{seawater}$ values ranging from -1.8‰ to -2.5‰ and~~Δ_{47} values of 0.725 to 0.746‰,
507 corresponding to much cooler temperatures of 9-15°C~~.~~ and $\delta^{18}O_{seawater}$ values ranging from -1.8‰ to
508 -3.4‰ (-2.8‰ on average). Shell $\delta^{13}C$ and $\delta^{18}O$ values from bulk samples of hinge carbonate
509 resemble values measured in the high-resolution transects, ~~further supporting the good~~
510 ~~preservation of~~showing that carbonate in ~~this area~~the shell hinges is well preserved.

511

512 **6. Discussion**

513 **6.1 Shell preservation**

514 **6.1.1 Visualization of diagenesis**

515 ~~The preservation~~Results of ~~fine shell porosity measured by~~ CT~~-~~ scanning ~~shows~~and microscopy show
516 that ~~if any~~, while calcite in the vesicular microstructure was affected by recrystallization ~~occurred in~~
517 ~~the shells, it was~~, the original porosity in *P. vesicularis* shells has been preserved almost completely,
518 and the filling of pores by calcite cementation is relatively uncommon (see **Figure 3D-E**). Microscopic
519 images of the foliated calcite microstructure (e.g. **Figure 3F-G**) and comparison with modern oyster
520 studies further show that the elongated crystal microstructure characteristic of pristine foliated shell
521 calcite has not ~~so extensive that the pores in the vesicular layers were filled by secondary calcite.~~
522 ~~Yet, identifying~~been compromised by diagenesis ~~in *P. vesicularis* shells cannot be done based on~~
523 ~~simple visual inspection alone. Recrystallized calcite is often characterized by elevated~~(Ullmann et
524 al., 2010). Elevated concentrations of ~~Mn and Fe, which are released into~~Fe and Mn in the shells can
525 be used as an indicator for recrystallization, since these elements are incorporated in secondary
526 calcite from reducing pore waters ~~of~~in the sediment surrounding the shell ~~under reducing~~
527 ~~conditions~~during burial (Al-Aasm and Veizer, 1986~~a~~). This ~~allows the distribution~~makes µXRF maps of
528 Fe and Mn concentrations ~~in the shells to be used as an indicator~~excellent tools for the
529 ~~amount~~assessment of ~~recrystallization and the~~primary calcite preservation ~~of the shell.~~. The map~~s~~ in
530 **Figure 3B and C** shows that such recrystallization is predominantly observed in the vesicular calcite
531 and that Fe and Mn concentrations in foliated calcite layers are low. Coronas of elevated Fe and Mn
532 concentrations around ~~the~~bore holes ~~in the shells~~confirm that ~~increased concentrations of~~Mn and
533 Fe ~~a~~we~~re~~ leached into the shell through these holes ~~as penetrating~~when pore fluid ~~carrying these~~
534 ~~ions can more easily infiltrate the~~infiltrated the shell and were distributed through the porous
535 vesicular calcite layers ~~than the foliated calcite.~~. The layered macrostructure of ostreid shells
536 facilitated this penetration of pore fluids. The fact that shells M6 and M11, ~~which contain~~containing
537 the most bore holes (see **Figure 2**), have the highest Mn and Fe values (**Figure 5**) supports this
538 hypothesis. ~~This pattern is confirmed by the cathodoluminescence~~CL microscopy images~~, which~~
539 ~~show~~ showing minimal dull luminescence in the foliated calcite~~, indicative of limited contamination~~
540 ~~of the~~ and bright luminescence in vesicular calcite ~~by~~ confirm leaching of Mn and Fe into the shells
541 (Barbin, 2000). ~~Thin lamina~~Brightly luminescing laminae between foliated calcite layers ~~show~~

12

542 ~~brighter luminescence,~~ in the shell hinge are associated with ~~higher concentrations of Fe and Mn.~~
543 ~~This is in agreement with~~ peaks in Mn and Fe observed in the μXRF profiles of M11 (**Figure 5**).
544 ~~Microscopic images of the foliated calcite structure (e.g. **Figure 3F-G**) further show that the~~
545 ~~elongated crystal structure characteristic of pristine foliated shell calcite has not been compromised~~
546 ~~by diagenesis (Ullmann et al., 2010).~~ Comparison between the CL composite and the μXRF map
547 shows that, while μXRF mapping does pick up large scale diagenetic features in the shell, it fails to
548 reveal most of the small layers intercalated between foliated calcite layers in the shell hinge because
549 they are smaller than the spot size of the μXRF scanner (25 μm). This illustrates that μXRF mapping is
550 a useful tool for screening ~~for diagenesis~~ diagenetic overprint, but fails to pick up the fine details that
551 are visualized by CL-microscopy. Similarly, Mn and Fe profiles in μXRF line scanning will miss or
552 average out the small layers of vesicular calcite present in some parts of the shell hinges of *P.*
553 *vesicularis* and CL-microscopy remains a necessary tool for thorough screening for diagenesis.

554 **6.1.2 Diagenesis in trace element profiles**

555 Quantitative XRF line scans through the hinge~~s~~ of ~~the~~ *P. vesicularis* ~~specimens~~ show that absolute
556 concentrations of Fe and Mn rarely exceed 800 μg/g in all shells except for M11 (**Figure 5**). ~~While~~ Mn
557 concentrations measured in the hinges ~~of *P. vesicularis*~~ are higher than is considered typical for well-
558 preserved bivalve calcite and often exceed the diagenesis threshold of 300 μg/g proposed by
559 Steuber (1999~~),~~). However, high concentrations of Sr (>700 μg/g) and Mg (>1000 μg/g),
560 comparatively low Fe concentrations and the observation of non-luminescent, well-preserved
561 foliated calcite crystals (**Figure 3**) suggest preservation of the original trace element signature
562 (Veizer, 1983; Al-Aasm and Veizer, 1986a; Steuber, 1999). The ~~peaks of high Fe concentrations in the~~
563 ~~M11 shell and elevated Fe concentrations in M6 compared to the other~~ fact that parts of shells
564 ~~coincide with decreases in δ¹⁸O and δ¹³C. In general,~~ with more depleted stable isotope ~~values~~
565 ~~are~~ ratios and lower ~~in intervals of the records characterized by elevated levels of Mn and Fe that~~
566 ~~exceed the baseline variation. Similarly, concentrations of~~ Sr ~~are~~ concentrations generally ~~lower in~~
567 ~~samples with higher Mn concentrations (**Figure 6B**). This trend is especially clear in samples of which~~
568 ~~Mn concentrations exceed 800 μg/g. This suggests that in these specimens of *P. vesicularis*, Fe and~~
569 ~~Mn concentrations~~ coincide with peaks in Fe and Mn exceeding 800 μg/g shows that these results
570 likely signify areas where recrystallization has occurred (see also **Figure 5 and 6A-C**). We therefore
571 propose 800 μg/g as a tentative maximum threshold for Mn and Fe concentrations for the
572 preservation of pristine calcite in shells of *P. vesicularis* in this setting, and consider samples
573 exceeding this threshold in concentration for either Mn or Fe as diagenetically altered. Evidence of
574 such alteration is most common in shells M6 and M11. Except for a few measurements in shells M6
575 and M11, low Si concentrations and high Ca concentrations ~~in the trace element records shown in~~
576 (**Figure 5**) indicate limited incorporation of detrital material into the hinge of the shell (see de Winter
577 and Claeys, 2017; de Winter et al., 2017a). ~~This shows that the infills of~~ Indeed, bore holes filled by
578 detrital material ~~have not significantly influenced the chemical signal of the hinges of the shells.~~
579 ~~Indeed, the locations of these bore holes~~ are almost exclusively observed away from the shell hinge
580 ~~are observed in~~ and did not significantly influence XRF records (**Figure 2 and 3**~~.~~). From this it follows
581 that the majority of post-mortem alteration of the shells occurred through the process of chemical
582 alteration (e.g. recrystallization) rather than physical processes (e.g. predatory burrowing). As
583 described above (see 5.1.1), the role of bore holes in the shells (especially M6 and M11) in the
584 diagenetic process was predominantly to provide entries through which pore waters could enter to
585 cause recrystallization. Bore holes elsewhere in the shells may lead to migration of fluids through the
586 shell, ultimately resulting in elevated concentrations throughout the shell.

587 **6.1.3 Diagenesis in stable isotope records**

13

Formatted: Font: Not Italic

588   The majority of the stable isotope ratios measured the shell records are in agreement with those of
589   well-preserved Low Magnesium Calcite ~~(LMC)~~ of fossil (Steuber, 1996; 1999; Tripati et al., 2001) and
590   modern marine mollusc shells (Klein et al., 1996a;b; Goodwin et al., 2001; Lécuyer et al., 2004). ~~The~~
591   ~~low~~ $\delta^{18}O$ and $\delta^{13}C$ values ~~characterizing~~below -4‰ and 1‰ respectively (a drop of 2-3‰ for $\delta^{18}O$
592   and 1-2‰ for $\delta^{13}C$) in the central part of the M6 shell hinge record ~~is~~are an exception to this and
593   ~~these values are~~ likely ~~explained by~~represent incorporation of diagenetically altered vesicular calcite
594   into micromilled IRMS samples. The scan image of M6 (**Figure 2**) shows that an extension of
595   vesicular calcite into the ~~micromilled samples. It is evident from the scan image of M6 in~~ **Figure 2**
596   ~~how an extension of this shell mineral phase into the umbo has~~hinge region resulted in the sampling
597   of vesicular calcite in the ~~centre of~~stable isotope and trace element records. Similarly, the stable
598   isotope record of specimen M4 was affected by lobes of vesicular calcite extending close to the
599   hinge line. A depletion of both $\delta^{18}O$ and $\delta^{13}C$ could potentially also be explained by an input of
600   freshwater into the ~~record. The resulting sudden decrease in $\delta^{18}O$ and $\delta^{13}C$ towards values below~~
601   ~~4‰ and 1‰ respectively (a drop of 2-3‰ for $\delta^{18}O$ and 1-2‰ for $\delta^{13}C$) illustrates that stable isotope~~
602   ~~composition of this vesicular calcite deviates significantly from~~basin (Gillikin et al., 2006), but the
603   scale of the isotopic shift and the fact ~~that~~ ~~of the foliated calcite. Similarly, the record from specimen~~
604   ~~M4 also has several stable isotope samples that most likely contain vesicular calcite. Lobes of~~they
605   coincide with increases in vesicular calcite ~~in this specimen extend close to the hinge line, making~~
606   ~~incorporation of this microstructure~~shows that diagenetic alteration is a more likely. ~~Several samples~~
607   ~~in the isotopic record of M4 are indeed characterized by unusually low isotopic values. We consider~~
608   ~~it likely that small amounts of~~ explanation. Low $\delta^{18}O$ values in vesicular calcite ~~were incorporated in~~
609   ~~these~~samples~~.~~

610   ~~The exceedingly low $\delta^{18}O$ values in some samples from the vesicular calcite suggests that the original~~
611   ~~composition is either not preserved due to alteration or~~ could also suggest that this vesicular calcite
612   was initially precipitated in disequilibrium with respect to ambient sea water (Grossman and Ku,
613   1986; Woo et al., 1993; Steuber, 1999). The latter could be in agreement with the hypothesis that
614   vesicular microstructures in oyster shells are formed by microbes instead of by the bivalve itself
615   (Vermeij, 2014). However, microscopic images of the vesicular microstructure reveal blocky calcite
616   crystals in some areas (**Figure ~~3D~~3E-F**), which suggest recrystallization (e.g. Folk and Land, 1975;
617   Schlager and James, 1978). Indeed, the offset in stable isotope ratios of vesicular calcite compared
618   to foliated calcite is not found in modern oyster shells (Surge and Lohmann, 2008; Ullmann et al.,
619   2010~~), and is therefore most likely a result of preferential diagenetic alteration of the vesicular~~
620   ~~calcite.~~). Elevated Mn and Fe concentrations found in XRF mapping (**Figure ~~3~~3B-C**), and the notion
621   that similar chalky or vesicular phases in modern oyster shells are less crystalline and grow faster
622   (Chinzei and Seilacher, 1993; Ullmann et al., 2010), further attest to the fact that vesicular calcite in
623   *P. vesicularis* (and likely in other fossil members of the Gryphaeidae) is more prone to diagenetic
624   alteration than its foliated counterpart, and therefore provides no suitable record of palaeoclimatic
625   information.

626   This conclusion is also supported by the clumped isotope analysis results. Bulk samples from the
627   ventral margin of the shell (containing more vesicular calcite, see **Figure 2 and 3**) contain lower
628   stable isotope ratios and higher reconstructed temperatures than samples from the dense shell
629   hinge (**Table 1**; ~~Figure 7~~). Elevated temperatures in ~~these~~altered samples likely reflect
630   recrystallization of shell material from slightly warmer pore fluids after burial. ~~However,~~
631   ~~temperatures~~Comparison of Δ_{47} with $\delta^{18}O$ and $\delta^{13}C$ measurements (**Figure 7**) clearly show how the
632   sensitivity of clumped isotope analysis can be used to demonstrate the effect of calcite
633   recrystallization within *P. vesicularis*. Sequential sampling for Δ_{47} measurements in bivalve calcite
634   therefore may provide a useful tool to trace intra-shell variability in preservation and calcification

14

635 temperature. Temperatures from diagenetic samples (average = 23°C) are relatively low compared
636 to typical pore fluid temperatures measured from diagenetic calcite in other studies (30-120°C;
637 Huntington et al., 2011; Loyd et al., 2012; Dale et al., 2014~~). Together with the fact that the~~
638 ~~difference between altered)~~, and ~~unaltered~~do not deviate much from those of pristine samples
639 (23°C vs. 11°C; **Table 1**~~) is relatively small and that the dense calcite portions seem to be unaffected~~
640 ~~by diagenesis, which~~). This suggests that burial was shallow and recrystallization not extensive. The
641 shallow burial history is also demonstrated by the preservation of organic biomarkers in the Bajada
642 de Jagüel section (Woelders et al., 2017). With a maximum burial temperature of 25°C during
643 recrystallization, the burial depth of the late Maastrichtian strata in the Neuquèn Basin is likely to be
644 very shallow and at the very maximum no more than 500 meters (Klein et al., 1999; Dale et al.,
645 2014).

6.1.4 Implications for sampling strategy

647 Contrary to what may be expected ~~based on the XRF map of M11 in~~ **Figure 3**, the incorporation of
648 vesicular calcite into the ~~microdrilled~~stable isotope samples of M6 **(Figure 2 and 5)** is not always
649 reflected ~~in~~by elevated Mn and Fe concentrations in the µXRF line scans. This could suggest that
650 trace element signatures in vesicular calcite ~~this~~ close to the ~~shell~~ hinge are ~~not strongly~~less affected
651 by the leaching of reducing pore waters ~~that likely elevated the concentrations of these elements in~~
652 ~~the vesicular calcite of the~~than in the rest of the shell. Alternatively, it is likely that the 2 mm wide
653 sampling track for stable isotope measurements contains more ~~of the~~vesicular calcite ~~was~~
654 ~~incorporated in the microdrilled samples for stable isotopes,~~than ~~in the XRF line scan, as the line~~
655 ~~scan is only~~the 25 µm wide ~~and relatively close to the hinge line, whereas the linear sampling paths~~
656 ~~of the microdrilling covered a much larger area (up to 2 mm wide parallel to the growth increments).~~
657 ~~The~~XRF line. This shows that the wide sampling ~~line~~track needed to sample for stable isotope
658 analysis at ~~this~~high spatial resolution (100 µm in the direction of growth) increases the chance of
659 incorporating vesicular calcite~~into the samples~~, particularly in samples further away from the hinge
660 line and in shells where vesicular calcite layers penetrate close to the hinge line (e.g. M4 and M11,
661 see **Figure 2, Figure 3 and Figure 6D**). This ~~result~~ illustrates a disadvantage of the abrasion-style
662 microdrilling method applied in this study for spatially heterogeneous bivalves~~. It~~, and shows that
663 thorough screening for diagenesis ~~using both trace element analysis and cathodoluminescence~~by CL-
664 microscopy and µXRF mapping is essential to correctly interpret the stable isotope results.

665 Summarizing, shells M6 and M11 are characterized by elevated Fe and Mn concentrations in the
666 shell hinge line, signifying that these specimens contain larger amounts of recrystallized vesicular
667 calcite in their shell hinge. Specimen M4 shows lower Fe and Mn concentrations in the shell hinge,
668 but low stable isotope ratios show that several microdrilled samples contain diagenetically altered
669 vesicular calcite. Stable carbon and oxygen isotope ratios in shells M4, M6 and M11 all show a
670 significant positive relationship, while such a relationship is absent in M0. As a result, of the 4
671 specimens investigated, specimen M0 is considered to represent the best preserved specimen, most
672 likely providing the most reliable results in terms of palaeoenvironmental reconstruction. Coloured
673 vertical bars in **Figure 5** illustrate parts of the shell records that were considered ~~diagenetically~~
674 altered based on one or more of the criteria described above: 1) Bright luminescence in CL-
675 microscopy. 2) ~~e~~Elevated (>800 µg/g) Fe and/or Mn concentrations. 3) Elevated Si (>0.5 mass%) and
676 reduced Ca (<38 mass%) concentrations. 4) Decreased stable isotope ratios ($\delta^{18}O$ < -3‰ and $\delta^{13}C$ <
677 1.5‰).

6.2 Periodic variations

6.2.1 Shell chronology

While earlier studies have been successful in determining the chronology of geochemical records from ~~comparatively young (Quarternary)~~Quaternary fossil bivalves (e.g. Scourse et al., 2006; Marali and Schöne, 2014), attempts at palaeoseasonality reconstruction~~s~~ based on more ancient ~~(pre-Quarternary)~~ shells have shown that this is not straightforward (Dettmann and Lohmann, 1993; Bougeois et al., 2014; de Winter and Claeys, 2016; de Winter et al., 2017a). ~~Quasi~~In this study, quasi-periodic variations in stable oxygen isotopes, Sr/Ca ratios and Mg/Ca ratios seem to represent seasonal cycles in shell growth (**Figure 5**), but on closer inspection it is difficult to find a consistent phase relationships between these records through all four shells. The ~~most well~~best-preserved ~~shell~~ record (M0) was tentatively subdivided into annual cycles based on Sr/Ca and $\delta^{18}O$ seasonality. **Figure 8** shows a stack of the trace element records created based on these subdivisions. Similar year stacks of the other three shells yielded different phase relationships between proxies (**supplementary data 5**). These differences are likely explained by the incorporation of diagenetically altered vesicular calcite in some of the microdrilled samples, resulting in significantly lighter ~~carbon~~$\delta^{18}O$ and ~~oxygen isotopic~~$\delta^{13}C$ values. ~~Especially in the~~The record of shell M4 (**Figure 5**~~), it is clear~~) clearly illustrates how diagenesis can preferentially influence one season over the other and result in a change of the phase relationship between proxies in the shell. ~~In the case of M4, the~~Since incorporation of lobes of vesicular calcite into the shell hinge seems to be paced to the seasonal cycle, ~~making~~ it is difficult to disentangle patterns ~~in~~of diagenetic alteration from seasonal patterns ~~in the shell records. The incorporation of diagenetically altered vesicular calcite into the~~ in the shell ~~hinge has influenced stable isotope profiles in shells M4, M6 and M11 more than M0, as is evident~~ ~~from the significant correlation between~~ $\delta^{18}O$ ~~and~~ $\delta^{13}C$ ~~in these shells, which is absent in M0 (~~**Figure 6D)**~~.~~ Such preferential incorporation of vesicular calcite into the hinge during one season can occur when the bivalve experiences more physiological stress in that season (Müller, 1970). Indeed, even when diagenetically altered parts of these records (according to the threshold of 800 µg/g for Fe and Mn and -3‰ for $\delta^{18}O$) are excluded, seasonal patterns in year stacks of shells M4, M6 and M11 do not fully agree with those in the better preserved M0 shell~~. This leads to the assumption~~, showing that poorer preservation prevents the establishment of~~ ~~a reliable chronology for these shells. That said, records from shells M4, M6 and M11 should not be dismissed, as variation in the geochemical proxies measured in pristine parts of these shells could still yield valuable information about the extent of seasonality during their growth, even though phase relationships are blurred by diagenetic overprinting. Moreover, since the exact stratigraphic level of the shells is not fully constrained, small differences in expression of the proxies due to changes in environment between their lifetimes cannot be fully excluded. The fact that ~~stable isotope measurements~~microdrill and µXRF tracks in these shells were not ~~taken from~~exactly the ~~exact~~ same ~~location as trace element measurements (due to different sampling and measurement techniques)~~ further complicates the establishment of consistent phase relationships between geochemical records in the shells. ~~The most obvious way in which this affected phase relationships between records is the fact that~~For example, stable isotope samples were more severely laterally averaged (2 mm wide tra~~nsec~~t~~k~~ compared to 25 µm wide ~~transect of~~ µXRF ~~measurements~~transect), and ~~the fact that stable isotope records were~~had to be rescaled to the length of XRF records before being plotted in **Figure 5** (see section 4.5).

6.2.2 Phase relationships

~~Since only one of the shells measured in this study (M0) showed good enough preservation for a~~ ~~discussion of phase relationships between records, care must be taken in extrapolating the~~ ~~conclusions drawn from the year stack of this single shell. However, a tentative discussion of these~~ ~~phase relationships may still shed some light on the mechanisms that drive the incorporation of~~ ~~these proxies into the shell of P. vesicularis.~~ The year stack of the well-preserved specimen M0 (**Figure 8**) shows that the $\delta^{18}O$, $\delta^{13}C$ and Sr/Ca records exhibit a sinusoidal pattern with one peak per

727 year. In contrast, records of Zn/Ca, S/Ca and Mg/Ca ~~contain a double peak~~show two peaks in each

728 year. Comparing these observations with the records in **Figure 5** shows that the same seems to be

729 true for the pristine parts of the other three shells. In addition, the M0 year stack shows that

730 maxima in $\delta^{13}C$ ratios coincide with minima in Sr/Ca and Zn/Ca and that minima in δ^{18}~~O~~^3C ratios

731 shortly follow m~~ax~~inima in ~~$\delta^{13}C$ after about one quarter of an annual cycle~~$\delta^{18}O$. Zn/Ca and S/Ca

732 records show an antiphase relationship, and the Mg/Ca record has one minimum that coincides with

733 a minimum in $\delta^{18}O$ ratios and another ~~half a cycle earlier.~~ offset by half a cycle. Yet, since only one of

734 the shells measured in this study (M0) showed good enough preservation for a discussion of phase

735 relationships between records, care must be taken in extrapolating the conclusions drawn from the

736 year stack of this single shell.

737 **6.3 Interpreting geochemical records in *Pycnodonte vesicularis***

738 6.3.1 Comparison with other taxa

739 Carbon isotope values found in this study are higher than in oysters living in modern coastal

740 temperate environments (Surge et al., 2001; Ullmann et al., 2010), but more similar to oysters living

741 in warmer, high-salinity or tropical settings (Klein et al., 1996a; Surge and Lohmann, 2008; Titschack

742 et al., 2010). Oxygen isotope ratios are generally lower than modern coastal mid latitude bivalves

743 (Klein et al., 1996b; Ullmann et al., 2010~~; Klein et al., 1996b~~) and in better agreement with warmer,

744 low latitude studies (Lécuyer et al., 2004) and other Cretaceous bivalves (Steuber, 1999). This is in

745 agreement with reconstructions of $\delta^{18}O$ ratios in Late Cretaceous oceans that were ~1‰ lower

746 compared to the present-day ocean due to the absence of extensive polar ice sheets ~~in the Late~~

747 ~~Cretaceous~~ (e.g. Hay, 2008~~). These results are in agreement~~), and also with the warmer

748 palaeoenvironmental setting inferred for the Late Cretaceous of Neuquén Basin, based on TEX_{86}-

749 palaeothermometry (Woelders et al., 2017). However, the clumped isotope thermometry results of

750 this study suggests rather cooler temperatures. In order to properly interpret geochemical records

751 from *P. vesicularis*, it is important to compare the results of this study with those from closely

752 related bivalves. Although the genus *Pycnodonte* has no living members, two sister taxa in the

753 subfamily Pycnodonteinae (Stenzel, 195~~9~~6) contain extant members: *Hyotissa* and *Neopycnodonte*

754 (Stenzel, 1971).

755 6.3.2 *Hyotissa hyotis* (Linnaeus, 1758)

756 The microstructure of *Hyotissa hyotis* is similar to that of *P. vesicularis*, with porous vesicular phases

757 alternat~~ed~~ing with dense foliated calcite layers. A specimen of *Hyotissa hyotis* in the northern Red

758 Sea was subject to a stable isotope study by Titschack et al. (2010). ~~That study illustrates that, in~~

759 ~~contrast~~In contradiction to ~~what was argued~~findings by Nestler (1965), ~~the microstructure~~

760 ~~alternations in pycnodontein bivalves do not correlate~~but similar to ~~annual growth increments. In~~

761 ~~the specimen of *H.*~~*H.* hyotis (Titschack et al., 2010~~), seasonal variations in $\delta^{18}O$~~) and ~~$\delta^{13}C$ were found~~

762 ~~to be independent of shell microstructure. Similarly, in~~ modern oysters like *Crassostrea virginica*

763 (Surge and Lohmann, 2008) and *Crassostrea gigas* (Ullmann et al., 2010), ~~no isotopic difference is~~

764 ~~observed between different~~ seasonal variations in $\delta^{18}O$ and $\delta^{13}C$ in *P. vesicularis* were found to be

765 independent of shell microstructure~~s~~ (foliated vs vesicular calcite). This ~~may explain why year stacks~~

766 ~~of *P. vesicularis* shells~~shows that ~~were affected by diagenesis differ from those of~~ the ~~well-preserved~~

767 ~~M0 specimen. The~~isotopically ~~lighter values observed in~~light signal of the vesicular calcite ~~of *P.*~~

768 ~~vesicularis* result from~~in the records of M4, M6 and M11 was caused by recrystallization, ~~not of~~

769 ~~annual cyclicity, and this incorporation of diagenetically altered samples into the record~~

770 ~~disturbed~~disturbing the ~~original~~seasonality signal in their stable isotope ~~seasonality.~~records,

771 hampering the interpretation of shell chronology (see 6.2.1). Stable carbon isotope ratios in ~~*H. hyotis*~~

772 ~~are very similar to *P. vesicularis*~~ resemble those measured in ~~*P. vesicularis.*~~*H. hyotis* in terms of
773 absolute values and seasonal amplitude. In principle, the $\delta^{13}C$ ~~signal of shells~~shell carbonate is
774 controlled by the $\delta^{13}C$ value of the dissolved inorganic carbon (DIC) of the organism's extrapallial
775 ~~F~~fluid (EPF), from which the shell is precipitated (Kirby, 2000). In marine bivalves, the ~~carbon isotope~~
776 ~~composition~~$\delta^{13}C$ of the EPF is controlled by the $\delta^{13}C$ of ambient seawater, the carbonate ion
777 ~~effects~~pump, pH, food availability, growth, valve gape/closure intervals, and seasonal changes in
778 metabolic rate (Romanek et al~~.~~., 1992; McConnaughey et al~~.~~., 1997; Kirby et al~~.~~., 1998; Owen et al~~.~~.,
779 2002; Geist et al~~.~~., 2005; McConnaughey and Gillikin, 2008; Lartaud et al~~.~~., 2010b). ~~All~~The variation in
780 all these processes ~~vary in strength and time, which~~ complicates practical interpretation of the $\delta^{13}C$
781 signal (Lorrain et al~~.~~., 2004; Omata et al~~.~~., 2005). ~~According to Titschack et al. (2010),~~In *H. hyotis*,
782 $\delta^{13}C_{shell}$ ~~of *H. hyotis* is most strongly~~is controlled by bivalve respiration, which ~~is increased~~increases
783 during periods of enhanced planktonic food supply~~. They recorded a~~ (Titschack et al., 2010). A
784 shifted phase relationship between $\delta^{18}O$ and $\delta^{13}C$ ~~records~~in *H. hyotis*, similar to the phase shift
785 observed in **Figure 8**, ~~which was~~is attributed to phase-shifted cycles in sea surface temperature and
786 productivity. ~~In~~Comparison with modern *H. hyotis* ~~there is an anti-phase relationship between $\delta^{13}C$~~
787 ~~and daily sunshine hours, suggesting~~therefore suggests that ~~in our records of the closely related *P.*~~
788 ~~*vesicularis*, the lowest~~ annual lows in $\delta^{13}C$ values ~~likely correspond to mid-summer (December).~~in *P.*
789 *vesicularis* also indicate periods of increased food supply, such as plankton blooms.

790 6.3.3 *Neopycnodonte zibrowii* (Videt, 2004)

791 ~~A specimen of~~While the large bivalve *Neopycnodonte zibrowii* ~~(Videt, 2004) was subject to detailed~~
792 ~~multi-proxy analysis in Wisshak et al. (2008). This large, deep dwelling (450–500m) bivalve from the~~
793 ~~Azores~~ shows similar alternations in vesicular and foliated calcite as *P. vesicularis*, ~~but~~ it is deep
794 dwelling (450–500m), in contrast with the shallow marine taxa *P. vesicularis* and *H. hyotis*, and has a
795 much longer lifespan. ~~Trace element records in *N. zibrowii* show~~A specimen of *N. zibrowii* (Videt,
796 2004) was subject of a detailed multi-proxy analysis in Wisshak et al. (2009). The shell of *N. zibrowii*
797 is characterized by much higher Mg/Ca and S/Ca and lower Sr/Ca ratios ~~compared to those found~~
798 ~~in~~than that of *P. vesicularis* ~~in this study. Consecutive~~. Coincidence of peaks in Mg/Ca and S/Ca
799 coinciding with minima in Ca and Sr ~~concentration in this shell are interpreted as a sign of a strong~~
800 ~~control of growth and reproductive cycle on trace element ratios. The covariation of Mg/Ca and S/Ca~~
801 ~~records in bivalve calcite has often been~~concentrations in *N. zibrowii* can be interpreted as evidence
802 ~~of internal control on~~for strong vital effects controlling trace element concentrations rather than
803 external forcing (e.g. by temperature; Lorens and Bender, 1980; Rosenberg and Hughes, 1991). ~~~~Such
804 relationships between Mg/Ca, S/Ca and Sr/Ca are~~, however,~~ not observed in *P. vesicularis* (**Figure 5**,
805 **Figure 6** and **Figure 7**). ~~While $\delta^{13}C$ values in *N. zibrowii* are similar to those found in this study, $\delta^{18}O$~~
806 ~~in *N. zibrowii* are much higher and are interpreted to be controlled by strong vital effects (Wisshak et~~
807 ~~al., 2008).~~ Contrary to other modern oyster studies (Surge and Lohmann, 2008; ~~Ullmann et al., 2010;~~
808 Titschack et al., 2010; Ullmann et al., 2010), Wisshak et al. (~~2008) do~~2009) report an isotopic offset
809 between vesicular and foliated calcite~~, but~~. However, $\delta^{18}O$ values in vesicular calcite of *N. zibrowii*
810 are ~~reported~~higher than in its foliated calcite, opposite to ~~what was observed in the specimens in~~
811 ~~this study~~*P. vesicularis* (**Figure 5**). ~~A~~Similarly, a strong negative ontogenetic trend in $\delta^{13}C$~~observed in~~
812 ~~the juvenile part of *N. zibrowii* records is again opposite to the trend in $\delta^{13}C$ observed in this study.~~
813 ~~This shows that the common explanation of incorporation of isotopically light CO_2 into the shell due~~
814 ~~to enhanced metabolic rate in the juvenile stage (e.g. Jones et al., 1986; Lorrain et al., 2005; Gillikin~~
815 ~~et al., 2007; Wisschak et al., 2008) does not explain the $\delta^{13}C$ trend in M6 and M11 shells in this study~~
816 ~~(**Figure 5**). Instead, any trends in $\delta^{13}C$ in these shells are most likely caused by the effects of sampling~~
817 ~~and incorporating recrystallized vesicular calcite into the stable isotope samples~~, which is ~~also~~
818 ~~evident from the elevated Fe concentrations in these shells. The fact that Fe concentrations in M11~~

819 ~~are highest in the ontogenetically oldest part of the record further confirms that the observed drop~~
820 ~~in stable isotope values towards the ontogenetically oldest part of this record is caused by~~
821 ~~diagenesis, and is not an ontogenetic trend. This is in agreement with work on~~ absent in *P.*
822 *vesicularis* and most extant oysters~~, in which such an ontogenetic trend is generally absent (~~ (**Figure**
823 **5**; Surge et al., 2001; Surge and Lohmann, 2008; Ullmann et al., 2010~~)~~.~~)~~, was observed in the juvenile
824 part of *N. zibrowii* records. While such a juvenile trend in δ¹³C is uncommon, trends later in life have
825 been reported for other taxa and are thought to be caused by increasing utilisation of isotopically
826 light metabolic carbon for shell calcification (Lorrain et al., 2004; Gillikin et al., 2007). The vast
827 difference in geochemical records between these closely related bivalve taxa ~~shows that vital~~
828 ~~effects~~(*Neopycnodonte* and *Pycnodonte*) shows that environmental setting and mode of life (growth
829 and metabolic rates) play a large role in ~~their mineralization~~governing vital effects. Geochemical
830 records in the shell of the deep-dwelling *N. zibrowii* are clearly strongly controlled by vital effects,
831 and ~~that independent control on the growth rates of these bivalves could be crucial in disentangling~~
832 ~~internal from external forcing in bivalve shells. In terms of their expression of proxy records~~both
833 shell chemistry and ~~their~~ environmental ~~niche, records from~~setting of *P. vesicularis* ~~shells obtained in~~
834 ~~this study~~ show much closer resemblance to ~~those of~~ *H. hyotis* and marine *Crassostrea gigas* (Surge
835 and Lohmann, 2008; Ullmann et al., 2010) than to those of *N. ~~zibrowii, making H. hyotis~~* ~~the best~~
836 ~~modern analogue to compare with records from shallow marine *Pycnodonte* shells~~zibrowii.

837 6.3.4 Timing of shell deposition and seasonality

838 The δ¹⁸O records of *H. hyotis* are strongly correlated with both Sea Surface Temperature (SST) and
839 Sea Surface Salinity (SSS; TItschak et al., 2010). The fact that δ¹⁸O values ~~of the specimens~~ in shells of
840 *H. hyotis* ~~studied by Titschak et al. (2010)~~ are higher than ~~the δ¹⁸O values of our specimens of~~ in *P.*
841 *vesicularis~~. Presumably, this~~* is likely because the ~~specimens studied by Titschak et al. (2010)~~former
842 grew in an environment characterized by ~~a strong evaporatic setting (~~net evaporative conditions
843 ~~(Safaga Bay). This setting likely resulted in a higher~~, Egypt). As a result, salinity and δ¹⁸O_{seawater}
844 ~~(~~+2.17‰~~)~~ ~~were higher~~ than in the Neuquén Basin (-2.8~~‰~~‰). Indeed, Woelders et al. (2017) argued
845 that the late Maastrichtian environmental setting of Bajada de Jaguël was influenced by freshwater
846 input, based on ~~clumped isotope results from well-preserved shells in this study). As a consequence,~~
847 ~~δ¹⁸O records H. hyotis in Titschack~~organic-walled dinoflagellate cysts, benthic foraminifera and
848 organic biomarker proxies. Crucially, the Neuquèn Basin is interpreted to have been characterized by
849 a strong summer precipitation maximum, suggesting that the lowest δ¹⁸O values in our yearstack
850 correspond to highest summer temperatures and lowest salinities (December - January). The δ¹⁸O
851 curve in our yearstack is strongly asymmetrical, the δ¹⁸O minimum peak being truncated. Such a
852 truncation potentially reflects slower growth or a growth stop in the summer season. We propose
853 that, while in modern oysters growth is often limited by low water temperature in the winter season
854 (e.g. Ullmann et al., ~~(2010) are strongly correlated with both Sea Surface Temperature (SST) and Sea~~
855 ~~Surface Salinity (SSS). Such an interplay~~2010, 2013), increased temperatures and low salinities in the
856 summer season of the Late Cretaceous Neuquèn Basin have limited growth of ~~salinity and~~
857 ~~temperature on stable isotope composition~~*P. vesicularis*. The effect of a similarly co-varying SSS and
858 SST on bivalve ~~calcite~~δ¹⁸O and δ¹³C has been studied in *Crassostrea virginica* ~~that grew~~growing under
859 changing salinity conditions (Surge et al., 2001). However, in contrast to estuarine *C. virginica*
860 studied by Surge et al. (2001), where both stable isotope records are in phase, the best preserved
861 specimen in our study (M0) presents a ~~(shifted)~~ ~~anti~~ phase relationship between δ¹⁸O and δ¹³C.
862 ~~Following~~Counterintuitively, following the rationale that ~~annual lows in δ¹³C occur in mid-summer in~~
863 ~~P. vesicularis, this would suggest that the lowest δ¹⁸O values are reached in spring (September-~~
864 ~~November). As δ¹⁸O is negatively correlated to temperature and positively correlated to salinity, this~~
865 ~~would suggest that δ¹⁸O_{shell} variations in our records are more strongly forced by changes~~the lowest

19

866 δ^{18}O values ~~in salinity rather than in temperature, since sea surface temperature is unlikely to be~~
867 ~~higher in spring than in summer. If so,~~ our record ~~suggests that the Neuquén basin experienced a~~
868 ~~decrease in salinity in the spring. Highest salinities are reached in summer and autumn and lowest~~
869 ~~salinities in winter to spring, possibly~~reflect to the summer precipitation maximum, the annual drop
870 in δ^{13}C, corresponding to ~~a winter-spring precipitation maximum similar to the present day situation~~
871 ~~at this latitude in this region (Servicio Meteorológico Nacional, 2017).~~months with the highest
872 planktonic food supply, would occur shortly after growth-limiting summer conditions (February -
873 March).

6.3.5 Palaeoproductivity

875 The ~~fact that a minimum~~coinciding of minima in Zn/Ca ~~coincides~~ with ~~a maximum~~maxima in S/Ca
876 and ~~δ^{13}C and a minimum~~minima in δ^{18}O in the well preserved M0 specimen (**Figure 5 and 6**) is in
877 agreement with the ~~proposed explanation~~interpretation of the~~se~~ seasonal
878 ~~records.~~palaeoproductivity cycle. Zn concentrations in bivalve shells drop during ~~a~~ productivity
879 bloom~~s~~, which ~~occurs~~occur late in the ~~spring~~summer season (~~September-November~~February-March;
880 Calvert and Pedersen, 1993; Jackson et al., 1993; Guo et al., 1997, de Winter et al., 2017a). ~~The~~
881 ~~observation that a minimum in Zn/Ca coincides with the lowest δ^{18}O values which occurred in spring~~
882 ~~and precedes the minimum in δ^{13}C that occurred in mid-summer is consistent with the hypothesis of~~
883 ~~spring blooms affecting~~Spring blooms affected the amount of bio-available Zn in the surface ocean
884 and ~~forcing~~forced a drop in Zn/Ca ratios in the shells of *P. vesicularis* (Guo et al., 2002). This
885 ~~explanation is further supported by the timing of the onset of the drop in Zn/Ca synchronous with a~~
886 ~~maximum in δ^{13}C. The annual δ^{13}C cycle in the closely related *H. hyotis* was also proposed to~~explains
887 why minima in Zn/Ca coincide with the lowest δ^{18}O values, which occur in summer and precede the
888 minima in δ^{13}C which reflect a seasonality in productivity ~~by Titschack et al. (2010), showing that the~~
889 ~~drop in Zn/Ca may indeed be related to a spring bloom in productivity.~~as in *H. hyotis*. Increased fresh
890 water input into the basin during ~~spring~~summer, which caused the warm, low salinity conditions ~~that~~
891 ~~are~~observed in the δ^{18}O records, could have provided the nutrients that initiated this productivity
892 bloom. ~~Seasonal decreases in salinity are in agreement with reconstructions by Woelders et al.~~
893 ~~(2017).~~

6.3.6 Physiological effects

895 The observed ~~anticorrelation~~anti-correlation between δ^{18}O and S/Ca in ~~specimen~~ M0 suggests that
896 S/Ca in *P. vesicularis*~~, S/Ca responds as a physiological parameter that co-varies with~~ responded to
897 seasonal changes~~, such as~~ in food availability, growth or respiration rate. ~~This response has also been~~
898 ~~inferred for~~In other groups of bivalves~~, where~~ S/Ca ratios were ~~considered~~shown to reflect periods
899 of high metabolic ~~rates~~rate and slow shell growth (e.g. Rosenberg and Hughes, 1991). ~~A peak in S/Ca~~
900 ~~during the spring season, when a productivity bloom coincides with a potential decrease in salinity is~~
901 ~~in agreement with this explanation. Such~~Similarly, environmental ~~perturbations affected the growth~~
902 ~~of the bivalve and~~stress, such as temperature or salinity extremes, have been linked to a decrease in
903 growth rate ~~an increase in the incorporation of sulphur into the organic matrix of the bivalve shell~~
904 (Lorens and Bender, 1980). ~~The fact~~Therefore, a peak in S/Ca during the summer season, when
905 growth rate presumably decreased, is in agreement with this explanation. The observation that the
906 amplitude of S/Ca variations in the record of M6 increases in the part of the shell where vesicular
907 calcite penetrates the shell hinge (**Figure 5**) supports the hypothesis that these disturbances of the
908 shell hinge indicate periods of physiological stress experienced by the bivalve (Müller, 1970).
909 ~~Interestingly, the year stack of specimen M0 shows a smaller second peak in Zn/Ca and S/Ca that~~
910 ~~coincides with autumn if the interpretation of phase relationships between records is correct. This~~
911 ~~may reflect a smaller productivity bloom in autumn. Similarly, a decrease in Sr/Ca ratios synchronous~~

912 ~~with the peak in $\delta^{13}C$ suggests a physiological origin of the seasonality in this proxy. The fact that~~
913 ~~Sr/Ca ratios are lower during the low-salinity, high-productivity spring season in which growth was~~
914 ~~probably slower is in agreement with relationships between Sr/Ca and growth rate found in modern~~
915 ~~bivalves (e.g. Lorrain et al., 2005; Gillikin et al., 2005a). As mentioned above, care must be taken to~~
916 ~~extrapolate these interpretations since they are based on only one well-preserved shell~~The anti-
917 phase relationship between S/Ca with Zn/Ca and $\delta^{13}C$ minima show that the productivity blooms
918 discussed above affected growth and metabolic rate in *P. vesicularis*.

919 Similarly, a decrease in Sr/Ca ratios synchronous with the peak in $\delta^{13}C$ suggests that both proxies are
920 controlled by physiology. The interpretation that Sr/Ca ratios are lower during the low-salinity
921 summer season in which growth was slower is in agreement with relationships between Sr/Ca and
922 growth rate found in modern bivalves (e.g. Gillikin et al., 2005a; Lorrain et al., 2005). However, if
923 Sr/Ca is indeed controlled by growth rate, one would expect to see an ontogenetic drift of Sr/Ca
924 towards lower ratios as the shell extends more slowly as the animal ages. Yet, this effect is not
925 clearly expressed by our specimens, indicating that either *P. vesicularis* did not exhibit such a
926 decreasing trend in growth rate with age or that the relationship between Sr/Ca and growth rate is
927 not straightforward.

928 **6.4 Temperature proxies**

929 An overview of all temperature proxies used in this study is plotted in **Figure 9**~~. This figure illustrates~~
930 ~~some of~~, illustrating the complexity of combining these different proxies in *P. vesicularis* to
931 reconstruct palaeoseasonality. Combination of the $\delta^{18}O_{sw}$ values reconstructed using clumped
932 isotope analysis with the high-resolution $\delta^{18}O$ records yields a ~~tentative~~ sub-annual
933 palaeotemperature reconstruction for all ~~shell~~ records. However, the variations in these records may
934 not reflect true sub-annual temperature variations, especially since it is likely that salinity in the
935 Neuquén Basin did not remain constant through the year (see ~~5~~6.3.4). ~~Temperature~~Clumped isotope
936 temperature reconstructions are similar to present-day average annual surface water temperatures
937 in the region (~10-15°C; Servicio Meteorológico Nacional, 2017), while they are below model and
938 proxy-based SST reconstructions for the Maastrichtian mid-latitudes (20-25°C; e.g. Donnadieu et al.,
939 2006; Brugger et al., 2017; O'Brien et al., 2017) and average air temperatures inferred for the
940 Maastrichtian Neuquén Basin based on ~~clumped isotope and $\delta^{18}O$ records are~~ the megathermal
941 vegetation (>24°; Barreda and Palazzesi, 2007; Palazzesi and Barreda, 2007; Barreda et al., 2012).
942 The systematically lower ~~than the TEX$_{86}$^{H}~~clumped isotope-based temperatures. ~~This offset~~ can
943 partially be explained by the fact that TEX$_{86}$^{H} is calibrated to sea surface temperatures while *P.*
944 *vesicularis* lived on the sea floor, at depths of 50-75 m ~~below sea level~~(Scasso et al., 2005~~), in~~). This
945 means that, while TEX$_{86}$^{H} reflects SSTs, the *P. vesicularis* clumped isotope-based temperatures reflect
946 the temperatures of the bottom waters ~~that were likely~~, which must have been slightly cooler than
947 those at the sea surface. However, this difference is ~~most~~ likely not enough to explain the offset of
948 ±15°C between clumped isotope and TEX$_{86}$^{H} temperature reconstructions. Over the past years,
949 several studies have highlighted the complexity of shallow marine TEX$_{86}$ records and have shown
950 that temperature reconstructions by this method may be biased (e.g. Jia et al~~-~~., 2017). Similarly, in
951 the compilation study of O'Brien et al. (2017), Cretaceous TEX$_{86}$-based sea surface temperatures are
952 systematically higher than planktic foraminiferal ~~δ~~$\delta^{18}O$-based temperatures. In some settings, TEX$_{86}$
953 ~~has been~~is shown to ~~predominantly reflect~~be biased towards summer temperatures (Schouten et
954 al., 2013). It is possible that the same bias also ~~in~~applies to the Neuqúen basin TEX$_{86}$^{H} ~~reconstructed~~
955 ~~temperatures are biased towards summer-season temperatures. In contrast~~reconstructions. On the
956 other hand, clumped isotope thermometry on ~~our~~ *P. vesicularis* ~~specimens reconstructs a~~relies on
957 bulk samples and yields mean value of the entire growth season of the bivalve. ~~Yet, it is likely~~

21

958 ~~that~~Since growth in ~~these bivalves~~*P. vesicularis* seems to have slowed or ceased during the spring
959 and summer season (~~as is evident from Sr/Ca ratios, see 5~~6.3.6). The year stack in **Figure 8** also
960 ~~shows that low δ¹⁸O values make up a much smaller portion of the year than the higher δ¹⁸O values,~~
961 ~~suggesting a growth stop~~4 and 6.3.6), summer temperatures are likely underrepresented in the ~~low~~
962 ~~δ¹⁸O season.~~clumped isotope reconstructions, biasing them towards lower temperatures. It is
963 therefore likely that ~~temperature reconstructions of both clumped isotope thermometry and TEX₈₆ᴴ~~
964 ~~measurements are seasonally biased and that~~ the mean annual temperature in this setting lies in
965 between ~~these two~~clumped isotope thermometry and TEX₈₆ᴴ estimates. ~~Alternatively, more~~
966 ~~vesicular calcite might have been incorporated~~Another source of bias for clumped isotope
967 thermometry on bulk samples is the incorporation of diagenetically altered vesicular calcite into the
968 shell hinge as a result of more stressful growth conditions (Müller, 1970; see 5~~6~~.2.1~~) causing these~~
969 ~~warm seasons to be selectively overprinted by diagenesis. Indeed, this seems to be the case in the~~
970 ~~record of M4, where low values in δ¹⁸O, associated with the spring season, are more characterized~~
971 ~~by diagenetic alteration than parts of the year (**Figure 9**). If vesicular calcite is avoided in clumped~~
972 ~~isotope sampling, this will cause a bias towards colder seasons for clumped isotope~~). However, this
973 would have biased the reconstruction towards higher temperatures~~. However, in~~, while the opposite
974 is observed. In practice it will be difficult to avoid these lobes of vesicular calcite and small amounts
975 are likely to be included in clumped isotope samples, leading to higher palaeotemperature
976 reconstructions.

977 ~~As mentioned above,~~While several temperature calibrations exist for Mg/Ca ratios in bivalves~~,~~. ~~T~~the
978 most likely candidates for temperature reconstruction based on Mg/Ca of *P. vesicularis* are the
979 calibrations based on other ostreid bivalves. ~~Promising examples are~~A good candidate would be the
980 ~~calibrations~~calibration by Surge and Lohmann (2008; based on *Crassostrea virginica*). An alternative
981 calibration by Mouchi et al. (2013~~,~~) was based on juvenile specimens of the pacific oyster
982 *Crassostrea gigas*~~) and Surge and Lohmann (2008; based on *Crassostrea virginica*). A factor that~~
983 ~~complicates the interpretation of~~ and is probably not suitable for application on records from
984 gerontic specimens. The Mg/Ca ~~ratios in terms of temperature is the fact that sea~~ratio of ocean
985 water ~~Mg/Ca~~(Mg/Ca_ocean) has changed drastically over geological timescales, and is thought to have
986 been much lower in the late Maastrichtian than in the present-day ocean (~~Maastrichtian Mg/Ca_ocean~~
987 ~~of~~ 1-2 mol/mol compared to 5 mol/mol in the modern ocean; Stanley and Hardie, 1998; Coggon et
988 al., 2010). This ~~complicates the use of modern transfer functions which were established for bivalves~~
989 ~~growing in modern ocean conditions. Since these changing ocean compositions have~~difference most
990 likely influenced Mg/Ca ratios in calcifying organisms (Lear et al., 2015), ~~temperature calibrations~~
991 ~~need~~and needs to be corrected ~~accordingly~~for (de Winter et al., 2017a~~). Therefore, here,~~) when
992 applying the Mg/~~Ca_ocean ratios of ~1.5 mol/mol were used to represent average Maastrichtian ocean~~
993 ~~water, about 3.3 times lower than in the modern ocean~~Ca thermometer. With this correction, the *C.*
994 *virginica* temperature calibration by Surge and Lohmann (2008; **Figure 9**) approach reconstructions
995 based on the other proxies in terms of temperature seasonality, ~~while the calibration of Mouchi et~~
996 ~~al. (2013) seems to significantly overestimate temperature (MAT >60°C). Reconstructions based on~~
997 ~~the Mg/Ca calibration of Surge and Lohmann (2008) yield~~yielding sea water temperatures ~~(~~of 20°C ±
998 10°C~~)~~, slightly higher than those observed in the δ¹⁸O_sw-corrected δ¹⁸O record.

999 Since Mg/Ca ratios yield temperatures between clumped isotope and TEX₈₆ᴴ reconstructions, it is
1000 ~~tentative~~tempting to assume that they more closely ~~represent~~approximate mean annual
1001 temperatures than the other proxies. However, while the seasonal bias caused by growth cessations
1002 in *P. vesicularis* should affect Mg/Ca as much as δ¹⁸O, there are large differences (>10°C) between
1003 temperature reconstructions of Mg/Ca and δ¹⁸O in some parts of the records. ~~Furthermore, the well~~
1004 ~~preserved M0 shell record shows an anticorrelation between the seasonal fluctuations of the two~~

1005 ~~temperature records in parts of the~~Moreover, Mg/Ca ratios and $\delta^{18}O$ are anti-correlated in parts of

1006 the well-preserved M0 record, suggesting that at least one of the proxies may largely be controlled

1007 by a factor other than ambient temperature ~~(although phasing arguments may be affected by the~~

1008 ~~relative scaling of trace element and stable isotope records)~~. Seasonal changes in salinity cannot

1009 account for this difference between the proxies, ~~as a seasonal increase in salinity of approximately~~

1010 ~~20 PSU would be required to account for the offset in temperature between the proxies (Ravelo and~~

1011 ~~Hillaire-Marcel, 2007). Such a severe~~since an unrealistic change in salinity would be required, which

1012 is not consistent with earlier palaeoenvironmental reconstructions in the Neuquén Basin (Prámparo

1013 et al. 1996; Prámparo and Papú 2006; ~~Woelders et al. 2017). Additionally, there seems to be no a~~

1014 ~~priori reason why Mg/Ca temperature calibration of Surge and Lohmann (2008) would be the most~~

1015 ~~suitable calibration for P. vesicularis, which may require its own species-specific calibration. If~~

1016 ~~seasonal growth cessations are present in P. vesicularis, they would affect Mg/Ca as well as $\delta^{18}O$ and~~

1017 ~~cause Mg/Ca records to have the same seasonal bias. It must be noted that the fact that trace~~

1018 ~~element records and stable isotope records were measured using different methods makes it~~

1019 ~~possible that the records are slightly shifted with respect to each other (see section 4.5). As a~~

1020 ~~consequence, phase relationships between Mg/Ca and $\delta^{18}O$ temperature reconstructions may have~~

1021 ~~been distorted. Closer observation of **Figure 9** indeed shows that temperature reconstructions based~~

1022 ~~on these two records are in some cases shifted with respect to each other. This might explain part of~~

1023 ~~the offset between the reconstructions and render Mg/Ca temperatures more probable.~~Ravelo and

1024 Hillaire-Marcel, 2007; Woelders et al., 2017). The shift between Mg/Ca and $\delta^{18}O$ records may also be

1025 a result of the relative scaling and aligning of records measured using two different methods.

1026 Nevertheless, the uncertainties of Mg/Ca temperature reconstructions in bivalves, together with the

1027 observed lack of temperature dependence of Mg/Ca ratios in the closely related ~~*Pycnodonte*~~*N.*

1028 *zibrowii*~~, leads to the conclusion~~ shows that temperature reconstructions based on Mg/Ca ratios in

1029 *Pycnodonte* oysters are ~~difficult~~probably not very robust.

1030 ~~In summary, $\delta^{18}O$ values in the shells of P. vesicularis have been shown to vary with changes in~~

1031 ~~salinity in this setting. Temperatures reconstructed by clumped isotope thermometry from well-~~

1032 ~~preserved parts of different bivalve shells agree and seem to be the most reliable method for~~

1033 ~~temperature reconstruction. These clumped isotope temperature reconstructions are in agreement~~

1034 ~~with present day average annual temperatures in the region (~10-15°C; Servicio Meteorológico~~

1035 ~~Nacional, 2017), while they are slightly below model and proxy-based SST reconstructions for the~~

1036 ~~Maastrichtian mid-latitudes (20-25°C; e.g.~~Based on these observations, the~~Donnadieu et al., 2006;~~

1037 ~~Brugger et al., 2017; O'Brien et al., 2017). Comparison of all palaeotemperature proxies in this study~~

1038 ~~shows that TEX$_{86}$^{H} temperature reconstructions (27-30°C) likely overestimate MAT, while clumped~~

1039 ~~isotope thermometry might underestimate it. Mg/Ca temperature reconstructions show promising~~

1040 ~~results (15-20°C), but depend heavily on the calibration that is used and are therefore considered~~

1041 ~~problematic. The~~ best approach to reconstruct palaeotemperature seasonality from *Pycnodonte*

1042 shells would be to microsample the foliated calcite of the shells for clumped isotope analysis. This

1043 microsampling can be guided by records of conventional stable isotope ratios and trace element

1044 concentrations to ensure the sampling of material from different seasons. Via this approach, both

1045 seasonality in temperature and salinity can be reconstructed from *Pycnodonte* shells, and the effects

1046 of salinity and temperature on $\delta^{18}O$ values can be disentangled.

1047 **7. Conclusions and recommendations**

1048 ~~This study represents a first attempt to employ the shells of the honeycomb oyster *Pycnodonte*~~

1049 ~~*vesicularis* for the reconstruction of late Maastrichtian palaeoseasonality.~~ The multi-proxy approach

1050 applied in this work demonstrates the complexity of ~~such attempts to reconstruct~~

Formatted: Font: Not Bold, No underline

23

1051 palaeoenvironmental ~~conditions. Yet, this approach also demonstrates the value of using a range of~~
1052 ~~different methods to characterize the preservation state and chemical composition of fossil bivalve~~
1053 ~~calcite.~~reconstruction on the seasonal scale. Based on ~~the results presented in~~ this ~~work~~study,
1054 several recommendations can be made for the use of ~~shells from~~ *P. vesicularis* shells for ~~the~~
1055 ~~reconstruction of~~ palaeoseasonality and palaeoenvironment reconstruction. Detailed analysis of
1056 shell structure and preservation shows that shells of *P. vesicularis*, like other species of the Order
1057 Ostreoida, are characterized by two major micromorphologies of calcite, which were referred to by
1058 Carriker et al. (1980b) as "chalky" and "foliated" calcite. In the case of *P. vesicularis*, CT scanning
1059 shows that these "chalky" (vesicular) calcite layers are ~~characterized by a high degree of porosity~~
1060 very porous (up to 65%) and ~~are therefore very~~ permeable for pore fluids (**Figure 4**~~). The thin walls~~
1061 ~~of the vesicular calcite structure provide a lot of surface contact between permeating pore fluid and~~
1062 ~~the calcite,~~), making it prone to recrystallization (**Figure 3**). ~~The recrystallization and the precipitation~~
1063 ~~of secondary carbonates in~~The presence of bore holes, such as those made by polychaete worms,
1064 facilitates this ~~porous micromorphology therefore~~penetration of pore fluids. Its susceptibility to
1065 diagenesis renders the vesicular calcite of pycnodontein bivalves poorly suitable for
1066 palaeoenvironmental reconstruction. Foliated calcite layers in the shell hinge of *P.* ~~In addition, pore~~
1067 ~~fluid can enter the shells of *P. vesicularis* post mortem through bore holes, for example made by~~
1068 ~~polychaete worms. Subsequently,~~vesicularis are less affected by diagenesis and seem to preserve
1069 primary calcite, making it suitable for palaeoseasonality reconstructions. However, lobes of vesicular
1070 calcite can extend into the hinge of the shells and complicate palaeoseasonality reconstructions
1071 based on stable and clumped isotope measurements. Highly localized recrystallization and
1072 precipitation of secondary carbonates in equilibrium with these reducing pore fluids incre~~a~~ses the
1073 concentrations of Mn and Fe (see XRF mapping and CL images in **Figure 3**) and lowers stable isotope
1074 ratios. ~~Hence, when selecting specimens of *P. vesicularis* for palaeoseasonality reconstructions,~~
1075 ~~specimens affected by boring organisms are best avoided or treated with care. Micro~~Hence, micro-
1076 analytical techniques such as cathodoluminescence microscopy, optical microscopy and µXRF
1077 mapping ~~allows to avoid~~allow these zones of recrystallization~~.~~ to be avoided.

1078 Palaeoseasonality reconstructions based on shells of *P. vesicularis* or other gryphaeid shells that
1079 contain multiple microstructures~~Foliated calcite layers in the shell hinge of *P. vesicularis* are less~~
1080 ~~affected by these diagenetic processes and stable isotope, clumped isotope and trace element~~
1081 ~~compositions of these layers suggest preservation of primary calcite, making it suitable for~~
1082 ~~palaeoseasonality reconstruction. However, care must be taken in sampling these parts of the shells~~
1083 ~~of *P. vesicularis*, as lobes of vesicular calcite can extend into the hinge of the shells. Such lobes of~~
1084 ~~vesulicar calcite can be very thin, and can be difficult to avoid while microsampling for stable isotope~~
1085 ~~ratios. Incorporation of vesicular calcite into stable isotope samples will significantly alter the~~
1086 ~~measured stable isotope ratios and influence the interpretation of palaeoseasonality. Clumped~~
1087 ~~isotope analysis of samples containing this vesicular calcite yield much higher temperatures than~~
1088 ~~samples of foliated calcite, suggesting diagenetic overprinting of the stable isotope signal. The multi-~~
1089 ~~proxy approach in this study allows the distinction of diagenetic parts in fossil bivalve shells and aids~~
1090 ~~in the evasion of diagenetically altered parts of the shells and the consideration of only well-~~
1091 ~~preserved parts.~~

1092 ~~Future work on *P. vesicularis* shells, as well as other gryphaeid shells that contain multiple~~
1093 ~~microstructures, aiming at the reconstruction of palaeoseasonality over geological time scales~~
1094 should benefit from the application of a multi-proxy approach that allows the interpretation of
1095 seasonally changing environmental parameters. ~~However, the establishment of a shell chronology~~
1096 ~~from these records can be difficult, as~~However, selective diagenetic overprinting, the occurrence of
1097 growth cessations and the complexity of synchronizing proxy records from multiple methods can

24

1098 complicate the interpretation of phase relationships between proxies. Multi-proxy analysis on one
1099 exceptionally well-preserved specimen demonstrates how the timing of seasonal deposition of the
1100 shell could be determined from the phase relationships between proxies. ~~If applied correctly, this~~
1101 ~~approach also allows the separation of the effects of, for example, temperature~~Stable and ~~salinity on~~
1102 ~~the stable~~clumped isotope ~~ratios in the shells. However, it must be noted that extrapolation of~~
1103 ~~results from one well-preserved specimen means that the interpretation of phase relationships in~~
1104 ~~this study must remain tentative. Even though the establishment of shell chronology for less well-~~
1105 ~~preserved samples is difficult, multi-proxy~~ records ~~from well-preserved parts of these shells can still~~
1106 ~~yield information about the sub-annual variation of proxies in P. vesicularis. Comparison of these~~
1107 ~~multi-proxy shell records with contextual proxy reconstructions allows palaeoseasonality~~
1108 ~~reconstructions to be placed in a larger geological context and allows the discussion of different~~
1109 ~~palaeotemperature proxies.~~

1110 ~~Records of uncontaminated~~of primary foliated calcite in the hinge of ~~well-preserved specimens of~~ P.
1111 vesicularis yield a ~~mean~~$\delta^{18}O_{seawater}$ of -2.8‰ indicative of seasonal freshwater input into the
1112 Neuquén Basin. Mean annual sea water ~~temperature in the late Maastrichtian Neuquén Basin~~
1113 ~~of~~temperatures were 11°C based on clumped isotope thermometry, which is much lower than
1114 reconstructions based on contextual TEX_{86}^H palaeothermometry ~~(±(~~27.3°C~~). This comparison~~
1115 ~~suggests~~ ± 2.5°C). We conclude that the TEX_{86}^H method likely overestimates mean annual
1116 temperatures in this setting, possibly representing summer surface water temperatures. Clumped
1117 isotope thermometry of bulk foliated calcite samples likely underestimates the annual mean
1118 because the warm spring and early summer season is underrepresented in the shells due to slower
1119 growth or growth cessations. A seasonality in $\delta^{18}O$ of about 1‰ is ascribed to a combination of
1120 decreased salinity by fresh water input in the ~~spring~~summer season and a moderate temperature
1121 seasonality~~, but the aforementioned seasonal bias prevents capture of the full seasonal cycle in this~~
1122 ~~record~~. Attempts to verify the seasonality in SST by Mg/Ca ratios of shell calcite are complicated by
1123 uncertainties about vital effects on the incorporation of Mg into the bivalve shell. ~~After correction~~
1124 ~~for lower sea water Mg/Ca ratios in the Late Cretaceous, Mg~~Records of Zn/Ca, S/Ca ~~temperatures~~
1125 ~~calculated using the oyster-based calibration of Surge~~ and ~~Lohmann (2008) fall between~~
1126 ~~temperatures of clumped isotope palaeothermometry and those of TEX_{86}^H palaeothermometry and~~
1127 ~~reveal a pattern similar to the δ^{18}O records. While it is tentative to conclude~~$\delta^{13}C$ show that ~~this~~
1128 ~~record most closely reconstructs the temperature seasonality, the uncertainties involved~~ the warm,
1129 low salinity summer season is followed by a peak in productivity which influenced the chemistry of
1130 the sea water in ~~bivalve Mg/Ca records precludes such a straightforward conclusion.~~

1131 ~~This multi-proxy work shows that, even using several independent palaeotemperature~~
1132 ~~reconstruction methods, the~~which P. vesicularis lived. The reconstruction of temperature seasonality
1133 from fossil bivalve calcite is ~~strongly~~ complicated by the influence of other palaeoenvironmental
1134 parameters that affect the chemistry of bivalve shells. Yet, the successful application of clumped
1135 isotope thermometry on fossil bivalve calcite in this study indicates that temperature seasonality in
1136 fossil ostreid bivalves may be constrained by the sequential analysis of foliated calcite samples using
1137 this method.

1138

References

Abele, D., Brey, T., Philipp, E., 2009. Bivalve models of aging and the determination of molluscan lifespans. Experimental gerontology 44, 307–315, 2009.

Al-Aasm, I.S., Veizer, J., 1986. Diagenetic stabilization of aragonite and low-Mg calcite, I. Trace elements in rudists. Journal of Sedimentary Research 56, 1986a.

Al-Aasm, I.S., Veizer, J., Diagenetic stabilization of aragonite and low-Mg calcite, II. Stable isotopes in rudists. Journal of Sedimentary Research 56, 1986b.

Andrews, J.E., Tandon, S.K., Dennis, P.F., 1995. Concentration of carbon dioxide in the Late Cretaceous atmosphere. Journal of the Geological Society 152, 1–3, 1995.

Ayyasami, K., 2006. Role of oysters in biostratigraphy: A case study from the Cretaceous of the Ariyalur area, southern India. Geosciences Journal 10, 237–247, 2006.

Baldoni, A.M., 1992. Palynology of the lower lefipan formation (upper cretaceous) of barranca de los perros, chubut province, Argentina. part I. Cryptogam spores and gymnosperm pollen. Palynology 16, 117–136, 1992.

Banner, J.L., Hanson, G.N., Calculation of simultaneous isotopic and trace element variations during water-rock interaction with applications to carbonate diagenesis. Geochimica et Cosmochimica Acta 54, 3123–3137, 1990.

Barbin, V., 2000. Cathodoluminescence of carbonate shells: biochemical vs diagenetic process, in: Cathodoluminescence in Geosciences. Springer, pp. 303–329, 2000.

Barreda, V., Palazzesi, L., 2007. Patagonian vegetation turnovers during the Paleogene-early Neogene: origin of arid-adapted floras. The botanical review 73, 31–50, 2007.

Barreda, V.D., Cúneo, N.R., Wilf, P., Currano, E.D., Scasso, R.A., Brinkhuis, H., 2012. Cretaceous/Paleogene floral turnover in Patagonia: drop in diversity, low extinction, and a *Classopollis* spike. PLoS One 7, e52455, 2012.

Berner, R., 1990. Atmospheric carbon dioxide levels over Phanerozoic time. Science 249, 1382–1386, 1990.

Bertels, A., 2013. Micropaleontología y estratigrafía del límite Cretácico-Terciario en Huantrai-co (provincia de Neuquén). Ostracoda. Parte 1: Cytherellidae, Bairdiidae, Pontocypridinae, Buntoniinae y Trachyleberidinae (pro parte). Ameghiniana 5, 279–298, 2013.

Bieler, R., Mikkelsen, P.M., Lee, T., Foighil, D.Ó., 2004. Discovery of the Indo-Pacific oyster *Hyotissa hyotis* (Linnaeus, 1758) in the Florida Keys (Bivalvia: Gryphaeidae). Molluscan Research 24, 149–159, 2004.

Brand, U., Veizer, J., 1981. Chemical diagenesis of a multicomponent carbonate system-2: stable isotopes. Journal of Sedimentary Research 51.

Brand, U., Veizer, J., 1980. Chemical diagenesis of a multicomponent carbonate system–1: Trace elements. Journal of Sedimentary Research 50, 1980.

Brezina, S.S., Romero, M.V., Casadío, S., Bremec, C., 2014. Boring Polychaetes Associated with *Pycnodonte* (Phygraea) *Vesicularis* (Lamarck) from the Upper Cretaceous of Patagonia. A Case of Commensalism? Ameghiniana 51, 129–140, 2014.

Brugger, J., Feulner, G., Petri, S., 2017. Baby, it's cold outside: Climate model simulations of the effects of the asteroid impact at the end of the Cretaceous: Chicxulub impact cooling. Geophysical Research Letters 44, 419–427. doi:10.1002/2016GL072241, 2017.

Butler, P.G., Wanamaker, A.D., Scourse, J.D., Richardson, C.A., Reynolds, D.J., Variability of marine climate on the North Icelandic Shelf in a 1357-year proxy archive based on growth increments in the bivalve *Arctica islandica*. Palaeogeography, Palaeoclimatology, Palaeoecology 373, 141–151, 2013.

Calmano, W., Hong, J., Förstner, U., Binding and mobilization of heavy metals in contaminated sediments affected by pH and redox potential. Water science and technology 28, 223–235, 1993.

Calvert, S.E., Pedersen, T.F., 1993. Geochemistry of Recent oxic and anoxic marine sediments: Implications for the geological record. Marine Geology, Marine Sediments, Burial, Pore Water Chemistry, Microbiology and Diagenesis 113, 67–88. doi:10.1016/0025-3227(93)90150-T, 1993.

Carré, M., Bentaleb, I., Blamart, D., Ogle, N., Cardenas, F., Zevallos, S., Kalin, R.M., Ortlieb, L., Fontugne, M., 2005. Stable isotopes and sclerochronology of the bivalve *Mesodesma donacium*: potential application to Peruvian paleoceanographic reconstructions. Palaeogeography, Palaeoclimatology, Palaeoecology 228, 4–25, 2005.

Carriker, Melbourne R., Palmer, R.E., Sick, L.V., Johnson, C.C., 1980a. Interaction of mineral elements in sea water and shell of oysters (Crassostrea virginica (Gmelin)) cultured in controlled and natural systems. Journal of experimental marine biology and ecology 46, 279–296, 1980a.

Carriker, M.R., Palmer, R.E., Prezant, R.S., 1980b. Ultrastructural morphogenesis of prodissoconch and early dissoconch valves of the oyster *Crassostrea virginica*. College of Marine Studies, University of Delaware, 1980b.

Chauvaud, L., Lorrain, A., Dunbar, R.B., Paulet, Y.-M., Thouzeau, G., Jean, F., Guarini, J.-M., Mucciarone, D., 2005. Shell of the Great Scallop *Pecten maximus* as a high-frequency archive of paleoenvironmental changes. Geochemistry, Geophysics, Geosystems 6, 2005.

Chinzei, K., Seilacher, A., 1993. Remote Biomineralization I: Fill skeletons in vesicular oyster shells.(With 7 figures in the text). Neues Jahrbuch fur Geologie und Palaontologie-Abhandlungen 190, 349–362, 1993.

Cleroux, C., Cortijo, E., Anand, P., Labeyrie, L., Bassinot, F., Caillon, N., Duplessy, J.-C., 2008. Mg/Ca and Sr/Ca ratios in planktonic foraminifera: Proxies for upper water column temperature reconstruction. Paleoceanography 23.

Coggon, R.M., Teagle, D.A., Smith-Duque, C.E., Alt, J.C., Cooper, M.J., 2010. Reconstructing past seawater Mg/Ca and Sr/Ca from mid-ocean ridge flank calcium carbonate veins. Science 327, 1114–1117, 2010.

Crippa, G., Angiolini, L., Bottini, C., Erba, E., Felletti, F., Frigerio, C., Hennissen, J.A.I., Leng, M.J., Petrizzo, M.R., Raffi, I., Seasonality

fluctuations recorded in fossil bivalves during the early Pleistocene: implications for climate change. Palaeogeography, Palaeoclimatology, Palaeoecology 446, 234–251, 2016.

Daëron, M., Blamart, D., Peral, M., Affek, H.P., Absolute isotopic abundance ratios and the accuracy of Δ_{47} measurements. Chemical Geology 442, 83–96, 2016.

Dale, A., John, C.M., Mozley, P.S., Smalley, P.C., Muggeridge, A.H., 2014. Time-capsule concretions: unlocking burial diagenetic processes in the Mancos Shale using carbonate clumped isotopes. Earth and Planetary Science Letters 394, 30–37, 2014.

de Winter, N.J., Zeeden, C., Hilgen, F.J., 2014. Low-latitude climate variability in the Heinrich frequency band of the Late Cretaceous greenhouse world. Climate of the Past 10, 1001–1015. doi:10.5194/cp-10-1001-2014, 2014.

de Winter, N.J., Claeys, P., 2016. Micro X-ray fluorescence (µXRF) line scanning on Cretaceous rudist bivalves: A new method for reproducible trace element profiles in bivalve calcite. Sedimentology. doi:10.1111/sed.12299, 2016.

de Winter, N.J., Goderis, S., Dehairs, F., Jagt, J.W.M., Fraaije, R.H.B., Van Malderen, S.J.M., Vanhaecke, F., Claeys, P., 2017a Tropical seasonality in the late Campanian (Late Cretaceous): Comparison between multiproxy records from three bivalve taxa from Oman. Palaeogeography, Palaeoclimatology, Palaeoecology, https://doi.org/10.1016/j.palaeo.2017.07.031, 2017a.

de Winter, N.J., Sinnesael, M., Makarona, C., Vansteenberge, S., Claeys, P., 2017b. Trace element analyses of carbonates using portable and micro-X-ray fluorescence: Performance and optimization of measurement parameters and strategies. Journal of Analytical Atomic Spectrometry, 2017b.

Defliese, W.F., Hren, M.T., Lohmann, K.C., 2015. Compositional and temperature effects of phosphoric acid fractionation on Δ 47 Δ_{47} analysis and implications for discrepant calibrations. Chemical Geology 396, 51–60, 2015.

Dennis, K.J., Affek, H.P., Passey, B.H., Schrag, D.P., Eiler, J.M., 2011. Defining an absolute reference frame for "clumped" isotope studies of CO 2. Geochimica et Cosmochimica Acta 75, 7117–7131.

Dettman, D.L., Kohn, M.J., Quade, J., Ryerson, F.J., Ojha, T.P., Hamidullah, S., 2001. Seasonal stable isotope evidence for a strong Asian monsoon throughout the past 10.7 my Myr. Geology 29, 31–34, 2001.

Dettman, D.L., Lohmann, K.C., Seasonal Change in Paleogene Surface Water δ^{18}O: Fresh-Water Bivalves of Western North America. Climate change in continental isotopic records 153–163, 1993.

Dettman, D.L., Lohmann, K.C., 2000. Oxygen isotope evidence for high-altitude snow in the Laramide Rocky Mountains of North America during the Late Cretaceous and Paleogene. Geology 28, 243–246. doi:10.1130/0091-7613(2000)28<243:OIEFHS>2.0.CO;2, 2000.

Dettman, D.L., Lohmann, K.C., 1993. Seasonal Change in Paleogene Surface Water δ18O: Fresh-Water Bivalves of Western North America. Climate change in continental isotopic records 153–163.

Dlugokencky, E., Tans P., 2017. NOAA/ESRL (www.esrl.noaa.gov/gmd/ccgg/trends/), accessed 31/01/2017.

Dodd, J.R., Crisp, E.L., 1982. Non-linear variation with salinity of Sr/Ca and Mg/Ca ratios in water and aragonitic bivalve shells and implications for paleosalinity studies. Palaeogeography, Palaeoclimatology, Palaeoecology 38, 45–56, 1982.

Donnadieu, Y., Pierrehumbert, R., Jacob, R., Fluteau, F., 2006. Modelling the primary control of paleogeography on Cretaceous climate. Earth and Planetary Science Letters 248, 426–437. doi:10.1016/j.epsl.2006.06.007, 2006

Dreier, A., Loh, W., Blumenberg, M., Thiel, V., Hause-Reitner, D., Hoppert, M., 2014. The isotopic biosignatures of photo-vs. thiotrophic bivalves: are they preserved in fossil shells? Geobiology 12, 406–423, 2014.

Duinker, J.C., Nolting, R.F., Michel, D., 1982. Effects of salinity, pH and redox conditions on the behaviour of Cd, Zn, Ni and Mn in the Scheldt estuary. Thalassia Jugosl 18, 191–202, 1982.

Dunbar, R.B., Wefer, G., 1984. Stable isotope fractionation in benthic foraminifera from the Peruvian continental margin. Marine Geology 59, 215–225, 1984.

Ekart, D.D., Cerling, T.E., Montanez, I.P., Tabor, N.J., 1999. A 400 million year carbon isotope record of pedogenic carbonate: implications for paleoatmospheric carbon dioxide. American Journal of Science 299, 805–827, 1999.

Elliot, M., Welsh, K., Chilcott, C., McCulloch, M., Chappell, J., Ayling, B., 2009. Profiles of trace elements and stable isotopes derived from giant long-lived *Tridacna gigas* bivalves: potential applications in paleoclimate studies. Palaeogeography, Palaeoclimatology, Palaeoecology 280, 132–142, 2009.

Folk, R.L., Land, L.S., 1975. Mg/Ca ratio and salinity: two controls over crystallization of dolomite. AAPG bulletin 59, 60–68, 1975.

Fossilworks.org: Pycnodonte genus, age range and distribution. Retrieved 14-02-2017

Freitas, P., Clarke, L.J., Kennedy, H., Richardson, C., Abrantes, F., 2005. Mg/Ca, Sr/Ca, and stable-isotope (δ^{18}O δ 18 O δ18O and δ^{13}C δ 13 C δ13C) ratio profiles from the fan mussel *Pinna nobilis* : Seasonal records and temperature relationships: *PINNA NOBILIS Pinna Nobilis* RATIO PROFILES. Geochemistry, Geophysics, Geosystems 6, n/a-n/a. doi:10.1029/2004GC000872, 2005

Freitas, P.S., Clarke, L.J., Kennedy, H., Richardson, C.A., Abrantes, F., 2006. Environmental and biological controls on elemental (Mg/Ca, Sr/Ca and Mn/Ca) ratios in shells of the king scallop *Pecten maximus*. Geochimica et Cosmochimica Acta 70, 5119–5133. doi:10.1016/j.gca.2006.07.029, 2006.

Freitas, P.S., Clarke, L.J., Kennedy, H.A., Richardson, C.A., 2008. Inter-and intra-specimen variability masks reliable temperature control on shell Mg/Ca ratios in laboratory and field cultured *Mytilus edulis* and *Pecten maximus* (bivalvia). Biogeosciences Discussions 5, 531–572, 2008.

Friedman, I., O'NEIL, J., CEBULA, G., 1982. Two New Carbonate Stable-Isotope Standards. Geostandards Newsletter 6, 11–12.

Friedrich, O., Norris, R.D., Erbacher, J., 2012. Evolution of middle to Late Cretaceous oceans—a 55 my record of Earth's temperature and carbon cycle. Geology 40, 107–110, 2012.

Geist, J., Auerswald, K., Boom, A., 2005. Stable carbon isotopes in freshwater mussel shells: Environmental record or marker for metabolic activity? Geochimica et Cosmochimica Acta 69, 3545–3554, 2005.

Gillikin, D.P., De Ridder, F., Ulens, H., Elskens, M., Keppens, E., Baeyens, W., Dehairs, F., 2005a. Assessing the reproducibility and reliability of estuarine bivalve shells (*Saxidomus giganteus*) for sea surface temperature reconstruction: implications for paleoclimate studies. Palaeogeography, Palaeoclimatology, Palaeoecology 228, 70–85, 2005a.

Gillikin, D.P., Lorrain, A., Meng, L., Dehairs, F., 2007. A large metabolic carbon contribution to the δ 13 C record in marine aragonitic bivalve shells. Geochimica et Cosmochimica Acta 71, 2936–2946.

Gillikin, D.P., Lorrain, A., Navez, J., Taylor, J.W., André, L., Keppens, E., Baeyens, W., Dehairs, F., 2005b. Strong biological controls on Sr/Ca ratios in aragonitic marine bivalve shells. Geochemistry, Geophysics, Geosystems 6, 2005b.

Gillikin, D.P., Lorrain, A., Bouillon, S., Willenz, P., Dehairs, F., Stable carbon isotopic composition of Mytilus edulis shells: relation to metabolism, salinity, δ^{13}C$_{DIC}$ and phytoplankton. Organic Geochemistry 37, 1371–1382, 2006.

Gillikin, D.P., Lorrain, A., Meng, L., Dehairs, F., A large metabolic carbon contribution to the δ^{13}C record in marine aragonitic bivalve shells. Geochimica et Cosmochimica Acta 71, 2936–2946, 2007.

Gillikin, D.P., Lorrain, A., Paulet, Y.-M., André, L., Dehairs, F., 2008. Synchronous barium peaks in high-resolution profiles of calcite and aragonite marine bivalve shells. Geo-Marine Letters 28, 351–358, 2008.

Goodwin, D.H., Flessa, K.W., Schöne, B.R., Dettman, D.L., 2001. Cross-calibration of daily growth increments, stable isotope variation,

27

and temperature in the Gulf of California bivalve mollusk *Chione cortezi*: implications for paleoenvironmental analysis. Palaios 16, 387–398, 2001.

Grossman, E.L., Ku, T.-L., 1986. Oxygen and carbon isotope fractionation in biogenic aragonite: temperature effects. Chemical Geology: Isotope Geoscience section 59, 59–74, 1986.

Guo, T., DeLaune, R.D., Patrick, W.H., 1997. The influence of sediment redox chemistry on chemically active forms of arsenic, cadmium, chromium, and zinc in estuarine sediment. Environment International 23, 305–316, 1997.

Gutiérrez-Zugasti, I., Clarke, L.J., Garcia-Escárzaga, A., Suárez-Revilla, R., G.N., González-Morales, M. Changes in seawater temperatures in northern Iberia during the Late Pleistocene and Early Holocene. 22nd Annual Meeting of the EAA 2016, TH5-13, Abstract 4, September 3, 2016.

Habermann, D., 2002. Quantitative cathodoluminescence (CL) spectroscopy of minerals: possibilities and limitations. Mineralogy and Petrology 76, 247–259, 2002.

Hallmann, N., Burchell, M., Brewster, N., Martindale, A., Schöne, B.R., 2013. Holocene climate and seasonality of shell collection at the Dundas Islands Group, northern British Columbia, Canada—A bivalve sclerochronological approach. Palaeogeography, Palaeoclimatology, Palaeoecology 373, 163–172, 2013.

Harzhauser, M., Piller, W.E., Müllegger, S., Grunert, P., Micheels, A., 2011. Changing seasonality patterns in Central Europe from Miocene Climate Optimum to Miocene Climate Transition deduced from the *Crassostrea* isotope archive. Global and Planetary Change 76, 77–84, 2011.

Hay, W.W., 2008. Evolving ideas about the Cretaceous climate and ocean circulation. Cretaceous Research 29, 725–753, 2008.

Hay, 2013.

Hayami, I., Kase, T., 1992. A new cryptic species of *Pycnodonte* from Ryukyu Islands: a living fossil oyster. Nihon Koseibutsu Gakkai hokoku, kiji 1070–1089, 1992.

Hays, P.D., Grossman, E.L., Oxygen isotopes in meteoric calcite cements as indicators of continental paleoclimate. Geology 19, 441–444. https://doi.org/10.1130/0091-7613(1991)019<0441:OIIMCC>2.3.CO;2, 1991.

Huber, B.T., Norris, R.D., MacLeod, K.G., 2002. Deep-sea paleotemperature record of extreme warmth during the Cretaceous. Geology 30, 123–126. doi:10.1130/0091-7613(2002)030<0123:DSPROE>2.0.CO;2, 2002.

Hunter, S.J., Valdes, P.J., Haywood, A.M., Markwick, P.J., 2008. Modelling Maastrichtian climate: investigating the role of geography, atmospheric CO_2 and vegetation. Climate of the Past Discussions 4, 981–1019, 2008.

Huntington, K.W., Budd, D.A., Wernicke, B.P., Eiler, J.M., 2011. Use of clumped-isotope thermometry to constrain the crystallization temperature of diagenetic calcite. Journal of Sedimentary Research 81, 656–669, 2011.

Iglesias, A., Wilf, P., Johnson, K.R., Zamuner, A.B., Cúneo, N.R., Matheos, S.D., Singer, B.S., 2007. A Paleocene lowland macroflora from Patagonia reveals significantly greater richness than North American analogs. Geology 35, 947–950, 2007.

IPCC, 2014: Climate Change 2014: Synthesis Report. Contribution of Working Groups I, II and III to the Fifth Assessment Report of the Intergovernmental Panel on Climate Change [Core Writing Team, R.K. Pachauri and L.A. Meyer (eds.)]. IPCC, Geneva, Switzerland, 151 pp, 2014.

Jackson, L.J., Kalff, J., Rasnnussen, J.B., 1993. Sediment pH and redox potential affect the bioavailability of Al, Cu, Fe, Mn, and Zn to rooted aquatic macrophytes. Canadian Journal of Fisheries and Aquatic Sciences 50, 143–148, 1993.

Jia, G., X. Wang, W. Guo, and L. Dong, 2017. Seasonal distribution of archaeal lipids in surface water and its constraint on their sources and the TEX_{86} temperature proxy in sediments of the South China Sea, J. Geophys. Res. Biogeosci., 122, doi:10.1002/2016JG003732, 2017.

Jones, D.S., 1980. Annual cycle of shell growth increment formation in two continental shelf bivalves and its paleoecologic significance. Paleobiology 6, 331–340, 1980.

Jones, D.S., 1983. Sclerochronology: reading the record of the molluscan shell: annual growth increments in the shells of bivalve molluscs record marine climatic changes and reveal surprising longevity. American Scientist 71, 384–391, 1983.

Jones, D.S., Williams, D.F., Romanek, C.S., 1986. Life history of symbiont-bearing giant clams from stable isotope profiles. Science 231, 46–49.

Kiessling, W., Aragón, E., Scasso, R., Aberhan, M., Kriwet, J., Medina, F., Fracchia, D., 2005. Massive corals in Paleocene siliciclastic sediments of Chubut (Argentina). Facies 51, 233–241, 2005.

Kirby, M.X., Soniat, T.M., Spero, H.J., Kim, S.-T., O'Neil, J.R., 1997. Equilibrium and nonequilibrium oxygen isotope effects in synthetic carbonates. Geochimica et Cosmochimica Acta 61, 3461–3475.

Kirby, M.X., 2000. Stable isotope sclerochronology of Pleistocene and Recent oyster shells (*Crassostrea virginica*). Palaios 13, 560–569, 1998.

Kirby, M.X. Paleoecological differences between Tertiary and Quaternary *Crassostrea* oysters, as revealed by stable isotope sclerochronology. Palaios 15, 132–141, 2000.

Kirby, M.X., Soniat, T.M., Spero, H.J., 1998. Stable isotope sclerochronology of Pleistocene and Recent oyster shells (*Crassostrea virginica*). Palaios 13, 560–569.

Klein, R.T., Lohmann, K.C., Thayer, C.W., 1996a. Bivalve skeletons record sea-surface temperature and δ^{18}O via Mg/Ca and ^{18}O/^{16}O ratios. Geology 24, 415–418, 1996a.

Klein, R.T., Lohmann, K.C., Thayer, C.W., 1996b. Sr/Ca and ^{13}C/^{12}C ratios in skeletal calcite of *Mytilus trossulus*: Covariation with metabolic rate, salinity, and carbon isotopic composition of seawater. Geochimica et Cosmochimica Acta 60, 4207–4221, 1996b.

Klein, J.S., Mozley, P., Campbell, A., Cole, R., Spatial distribution of carbon and oxygen isotopes in laterally extensive carbonate-cemented layers: implications for mode of growth and subsurface identification. Journal of Sedimentary Research 69, 1999.

Langlet, D., Alunno-Bruscia, M., Rafélis, M., Renard, M., Roux, M., Schein, E., Buestel, D., 2006. Experimental and natural cathodoluminescence in the shell of *Crassostrea gigas* from Thau lagoon (France): ecological and environmental implications. Marine Ecology Progress Series 317, 143–156, 2006.

Lartaud, F., De Rafélis, M., Ropert, M., Emmanuel, L., Geairon, P., Renard, M., 2010a. Mn labelling of living oysters: artificial and natural cathodoluminescence analyses as a tool for age and growth rate determination of *C. gigas* (Thunberg, 1793) shells. Aquaculture 300, 206–217, 2010a.

Lartaud, F., Emmanuel, L., De Rafélis, M., Pouvreau, S., Renard, M., 2010b. Influence of food supply on the δ^{13}C signature of mollusc shells: implications for palaeoenvironmental reconstitutions. Geo-Marine Letters 30, 23–34, 2010b.

Lazareth, C.E., Vander Putten, E., André, L., Dehairs, F., 2003. High-resolution trace element profiles in shells of the mangrove bivalve *Isognomon ephippium*: a record of environmental spatio-temporal variations? Estuarine, Coastal and Shelf Science 57, 1103–1114, 2003.

Lear, C.H., Elderfield, H., Wilson, P.A., 2000. Cenozoic deep-sea temperatures and global ice volumes from Mg/Ca in benthic foraminiferal calcite. Science 287, 269–272, 2000.

Lear, C.H., Coxall, H.K., Foster, G.L., Lunt, D.J., Mawbey, E.M., Rosenthal, Y., Sosdian, S.M., Thomas, E., Wilson, P.A., 2015. Neogene

28

ice volume and ocean temperatures: Insights from infaunal foraminiferal Mg/Ca paleothermometry. Paleoceanography 30, 1437–1454, 2015.

Lécuyer, C., Reynard, B., Martineau, F., 2004. Stable isotope fractionation between mollusc shells and marine waters from Martinique Island. Chemical Geology 213, 293–305, 2004.

Linnaeus, Carolus, Systema naturae per regna tria naturae : secundum classes, ordines, genera, species, cum characteribus, differentiis, synonymis, locis., 10th edition, Lars Salvi, Stockholm, 1758

Lorens, R.B., Bender, M.L., 1980. The impact of solution chemistry on *Mytilus edulis* calcite and aragonite. Geochimica et Cosmochimica Acta 44, 1265–1278, 1980.

Lorrain, A., Gillikin, D.P., Paulet, Y.-M., Chauvaud, L., Le Mercier, A., Navez, J., André, L., 2005. Strong kinetic effects on Sr/Ca ratios in the calcitic bivalve *Pecten maximus.* Geology 33, 965–968.

Lorrain, A., Paulet, Y.-M., Chauvaud, L., Dunbar, R., Mucciarone, D., Fontugne, M., 2004. δ13Cδ13C variation in scallop shells: increasing metabolic carbon contribution with body size? Geochimica et Cosmochimica Acta 68, 3509–3519, 2004.

Lorrain, A., Gillikin, D.P., Paulet, Y.-M., Chauvaud, L., Le Mercier, A., Navez, J., André, L., Strong kinetic effects on Sr/Ca ratios in the calcitic bivalve *Pecten maximus.* Geology 33, 965–968, 2005.

Loyd, S.J., Corsetti, F.A., Eiler, J.M., Tripati, A.K., 2012. Determining the diagenetic conditions of concretion formation: assessing temperatures and pore waters using clumped isotopes. Journal of Sedimentary Research 82, 1006–1016, 2012.

MacDonald, J., Freer, A., Cusack, M., Alignment of crystallographic c-axis throughout the four distinct microstructural layers of the oyster *Crassostrea gigas.* Crystal Growth & Design 10, 1243–1246, 2009.

Machel, H.G., Burton, E.A., 1991. Factors governing cathodoluminescence in calcite and dolomite, and their implications for studies of carbonate diagenesis, 1991.

Malumian, N., Nanez, C., 2011. The Late Cretaceous–Cenozoic transgressions in Patagonia and the Fuegian Andes: foraminifera, palaeoecology, and palaeogeography. Biological Journal of the Linnean Society 103, 269–288, 2011.

Marali, S., Schöne, B.R., Oceanographic control on shell growth of *Arctica islandica* (Bivalvia) in surface waters of Northeast Iceland—Implications for paleoclimate reconstructions. Palaeogeography, Palaeoclimatology, Palaeoecology 420, 138–149, 2015.

Marali, S., Schöne, B.R., Mertz-Kraus, R., Griffin, S.M., Wanamaker, A.D., Matras, U., Butler, P.G., Ba/Ca ratios in shells of *Arctica islandica*—Potential environmental proxy and crossdating tool. Palaeogeography, Palaeoclimatology, Palaeoecology 465, 347–361, 2017.

McConnaughey, T., 1989. 13C and 18O isotopic disequilibrium in biological carbonates: II. In vitro simulation of kinetic isotope effects, 1989. Geochimica et Cosmochimica Acta 53, 163–171.

McConnaughey, T.A., Burdett, J., Whelan, J.F., Paull, C.K., 1997. Carbon isotopes in biological carbonates: Respiration and photosynthesis. Geochimica et Cosmochimica Acta 61, 611–622. doi:10.1016/S0016-7037(96)00361-4, 1997.

McConnaughey, T.A., Gillikin, D.P., 2008. Carbon isotopes in mollusk shell carbonates. Geo-Marine Letters 28, 287–299, 2008.

Miller, K.G., Sugarman, P.J., Browning, J.V., Kominz, M.A., Hernández, J.C., Olsson, R.K., Wright, J.D., Feigenson, M.D., Van Sickel, W., 2003. Late Cretaceous chronology of large, rapid sea-level changes: Glacioeustasy during the greenhouse world. Geology 31, 585–588, 2003.

Morrison, J.M., Codispoti, L.A., Gaurin, S., Jones, B., Manghnani, V., Zheng, Z., 1998. Seasonal variation of hydrographic and nutrient fields during the US JGOFS Arabian Sea Process Study. Deep Sea Research Part II: Topical Studies in Oceanography 45, 2053–2101, 1998.

Mouchi, V., De Rafélis, M., Lartaud, F., Fialin, M., Verrecchia, E., 2013. Chemical labelling of oyster shells used for time-calibrated high-resolution Mg/Ca ratios: a tool for estimation of past seasonal temperature variations. Palaeogeography, Palaeoclimatology, Palaeoecology 373, 66–74, 2013.

Müller, A.H., 1970. Zur funktionellen Morphologie, Taxiologie und Ökologie von Pycnodonta (Ostreina, Lamellibranchiata). Monatsberichte der Deutschen Akademie der Wissenschaften zu Berlin 12, 902–923, 1970.

Nestler, H., 1965. Entwicklung und Schalenstruktur von *Pycnodonte uesicularis* (LAM.) und *Dimyodon nilssoni* (v. Hag.) aus der Oberkreide. Geologie L4 64–77, 1965.

O'Brien, C.L., Robinson, S.A., Pancost, R.D., Sinninghe Damsté, J.S., Schouten, S., Lunt, D.J., Alsenz, H., Bornemann, A., Bottini, C., Brassell, S.C., Farnsworth, A., Forster, A., Huber, B.T., Inglis, G.N., Jenkyns, H.C., Linnert, C., Littler, K., Markwick, P., McAnena, A., Mutterlose, J., Naafs, B.D.A., Püttmann, W., Sluijs, A., van Helmond, N.A.G.M., Vellekoop, J., Wagner, T., Wrobel, N.E., 2017. Cretaceous sea-surface temperature evolution: Constraints from TEX 86TEX86 and planktonic foraminiferal oxygen isotopes. Earth-Science Reviews 172, 224–247. doi:10.1016/j.earscirev.2017.07.012, 2017.

Omata, T., Suzuki, A., Kawahat, H., Okamoto, M., 2005. Annual fluctuation in the stable carbon isotope ratio of coral skeletons: the relative intensities of kinetic and metabolic isotope effects. Geochimica et cosmochimica acta 69, 3007–3016, 2005.

Otto-Bliesner, B.L., Brady, E.C., Shields, C., 2002. Late Cretaceous ocean: Coupled simulations with the National Center for Atmospheric Research Climate System Model. J. Geophys. Res. 107, ACL 11-1. doi:10.1029/2001JD000821, 2002.

Owen, R., Kennedy, H., Richardson, C., 2002. Experimental investigation on partitioning of stable isotopes between scallop (*Pecten maximus*) shell calcite and sea water. Palaeogeography, Palaeoclimatology, Palaeoecology 185, 163–174, 2002.

Palazzesi, L., Barreda, V., 2007. Major vegetation trends in the Tertiary of Patagonia (Argentina): a qualitative paleoclimatic approach based on palynological evidence. Flora-Morphology, Distribution, Functional Ecology of Plants 202, 328–337, 2007.

Pearson, P.N., Ditchfield, P.W., Singano, J., Harcourt-Brown, K.G., Nicholas, C.J., Olsson, R.K., Shackleton, N.J., Hall, M.A., 2001. Warm tropical sea surface temperatures in the Late Cretaceous and Eocene epochs. Nature 413, 481–487, 2001.

Pennington, J.T., Chavez, F.P., 2000. Seasonal fluctuations of temperature, salinity, nitrate, chlorophyll and primary production at station H3/M1 over 1989–1996 in Monterey Bay, California. Deep Sea Research Part II: Topical Studies in Oceanography 47, 947–973, 2000.

Petersen, S.V., Winkelstern, I.Z., Lohmann, K.C., Meyer, K.W., 2016. The effects of Porapak™ trap temperature on δ18O, δ13C, and Δ47 values in preparing samples for clumped isotope analysis. Rapid Communications in Mass Spectrometry 30, 199–208, 2016.

Pirrie, D., Marshall, J.D., 1990. Diagenesis of Inoceramus and Late Cretaceous paleoenvironmental geochemistry: a case study from James Ross Island, Antarctica. Palaios 336–345, 1990.

Prámparo, M.B., Papu, O.H., 2006. Late Maastrichtian dinoflagellate cysts from the Cerro Butaló section, southern Mendoza province, Argentina. Journal of Micropalaeontology 25, 23–33.

Prámparo, M.B., Papu, O.H., Milana, J.P., 1996. Estudios palinológicos del miembro inferior de la Formación Pachaco, Terciario de la provincia de San Juan. Descripciones sistemáticas. Ameghiniana 33, 397–407, 1996.

Prámparo, M.B., Papu, O.H., Late Maastrichtian dinoflagellate cysts from the Cerro Butaló section, southern Mendoza province, Argentina. Journal of Micropalaeontology 25, 23–33, 2006.

Pugaczewska, H., 1977. The Upper Cretaceous Ostreidae from the Middle Vistula Region (Poland). Acta palaeontologica polonica 22, 1977.

Quan, C., Sun, C., Sun, Y., Sun, G., 2009. High resolution estimates of paleo-CO 2CO2 levels through the Campanian (Late Cretaceous)

based on Ginkgo cuticles. Cretaceous Research 30, 424–428, 2009.

Ravelo, A.C., Hillaire-Marcel, C., 2007. Chapter Eighteen the use of oxygen and carbon isotopes of foraminifera in Paleoceanography. Developments in Marine Geology 1, 735–764, 2007.

Richardson, C.A., Peharda, M., Kennedy, H., Kennedy, P., Onofri, V., 2004. Age, growth rate and season of recruitment of *Pinna nobilis* (L) in the Croatian Adriatic determined from Mg: Ca and Sr: Ca shell profiles. Journal of Experimental Marine Biology and Ecology 299, 1–16, 2004.

Romanek, C.S., Grossman, E.L., Morse, J.W., 1992. Carbon isotopic fractionation in synthetic aragonite and calcite: effects of temperature and precipitation rate. Geochimica et Cosmochimica Acta 56, 419–430, 1992.

Rosenberg, G.D., Hughes, W.W., 1991. A metabolic model for the determination of shell composition in the bivalve mollusc, *Mytilus edulis*. Lethaia 24, 83–96, 1991.

Scasso, R.A., Concheyro, A., Kiessling, W., Aberhan, M., Hecht, L., Medina, F.A., Tagle, R., 2005. A tsunami deposit at the Cretaceous/Paleogene boundary in the Neuquén Basin of Argentina. Cretaceous Research 26, 283–297, 2005.

Schauer, A.J., Kelson, J., Saenger, C., Huntington, K.W., Choice of 17O correction affects clumped isotope (Δ_{47}) values of CO_2 measured with mass spectrometry. Rapid Communications in Mass Spectrometry 30, 2607–2616, 2016.

Schlager, W., James, N.P., 1978. Low-magnesian calcite limestones forming at the deep-sea floor, Tongue of the Ocean, Bahamas. Sedimentology 25, 675–702, 1978.

Schouten, S., Hopmans, E. C., & Damsté, J. S. S. 2013. The organic geochemistry of glycerol dialkyl glycerol tetraether lipids: a review. Organic geochemistry, 54, 19-61.

Schöne, B.R., Fiebig, J., Pfeiffer, M., Gleβ, R., Hickson, J., Johnson, A.L., Dreyer, W., Oschmann, W., 2005a. Climate records from a bivalved Methuselah (*Arctica islandica*, Mollusca; Iceland). Palaeogeography, Palaeoclimatology, Palaeoecology 228, 130–148, 2005a.

Schöne, B.R., Houk, S.D., Castro, A.D.F., Fiebig, J., Oschmann, W., Kröncke, I., Dreyer, W., Gosselck, F., 2005b. Daily growth rates in shells of *Arctica islandica*: assessing sub-seasonal environmental controls on a long-lived bivalve mollusk. Palaios 20, 78–92, 2005b.

Schöne, B.R., Pfeiffer, M., Pohlmann, T., Siegismund, F., A seasonally resolved bottom-water temperature record for the period AD 1866–2002 based on shells of *Arctica islandica* (Mollusca, North Sea). International Journal of Climatology 25, 947–962, 2005c.

Servicio Meteorológico Nacional, Republic of Argentina, http://www.smn.gov.ar/serviciosclimaticos/?mod=turismo&id=5&var=buenosaires, visited on 25-09-2017.

Schouten, S., Hopmans, E. C., & Damsté, J. S. S. The organic geochemistry of glycerol dialkyl glycerol tetraether lipids: a review. Organic geochemistry, 54, 19-61, 2013.

Stanley, S.M., Hardie, L.A., 1998. Secular oscillations in the carbonate mineralogy of reef-building and sediment-producing organisms driven by tectonically forced shifts in seawater chemistry. Palaeogeography, Palaeoclimatology, Palaeoecology 144, 3–19, 1998.

Stenzel, H. B. 1956. Cretaceous oysters of southwestern North America. Int. Geol. Congr. Mexico City, 15-37, 1956.

Stenzel, H.B., 1971. Oysters. University of Kansas Press and Geological Society of America, Part N, Mollusca, 1971.

Steuber, T., Stable isotope sclerochronology of rudist bivalves: Growth rates and Late Cretaceous seasonality. Geology 24, 315. doi:10.1130/0091-7613(1996)024<0315:SISORB>2.3.CO;2, 1996.

Steuber, T., 1999. Isotopic and chemical intra-shell variations in low-Mg calcite of rudist bivalves (Mollusca-Hippuritacea): disequilibrium fractionations and late Cretaceous seasonality. International Journal of Earth Sciences 88, 551–570, 1999.

Steuber, T., 1996. Stable isotope sclerochronology of rudist bivalves: Growth rates and Late Cretaceous seasonality. Geology 24, 315. doi:10.1130/0091-7613(1996)024<0315:SISORB>2.3.CO;2

Steuber, T., Rauch, M., Masse, J.-P., Graaf, J., Malkoč, M., 2005. Low-latitude seasonality of Cretaceous temperatures in warm and cold episodes. Nature 437, 1341–1344, 2005.

Surge, D., Lohmann, K.C., 2008. Evaluating Mg/Ca ratios as a temperature proxy in the estuarine oyster, *Crassostrea virginica*. J. Geophys. Res. 113, G02001. doi:10.1029/2007JG000623

Surge, D., Lohmann, K.C., Dettman, D.L., 2001. Controls on isotopic chemistry of the American oyster, *Crassostrea virginica*: implications for growth patterns. Palaeogeography, Palaeoclimatology, Palaeoecology 172, 283–296, 2001.

Surge, D., Lohmann, K.C., Evaluating Mg/Ca ratios as a temperature proxy in the estuarine oyster, *Crassostrea virginica*. J. Geophys. Res. Surge, D., Owens, S., 2003. Oxygen and Carbon Stable Isotope and Sr: Ca Records in Outer and Middle Microstructural Layers of Bivalve Shells (Mercenaria campechiensis), in: AGU Fall Meeting Abstracts. 113, 2001. doi:10.1029/2007JG000623, 2008.

Takesue, R.K., van Geen, A., 2004. Mg/Ca, Sr/Ca, and stable isotopes in modern and Holocene *Protothaca staminea* shells from a northern California coastal upwelling region. Geochimica et Cosmochimica Acta 68, 3845–3861, 2004.

Titschack, J., Zuschin, M., Spötl, C., Baal, C., 2010. The giant oyster *Hyotissa hyotis* from the northern Red Sea as a decadal-scale archive for seasonal environmental fluctuations in coral reef habitats. Coral Reefs 29, 1061–1075, 2010.

Torsvik, T.H., Van der Voo, R., Preeden, U., Mac Niocaill, C., Steinberger, B., Doubrovine, P.V., van Hinsbergen, D.J., Domeier, M., Gaina, C., Tohver, E., others, 2012. Phanerozoic polar wander, palaeogeography and dynamics. Earth-Science Reviews 114, 325–368, 2012.

Tripati, A., Zachos, J., Marincovich Jr., L., Bice, K., 2001. Late Paleocene Arctic coastal climate inferred from molluscan stable and radiogenic isotope ratios. Palaeogeography, Palaeoclimatology, Palaeoecology 170, 101–113. doi:10.1016/S0031-0182(01)00230-9, 2001.

Ullmann, C.V., Wiechert, U., Korte, C., Ullmann, C.V., Böhm, F., Rickaby, R.E., Wiechert, U., Korte, C., 2013. The Giant Pacific Oyster (Crassostrea gigas) as a modern analog for fossil ostreoids: isotopic (Ca, O, C) and elemental (Mg/Ca, Sr/Ca, Mn/Ca) proxies. Geochemistry, Geophysics, Geosystems 14, 4109–4120.

Ullmann, C.V., Wiechert, U., Korte, C., 2010. Oxygen isotope fluctuations in a modern North Sea oyster (*Crassostrea gigas*) compared with annual variations in seawater temperature: Implications for palaeoclimate studies. Chemical Geology 277, 160–166. doi:10.1016/j.chemgeo.2010.07.019, 2010.

Ullmann, C.V., Böhm, F., Rickaby, R.E., Wiechert, U., Korte, C., The Giant Pacific Oyster (*Crassostrea gigas*) as a modern analog for fossil ostreoids: isotopic (Ca, O, C) and elemental (Mg/Ca, Sr/Ca, Mn/Ca) proxies. Geochemistry, Geophysics, Geosystems 14, 4109–4120, 2013.

van Hinsbergen, D.J., de Groot, L.V., van Schaik, S.J., Spakman, W., Bijl, P.K., Sluijs, A., Langereis, C.G., Brinkhuis, H., 2015a. A paleolatitude calculator for paleoclimate studies. PloS one 10, e0126946, 2015.

van Hinsbergen, D.J., de Groot, L.V., van Schaik, S.J., Spakman, W., Bijl, P.K., Sluijs, A., Langereis, C.G., Brinkhuis, H., 2015b. A paleolatitude calculator for paleoclimate studies. PloS one 10, e0126946.

Van Rampelbergh, M., Verheyden, S., Allan, M., Quinif, Y., Keppens, E., Claeys, P., 2014. Seasonal variations recorded in cave monitoring results and a 10 year monthly resolved speleothem $\delta^{18}O$ and $\delta^{13}C$ record from the Han-sur-Lesse cave, Belgium. Climate of the

Past Discussions 10, 1821–1856, 2014.

Vander Putten, E., Dehairs, F., Keppens, E., Baeyens, W., 2000. High resolution distribution of trace elements in the calcite shell layer of modern *Mytilus edulis*: Environmental and biological controls. Geochimica et Cosmochimica Acta 64, 997–1011, 2000.

Vansteenberge, S., Verheyden, S., Goderis, S., Sinnesael, M., de Winter, N.J., Van Malderen, S.J.M., Vanhaecke, F., Claeys, P., Reconstructing seasonality through stable isotope and trace element analysis of the Proserpine stalagmite, Han-sur-Lesse Cave, Belgium: indicationis for climate-driven changes during the last 400 years. Chemical Geology, in review.

Veizer, J., 1983. Chemical diagenesis of carbonates: theory and application of trace element technique, 1983.

Vellekoop, J., Esmeray-Senlet, S., Miller, K.G., Browning, J.V., Sluijs, A., van de Schootbrugge, B., Damsté, J.S.S., Brinkhuis, H., 2016. Evidence for Cretaceous-Paleogene boundary bolide "impact winter" conditions from New Jersey, USA. Geology 44, 619–622, 2016.

Vermeij, G.J., 2014. The oyster enigma variations: a hypothesis of microbial calcification. Paleobiology 40, 1–13, 2014.

Videt, B. 2004. Dynamique des paléoenvironnements à huîtres du Cré-tacéCrétacé supérieur nord-aquitain (SW France) et du Mio-Pliocène andalou (SE Espagne): biodiversité, analyse séquentielle, biogéochimie. – Mém. Géosc. Rennes, 108, 1-261, 2004.

Wanamaker Jr, A.D., Kreutz, K.J., Wilson, T., Borns Jr, H.W., Introne, D.S., Feindel, S., 2008. Experimentally determined Mg/Ca and Sr/Ca ratios in juvenile bivalve calcite for *Mytilus edulis*: implications for paleotemperature reconstructions. Geo-Marine Letters 28, 359–368, 2008.

Wang, W.-X., Fisher, N.S., 1996. Assimilation of trace elements and carbon by the mussel *Mytilus edulis*: effects of food composition. Limnology and Oceanography 4, l, 1996.

Wang, Q.J., Xu, X.H., Jin, P.H., Li, R.Y., Li, X.Q., Sun, B.N., 2013. Quantitative reconstruction of Mesozoic paleoatmospheric CO2 based on stomatal parameters of fossil *Baiera furcata* of Ginkgophytes. Geological review 59, 1035–1045, 2013.

Watanabe, T., Winter, A., Oba, T., 2001. Seasonal changes in sea surface temperature and salinity during the Little Ice Age in the Caribbean Sea deduced from Mg/Ca and 18-O/16-O^{18}O/^{16}O ratios in corals. Marine Geology 173, 21–35, 2001.

Weidman, C.R., Jones, G.A., 1994. The long-lived mollusc Arctica islandica: A new paleoceanographic tool for the reconstruction of bottom temperatures for the continental shelves of the northern North Atlantic Ocean. Journal of Geophysical Research: Oceans 99, 18305–18314.

Weiner, S., Dove, P.M., 2003. An overview of biomineralization processes and the problem of the vital effect. Reviews in mineralogy and geochemistry 54, 1–29, 2003.

Wisshak, M., Correa, M.L., Gofas, S., Salas, C., Taviani, M., Jakobsen, J., Freiwald, A., 2009. Shell architecture, element composition, and stable isotope signature of the giant deep-sea oyster *Neopycnodonte zibrowii* sp. n. from the NE Atlantic. Deep Sea Research Part I: Oceanographic Research Papers 56, 374–407, 2009.

Woelders, L., Vellekoop, J., Kroon, D., Smit, J., Casadío, S., Prámparo, M.B., Dinarès-Turell, J., Peterse, F., Sluijs, A., Lenaerts, J.T.M., Speijer, R.P., 2017. Latest Cretaceous climatic and environmental change in the South Atlantic region. Paleoceanography 2016PA003007. doi:10.1002/2016PA003007, 2017.

Woo, K.-S., Anderson, T.F., Sandberg, P.A., 1993. Diagenesis of skeletal and nonskeletal components of mid-Cretaceous limestones. Journal of Sedimentary Research 63, 1993.

[FIGURE CAPTIONS]
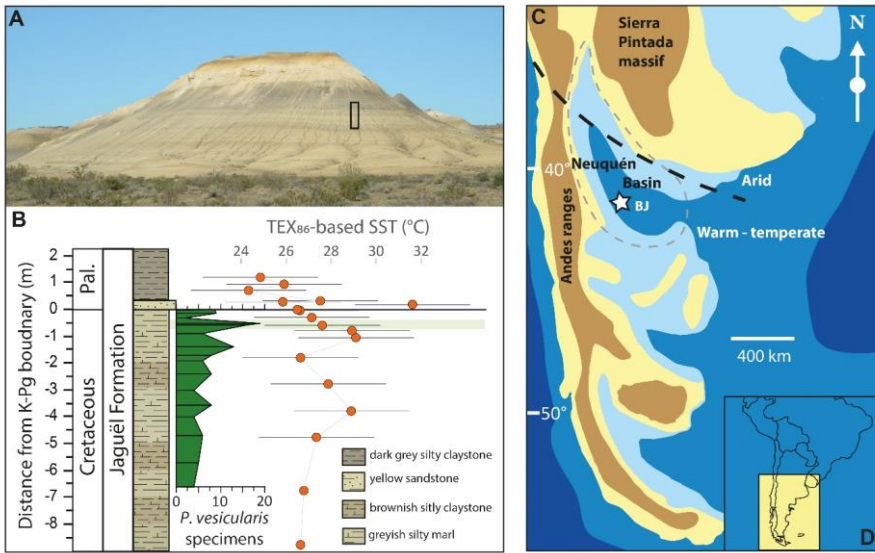
1550

1551 **Figure 1**
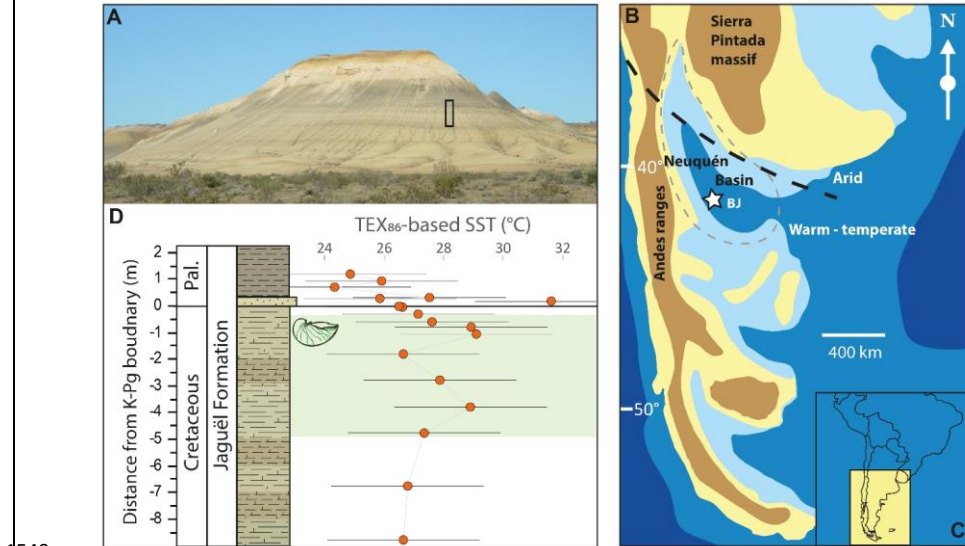
1552 ~~Origin and stratigraphy~~Background information of the studied *Pycnodonte vesicularis* specimens. A)
1553 ~~photograph of the~~The Bajada de Jaguël section in outcrop (BJ; modern location:
1554 38°06'10.5"S, 68°23'20.5"W, palaeolatitude = 43°S). ~~B~~B) ~~Palaeogeography of study area~~
1555 ~~during the latest Cretaceous. Palaeomap after Scasso et al. (2005) and Woelders et al.~~
1556 ~~(2017). C) Location of the study area in southern Argentina relative to modern day South~~
1557 ~~America. D~~) lithology, stratigraphy and TEX$_{86}$ record (Woelders et al., 2017) of the BJ section.
1558 The main *P. vesicularis* level is indicated in light green. The abundance of *P. vesicularis* is
1559 based on Aberhan and Kiessling (2014). C) Palaeogeography of study area during the latest
1560 Cretaceous. Palaeomap after Scasso et al. (2005) and Woelders et al. (2017). D) Location of
1561 the study area in southern Argentina relative to modern day South America.
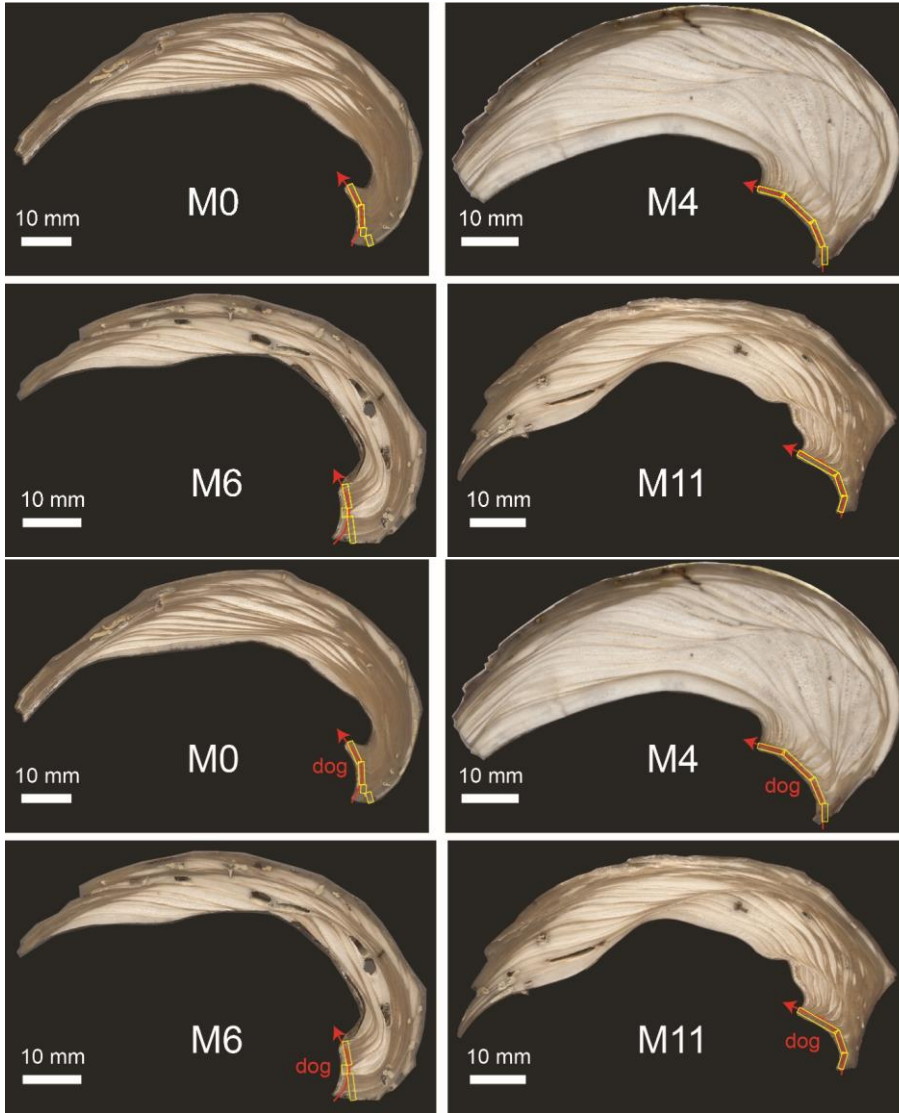
Figure 2

Colour scans of cross sections of the four shells subject to multi-proxy analysis. Red arrows indicate sampling location and direction. Yellow boxes indicate the location of stable isotope transects. XRF sampling is in the direction of growth ("dog").

1569

1570
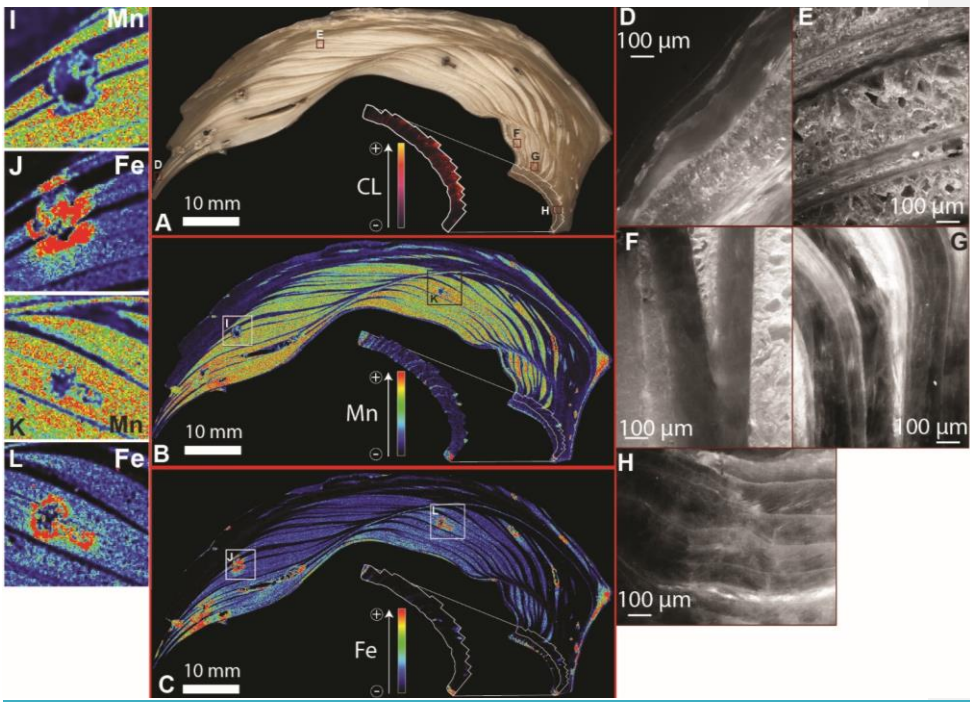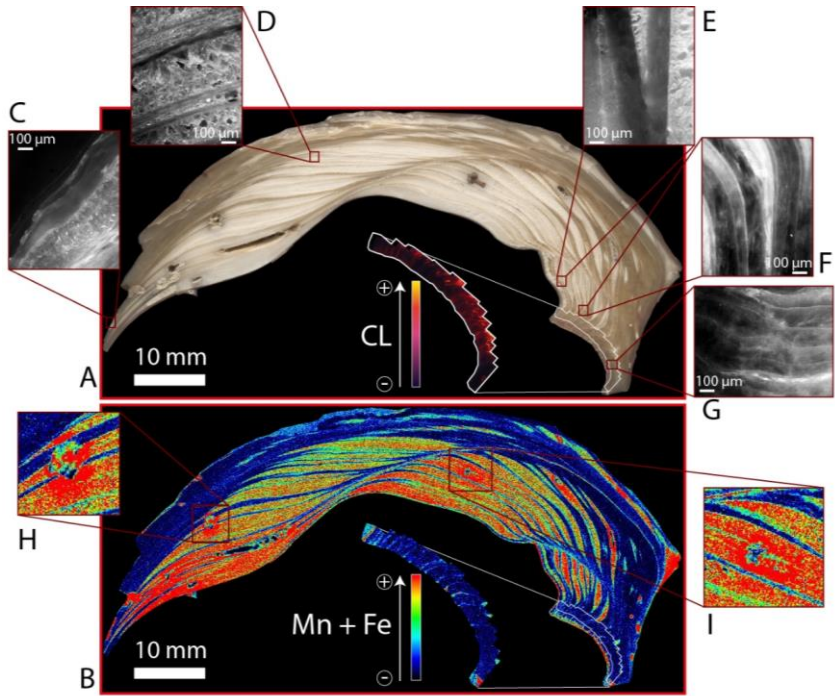
34

Figure 3

Overview of the results of colour scanning, microscopic analyses and µXRF mapping of specimen M11. A) Colour scan of cross section in growth direction through the shell, with close-up of cathodoluminescence microscopic image of the hinge line. B) µXRF mapping of Mn the cross section, with close-up of the µXRF map of the hinge line. C) Optical microscopic imageC) µXRF mapping of Fe the cross section, with close-up of the µXRF map of the hinge line. D) Micrograph of transitions between dense foliated calcite and porous vesicular calcite. near the edge of the shell. Note the blocky calcite crystals in the vesicular structure. D) Optical microscopic image of verymicrostructure. E) Micrograph of thin, alternating layers of foliated and vesicular calcite. E) Optical microscopic image ofF) Micrograph showing sharp transitions between dense foliated calcite and porous vesicular calcite F) Optical microscopic image of moreG) Micrograph of gradual transitions between foliated calcite and vesicular calcite. G) Optical microscopic image closer to the hinge. H) Micrograph of dense, foliated calcite layers in shell hinge line. Note the thin layer of vesicular calcite (white) intercalated between the foliated layers near the bottom of the image. H) and I-L) Close-ups of µXRF mapping of bore holes with coronas of elevated Fe and Mn concentrations.
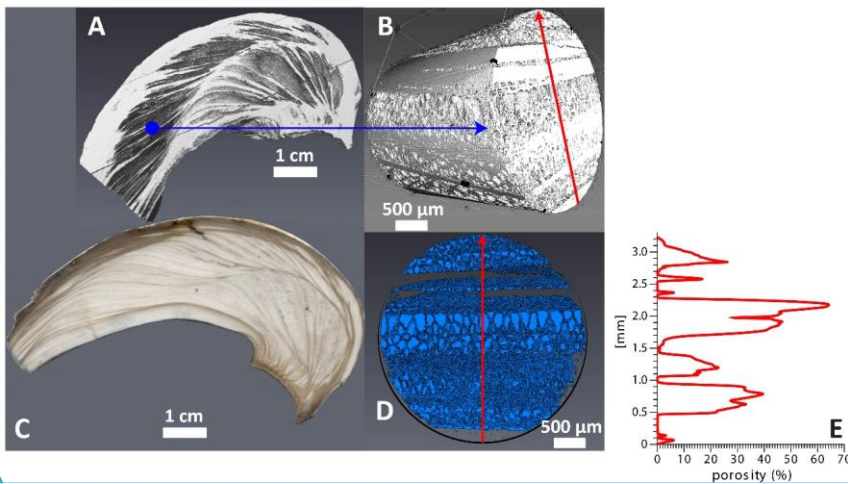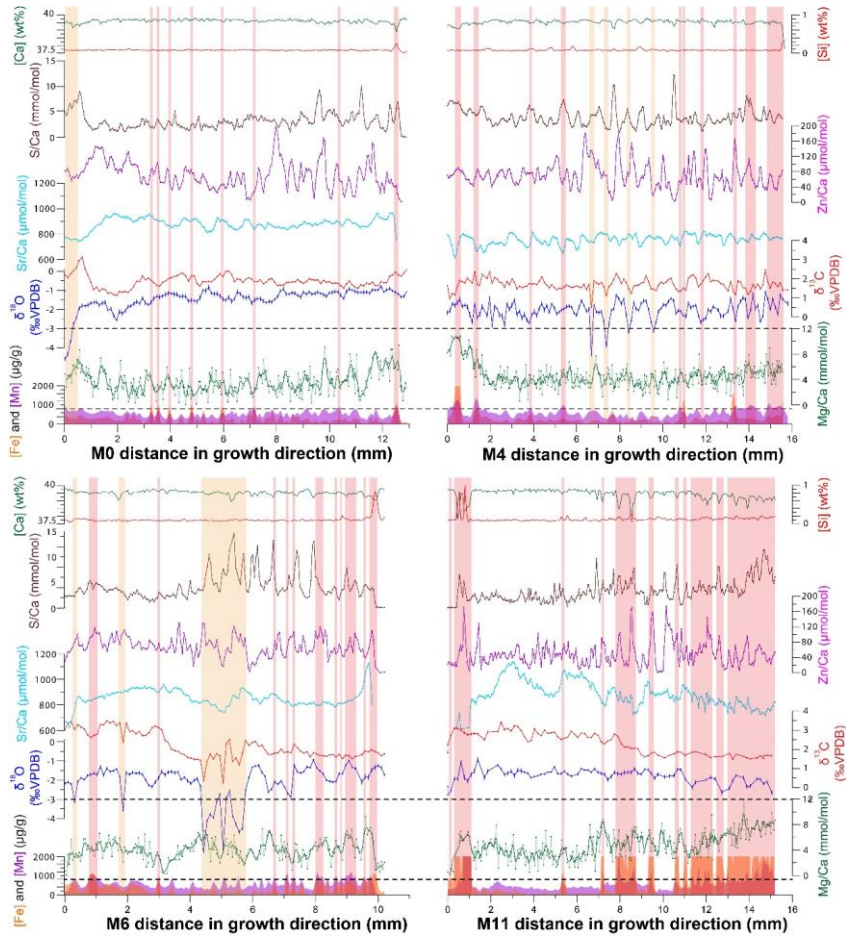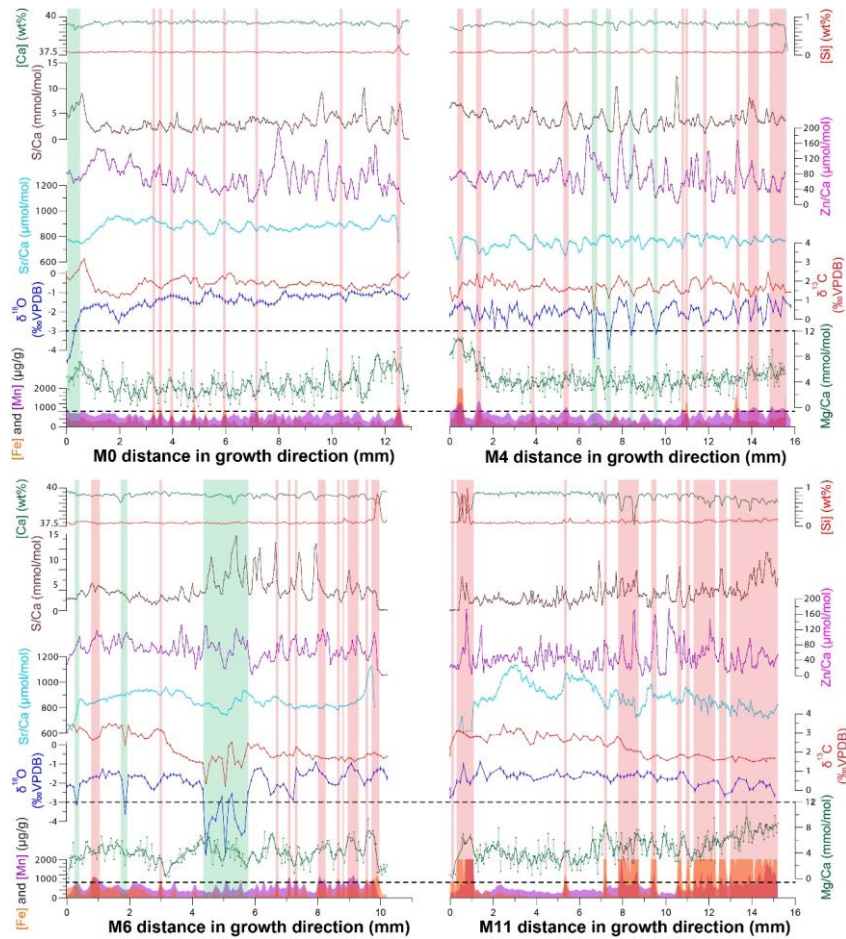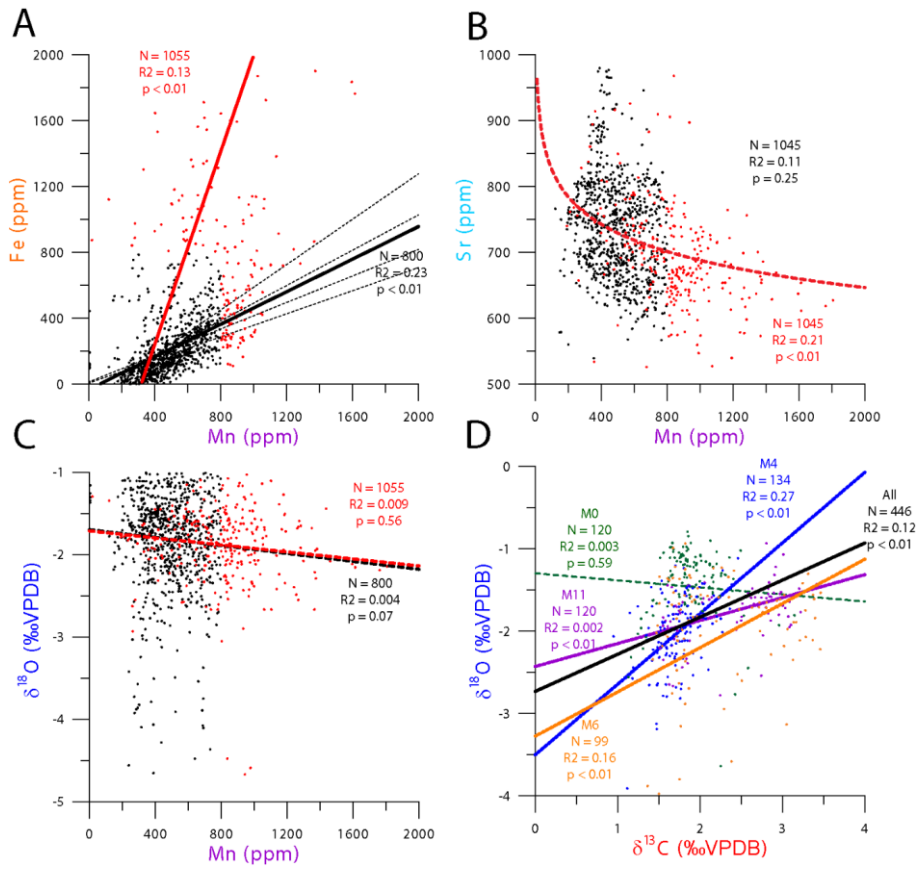

Figure 4

Overview of the results of CT-scanning and poreporosity analysis on specimen M4, with A) showing an overview of density variations in the shell (white = dense calcite, darker colours represent porosity). The blue dot shows the location of the part of the shell that was CT-scanned at high resolution. B) shows the shape and density of a part of the shell that was CT-scanned with higher spatial resolution as well as the location of the porograph shown in E). C) shows a colour scan of the shell cross section. D) shows a high-resolution cross-section through the high-resolution section through the shell with porosity in blue. (light blue = porosity, darker colours = dense calcite). The red line is in the same location as in B). E) shows a graph of porosity through the high resolution section perpendicular to the growth layers.

Figure 5

Overview of multi-proxy records through the hinges of 4 specimens of *P. vesicularis*. From top to bottom, records of [Ca] (green), [Si] (red), S/Ca ratios (brown), Zn/Ca ratios (purple), Sr/Ca ratios (light blue), δ¹³C (red), δ¹⁸O (blue), Mg/Ca (green), [Mn] (purple) and [Fe] (orange) are shown. Red arrows in Figure 2 indicate the direction of sampling. Vertical bars indicate parts of the records that were affected by diagenesis based on Mn and Fe concentrations (red bars) and stable isotope ratios (~~orange~~green bars). Note that the vertical scale of the Mn and Fe plots is clipped at 2000 µg/g.
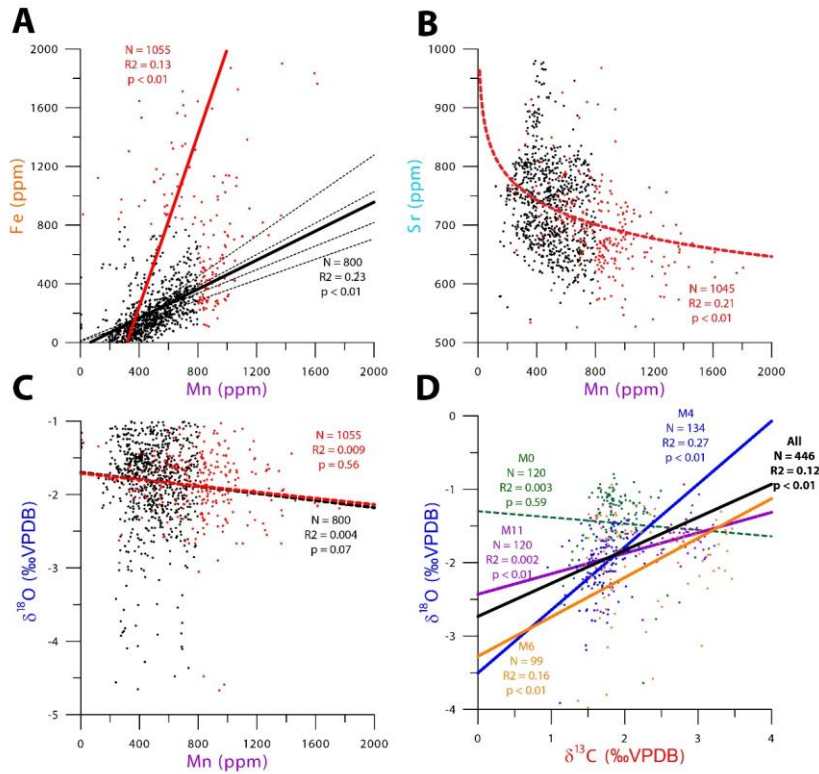
1609

Figure 6

1611 ~~Cross plots~~Figure showing cross plots between trace element and stable isotope measurements in
1612   the shells. Black lines indicate correlations through all measurements, red lines show
1613   correlations of diagenetically altered samples (according to the 800 μg/g threshold for Fe
1614   and Mn) and alternatively coloured lines indicate correlations in individual shells. Statistics
1615   of the regressions are indicated in matching colours. A) [Fe] vs [Mn] showing ~~how both~~a
1616   correlation between concentrations of these elements ~~increase with increasing diagenetic~~
1617   ~~overprinting~~in all shells. Steeper slopes suggest relatively more Fe is added in diagenetically
1618   altered samples. B) [Sr] vs [Mn] showing decreasing Sr concentrations corresponding to
1619   increasing [Mn], but only in diagenetically altered samples. No significant correlation was
1620   found for pristine samples ($R^2 = 0.11$, $p = 0.25$). C) $\delta^{18}O$ vs [Mn] showing lack of correlation~~,~~
1621   ~~although Mn-rich diagenetic samples generally have lower $\delta^{18}O$ values~~. D) $\delta^{18}O$ vs $\delta^{13}C$,
1622   showing positive correlation in specimens affected by diagenesis and no correlation in M0,
1623   which has pristine values.
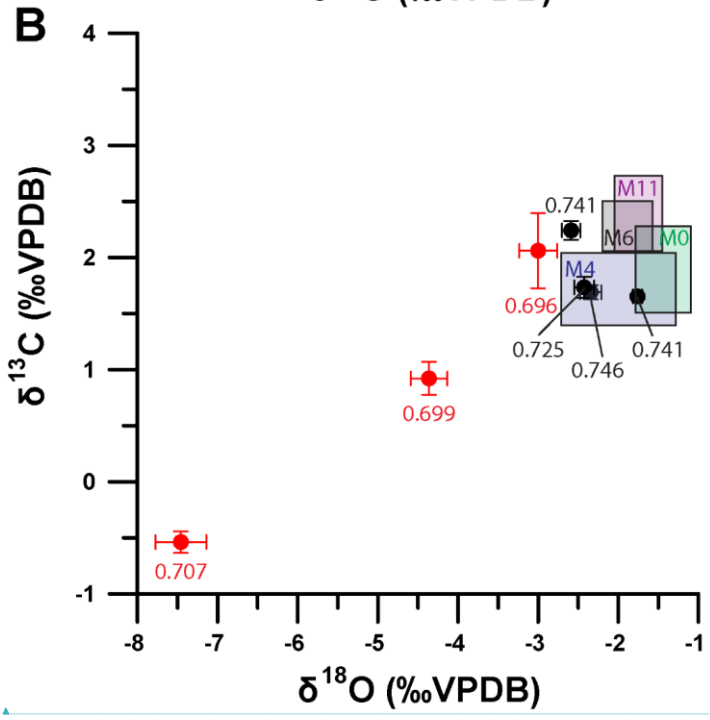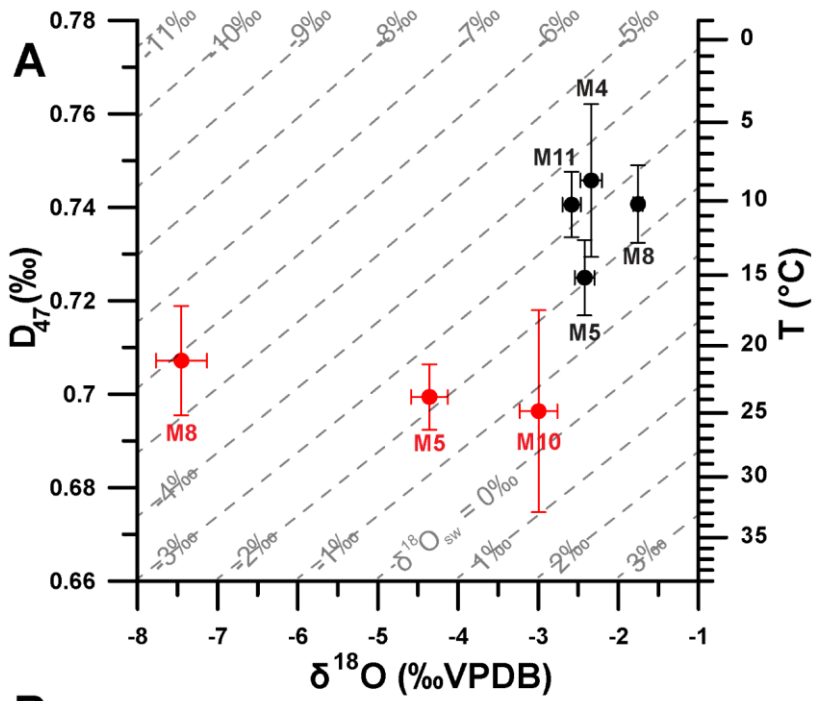
Figure 7

1626 Cross plots of clumped isotope results. A) Δ_{47} vs. $\delta^{18}O$ from clumped isotope measurements on all

1627 seven shells. Red dots and error bars represent measurements of samples from the ventral

1628 margin of the shells, while black dots and error bars indicate results from dense foliated

1629 calcite from the hinge of the shells. Dashed lines illustrate the $\delta^{18}O$ values of seawater that

1630 correspond to the combination of Δ_{47} and $\delta^{18}O$ values in the graph. B) $\delta^{13}C$ vs. $\delta^{18}O$ from

1631 clumped isotope measurements on all shells. ~~Red dots and error bars represent~~

1632 ~~measurements of samples from the ventral margin of the shells, while black dots and error~~

1633 ~~bars indicate results from dense foliated calcite from the hinge of the shells.~~Symbols as in A)

1634 Numbers next to the dots indicate Δ_{47} values measured in the same samples. Coloured

1635 rectangles indicate the range of pristine stable isotope values measured in high resolution

1636 transects through the hinges of shells M0, M4, M6 and M11.

1637

Annual stack of shell M0 (interpreted months)

1638
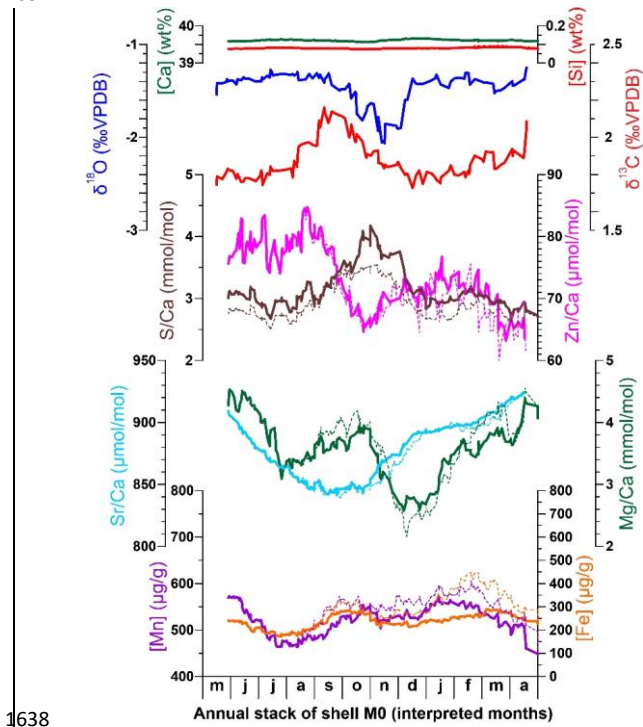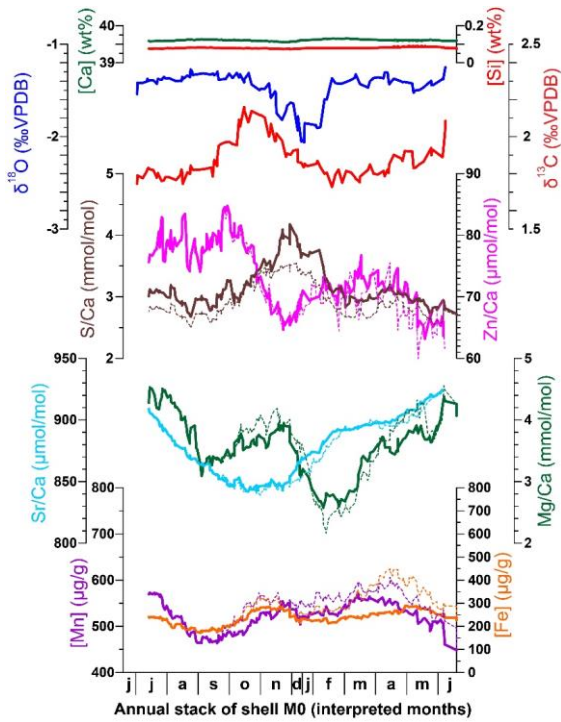
Figure 8

Stack of proxy records for shell M0 made according to a tentative interpretation of annual cyclicity based on δ18O and Sr/Ca ratios in **Figure 5**. Solid lines indicate annual stacks excluding diagenetically altered samples while dashed lines include all measured samples to show the effect of diagenesis. From top to bottom, stacks of [Ca] (green), [Si] (red), δ13C (red), δ18O (blue), S/Ca ratios (brown), Zn/Ca ratios (purple), Sr/Ca ratios (light blue), , Mg/Ca (green), [Mn] (purple) and [Fe] (orange) records are shown. Subdivisions of the stack into 12 time steps and corresponding months are based on an interpretation of the phase relationship between the proxies in terms of palaeoenvironmental seasonality. Note that summer months (December and January) are underrepresented in the record due to the interpreted decrease or cessation of shell growth.

Figure 9

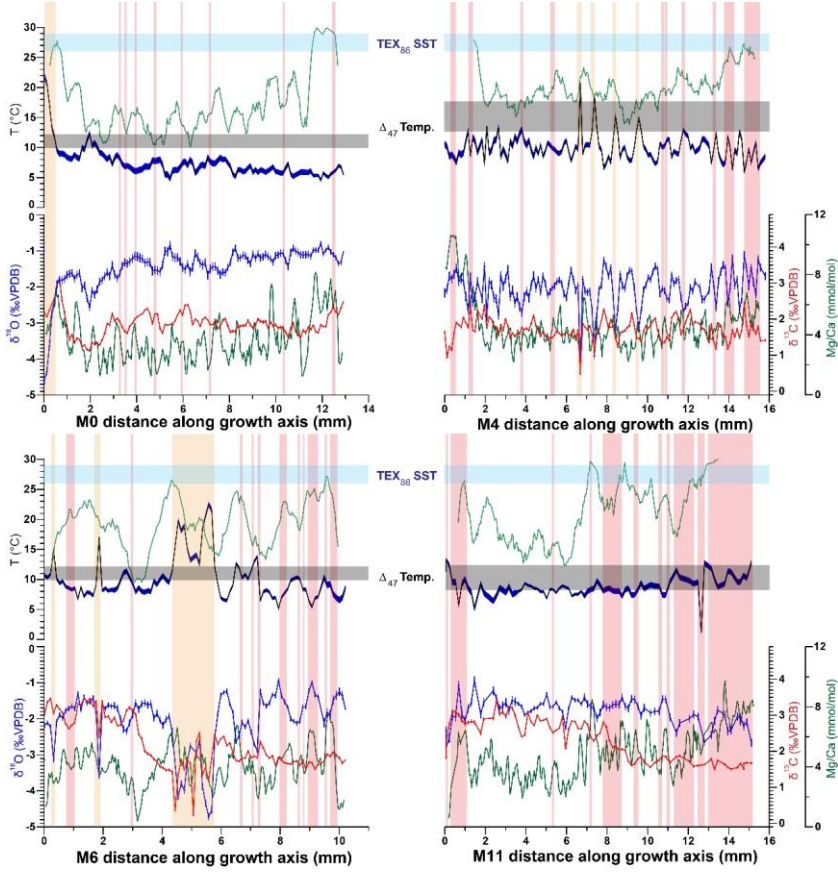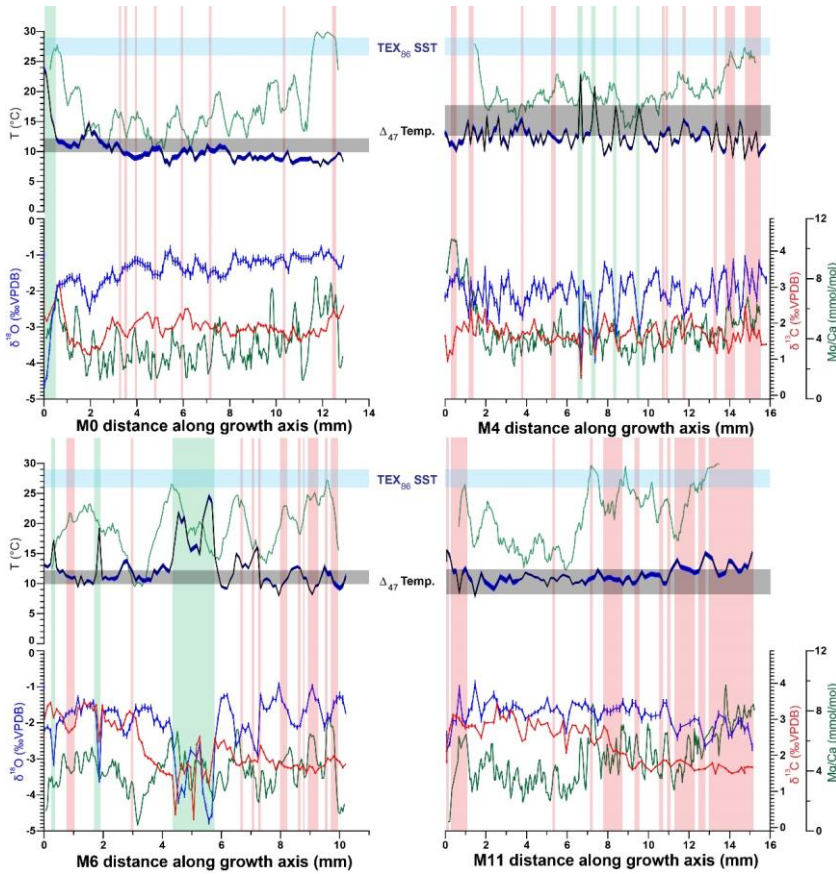Overview of stable isotope and Mg/Ca records (bottom) as well as tentative temperature and salinity reconstructions (top) based on δ18O (blue) and Mg/Ca (green), clumped isotope analysis (grey bars) and TEX86H palaeothermometry (light blue bars). Temperatures calculated from δ18O records (dark blue on top) are based on the calibration by ~~Kim~~Hays and ~~O'Neil (1997~~Grossman (1991) and the δ18Osw value of the clumped isotope measurements indicated in grey. Mg/Ca temperatures (green line on top) were calculated using the calibration reported in Surge and Lohmann (2008) with a factor 3.3 correction for lower Mg/Ca ratios in late Cretaceous ocean water. Temperatures of bulk samples of shells M4 and M11 measured using clumped isotope analysis are indicated by grey bars in graphs of M0 and M6 represent average clumped isotope temperatures of all pristine shell samples (see **Table 1**). Red and ~~orange~~green vertical bars indicate intervals were vesicular calcite was incorporated in the stable isotopic measurements (see **Figure 5**).

44

Shell name	Sampling Location	N	δ13Cav (VPDB) ±1σ		δ13C_record (VPDB) ±season		δ18Oav (VPDB) ±1σ		δ18O_record (VPDB) ±season		D47av ±1σ		T_av (°C) ±1σ		δ18Osw ±1σ	
M0	Shell hinge				1.91	±0.38			-1.43	±0.35						
M4	Shell hinge	3	1.74	±0.10	1.73	±0.32	-2.42	±0.12	-1.99	±0.72	0.725	±0.008	15.2	±2.6	-2.1	±0.7
M5	Shell hinge	3	1.70	±0.06			-2.34	±0.13			0.746	±0.016	9.0	±4.9	-3.4	±1.2
M6	Shell hinge				2.28	±0.23			-1.88	-±0.31						
M8	Shell hinge	4	1.66	±0.02			-1.75	±0.06			0.741	±0.008	10.3	±2.5	-2.5	±0.6
M11	Shell hinge	4	2.25	±0.08	2.40	±0.34	-2.58	±0.11	-1.74	±0.30	0.741	±0.007	10.3	±2.1	-3.3	±0.6
M5	Ventral margin	4	0.93	±0.15			-4.36	±0.23			0.699	±0.007	23.8	±2.5	-2.2	±0.7
M8	Ventral margin	4	-0.53	±0.10			-7.45	±0.32			0.707	±0.012	21.3	±4.0	-5.9	±1.1
M10	Ventral margin	3	2.07	±0.34			-2.99	±0.23			0.696	±0.022	25.4	±7.7	-0.6	±1.8
Average	Shell hinge	14									0.738	±0.004	11.1	±1.2	-2.8	±0.6
Average	Ventral margin	11									0.643	±0.007	23.3	±2.9	-3.1	±2.5
Shell name	Sampling Location	N	δ13Cav (VPDB) ±1σ		δ13C_record (VPDB) ±season		δ18Oav (VPDB) ±1σ		δ18O_record (VPDB) ±season		D47av ±1σ		T_av (°C) ±1σ		δ18Osw ±1σ	
M0	Shell hinge				1.91	±0.38			-1.43	±0.35						
M4	Shell hinge	3	1.74	±0.10	1.73	±0.32	-2.42	±0.12	-1.99	±0.72	0.725	±0.008	15.2	±2.6	-2.1	±0.7
M5	Shell hinge	3	1.70	±0.06			-2.34	±0.13			0.746	±0.016	9.0	±4.9	-3.4	±1.2
M6	Shell hinge				2.28	±0.23			-1.88	-±0.31						
M8	Shell hinge	4	1.66	±0.02			-1.75	±0.06			0.741	±0.008	10.3	±2.5	-2.5	±0.6
M11	Shell hinge	4	2.25	±0.08	2.40	±0.34	-2.58	±0.11	-1.74	±0.30	0.741	±0.007	10.3	±2.1	-3.3	±0.6
M5	Ventral margin	4	0.93	±0.15			-4.36	±0.23			0.699	±0.007	23.8	±2.5	-2.2	±0.7
M8	Ventral margin	4	-0.53	±0.10			-7.45	±0.32			0.707	±0.012	21.3	±4.0	-5.9	±1.1
M10	Ventral margin	3	2.07	±0.34			-2.99	±0.23			0.696	±0.022	25.4	±7.7	-0.6	±1.8
Average	Shell hinge	14									0.738	±0.004	11.1	±1.2	-2.8	±0.6
Average	Ventral margin	11									0.701	±0.007	23.3	±2.9	-3.1	±2.5

Table 1

Overview table of stable and clumped isotope results in this study. Rows highlighted in red represent samples from the ventral margin of the shells (which contain vesicular calcite). Rows with a white background represent samples of the dense foliated shell hinge. Note that for some shells (M5 and M8) both the ventral margin and the shell hinge was measured. Columns labelled "$\delta^{13}C\_record$" and "$\delta^{18}O\_record$" contain averages of the high-resolution stable isotope records measured in the shell hinges (if available, Figure 5). The bottom two rows contain average Δ_{47} and $\delta^{18}O_{sw}$ values of shell hinge (white) and ventral margin (red) samples, highlighting the difference between the two sampling strategies.